Emerging Technologies in Material Science

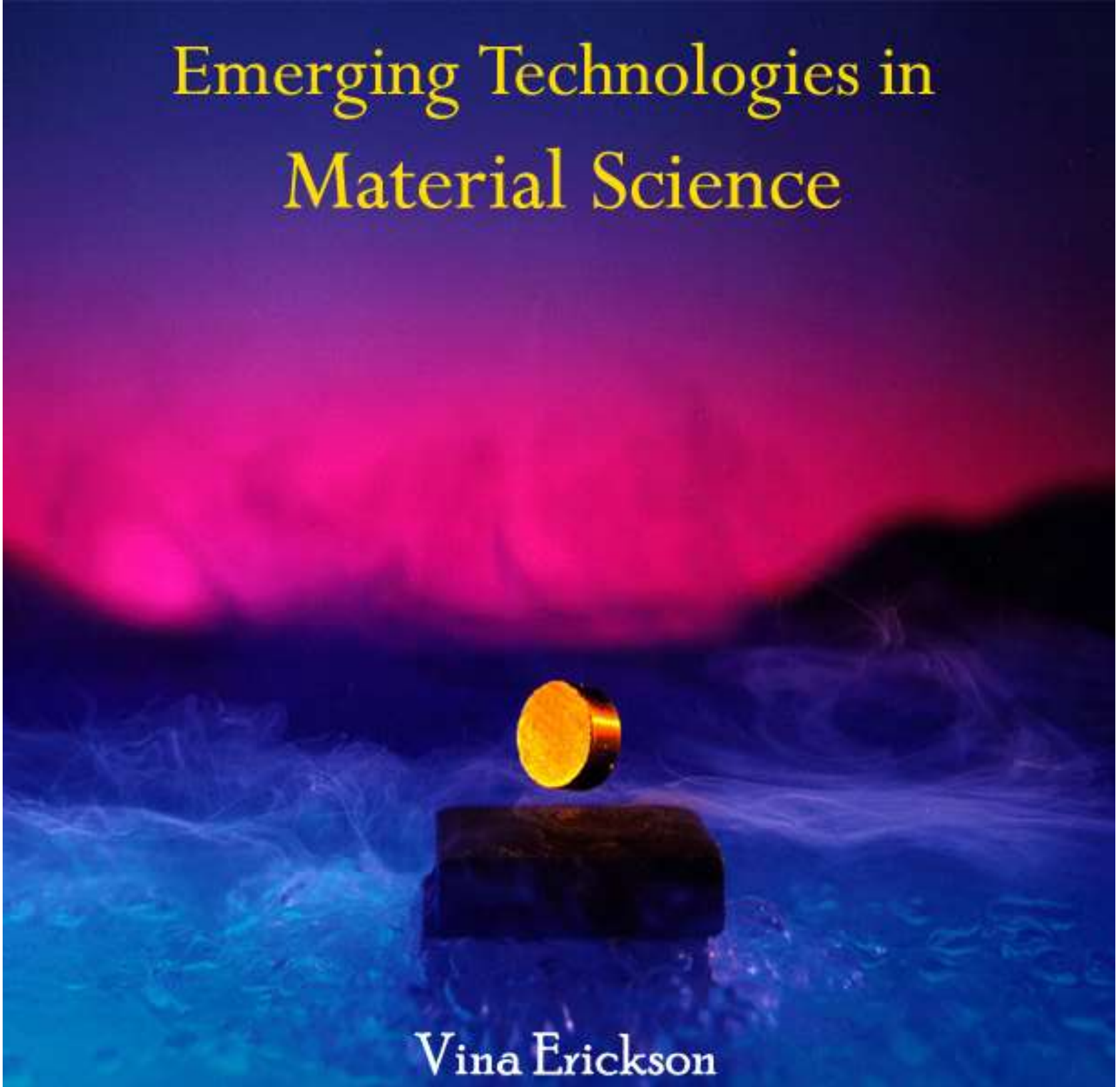

Vina Erickson

First Edition, 2012

ISBN 978-81-323-2323-5

© All rights reserved.

Published by:
Library Press
4735/22 Prakashdeep Bldg,
Ansari Road, Darya Ganj,
Delhi - 110002
Email: info@wtbooks.com

Table of Contents

WT

Chapter- 1

High-temperature Superconductivity

High-temperature superconductors (abbreviated **high-T_c** or **HTS**) are materials that have a superconducting transition temperature (T_c) above 30 K (−243.2 °C). From 1960 to 1980, 30 K was thought to be the highest theoretically possible T_c. The first high-T_c superconductor was discovered in 1986 by IBM Researchers Karl Müller and Johannes Bednorz, for which they were awarded the Nobel Prize in Physics in 1987. Until Fe-based superconductors were discovered in 2008, the term **high-temperature superconductor** was used interchangeably with **cuprate superconductor** for compounds such as bismuth strontium calcium copper oxide (BSCCO) and yttrium barium copper oxide (YBCO).

"High-temperature" has three common definitions in the context of superconductivity:

1. Above the temperature of 30 K that had historically been taken as the upper limit allowed by BCS theory. This is also above the 1973 record of 23 K that had lasted until copper-oxide materials were discovered in 1986.
2. Having a transition temperature that is a larger fraction of the Fermi temperature than for conventional superconductors such as elemental mercury or lead. This definition encompasses a wider variety of unconventional superconductors and is used in the context of theoretical models.
3. Greater than the boiling point of liquid nitrogen (77 K or −196 °C). This is significant for technological applications of superconductivity because liquid nitrogen is a relatively inexpensive and easily handled coolant.

Technological applications benefit from both the higher critical temperature being above the boiling point of liquid nitrogen and also the higher critical magnetic field (and critical current density) at which superconductivity is destroyed. In magnet applications the high critical magnetic field may be more valuable than the high T_c itself. Some cuprates have an upper critical field around 100 teslas. However, cuprate materials are brittle ceramics which are expensive to manufacture and not easily turned into wires or other useful shapes.

Two decades of intense experimental and theoretical research, with over 100,000 published papers on the subject, have discovered many common features in the properties of high-temperature superconductors, but as of 2009, there is no widely accepted theory to explain their properties. Cuprate superconductors (and other unconventional

superconductors) differ in many important ways from conventional superconductors, such as elemental mercury or lead, which are adequately explained by the BCS theory. There also has been much debate as to high-temperature superconductivity coexisting with magnetic ordering in YBCO, iron-based superconductors, several ruthenocuprates and other exotic superconductors, and the search continues for other families of materials. HTS are Type-II superconductors, which allow magnetic fields to penetrate their interior in quantized units of flux, meaning that much higher magnetic fields are required to suppress superconductivity. The layered structure also gives a directional dependence to the magnetic field response.

History and progress

- April 1986 - The term *high-temperature superconductor* was first used to designate the new family of cuprate-perovskite ceramic materials discovered by Johannes Georg Bednorz and Karl Alexander Müller, for which they won the Nobel Prize in Physics the following year. Their discovery of the first high-temperature superconductor, LaBaCuO, with a transition temperature of 30 K, generated great excitement.

- LSCO ($La_{2-x}Sr_xCuO_4$) discovered the same year.

- January 1987 - YBCO was discovered to have a T_c of 90 K.

- 1988 - BSCCO discovered with T_c up to 108 K, and TBCCO (T=thallium) discovered to have T_c of 127 K.

- As of 2009, the highest-temperature superconductor (at ambient pressure) is mercury barium calcium copper oxide ($HgBa_2Ca_2Cu_3O_x$), at 135 K and is held by a cuprate-perovskite material, possibly 164 K under high pressure.
- Recently, iron-based superconductors with critical temperatures as high as 56 K have been discovered. These are often also referred to as high-temperature superconductors.

After more than twenty years of intensive research the origin of high-temperature superconductivity is still not clear, but it seems that instead of *electron-phonon* attraction mechanisms, as in conventional superconductivity, one is dealing with genuine *electronic* mechanisms (e.g. by antiferromagnetic correlations), and instead of s-wave pairing, d-waves are substantial.

One goal of all this research is room-temperature superconductivity.

Examples

Examples of high-T_c cuprate superconductors include $La_{1.85}Ba_{0.15}CuO_4$, and YBCO (Yttrium-Barium-Copper-Oxide), which is famous as the first material to achieve superconductivity above the boiling point of liquid nitrogen.

Transition temperatures of well-known superconductors (Boiling point of liquid nitrogen for comparison)

Transition temperature (in kelvins)	Material	Class
133	$HgBa_2Ca_2Cu_3O_x$	Copper-oxide superconductors
110	$Bi_2Sr_2Ca_2Cu_3O_{10}$(BSCCO)	
90	$YBa_2Cu_3O_7$ (YBCO)	
77	Boiling point of liquid nitrogen	
55	SmFeAs(O,F)	Iron-based superconductors
41	CeFeAs(O,F)	
26	LaFeAs(O,F)	
20	Boiling point of liquid hydrogen	
18	Nb_3Sn	Metallic low-temperature superconductors
10	NbTi	
9.2	Nb	
4.2	Hg (mercury)	

Cuprates

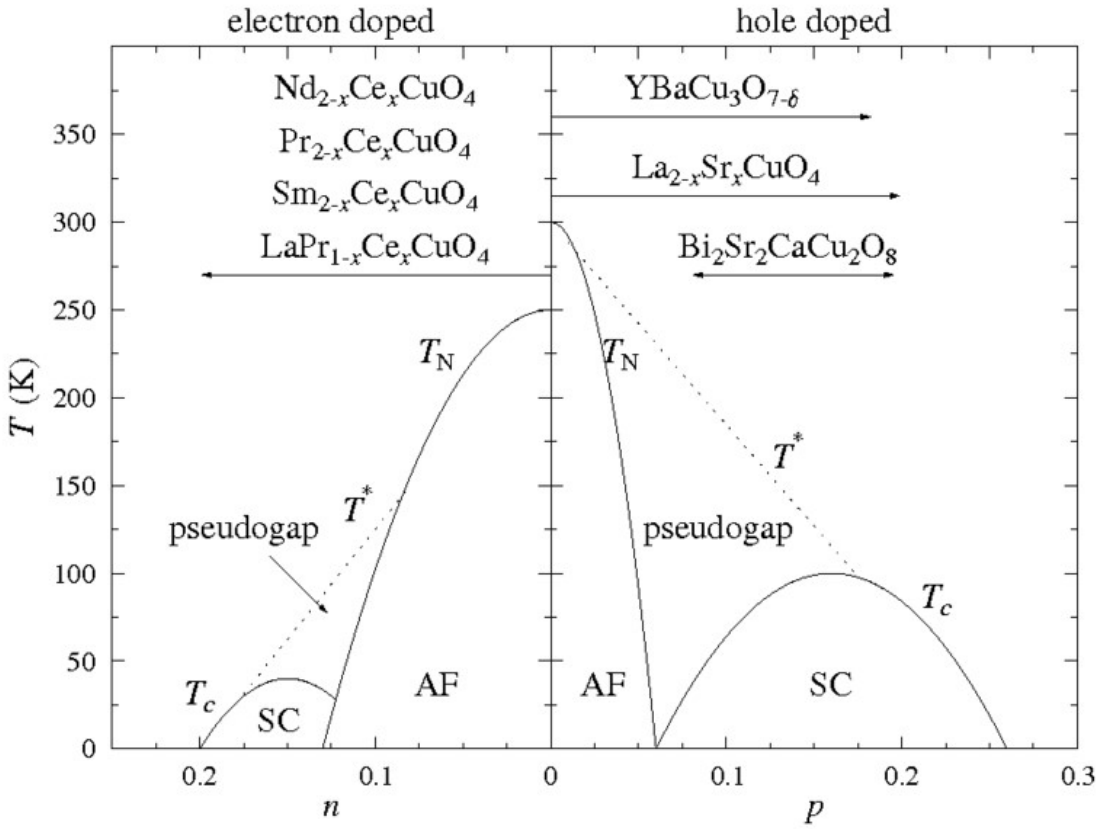

Simplified doping dependent phase diagram of cuprate superconductors for both electron (n) and hole (p) doping. The phases shown are the antiferromagnetic (AF) phase close to zero doping, the superconducting phase around optimal doping, and the pseudogap phase. Doping ranges possible for some common compounds are also shown.

Cuprate superconductors are generally considered to be quasi-two-dimensional materials with their superconducting properties determined by electrons moving within weakly coupled copper-oxide (CuO_2) layers. Neighbouring layers containing ions such as lanthanum, barium, strontium, or other atoms act to stabilize the structure and dope electrons or holes onto the copper-oxide layers. The undoped 'parent' or 'mother' compounds are Mott insulators with long-range antiferromagnetic order at low enough temperature. Single band models are generally considered to be sufficient to describe the electronic properties.

The cuprate superconductors adopt a perovskite structure. The copper-oxide planes are checkerboard lattices with squares of O^{2-} ions with a Cu^{2+} ion at the centre of each square. The unit cell is rotated by 45° from these squares. Chemical formulae of superconducting materials generally contain fractional numbers to describe the doping required for superconductivity. There are several families of cuprate superconductors and

they can be categorized by the elements they contain and the number of adjacent copper-oxide layers in each superconducting block. For example, YBCO and BSCCO can alternatively be referred to as Y123 and Bi2201/Bi2212/Bi2223 depending on the number of layers in each superconducting block (*n*). The superconducting transition temperature has been found to peak at an optimal doping value (*p=0.16*) and an optimal number of layers in each superconducting block, typically *n = 3*.

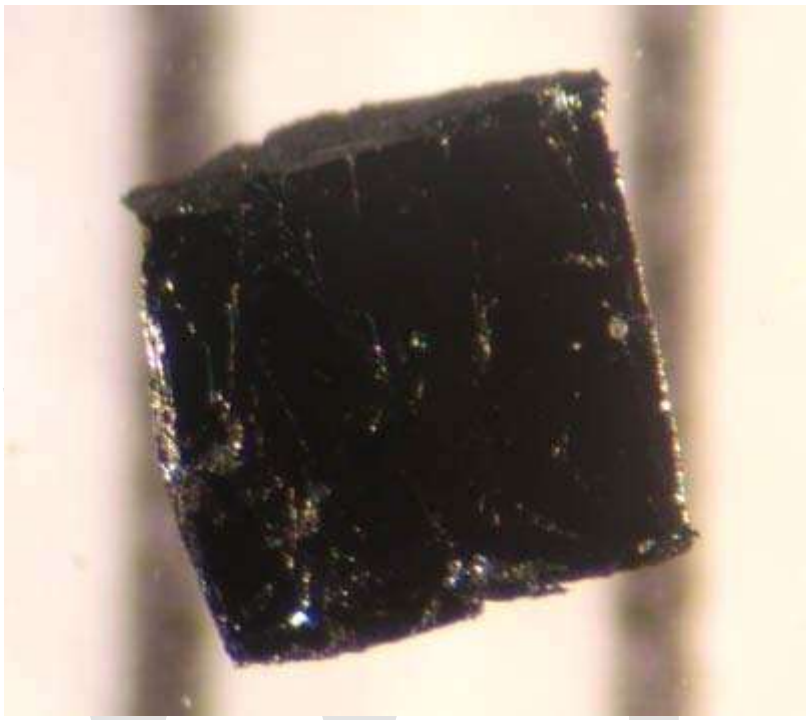

A small sample of the high-temperature superconductor BSCCO-2223

Possible mechanisms for superconductivity in the cuprates are still the subject of considerable debate and further research. Certain aspects common to all materials have been identified. Similarities between the antiferromagnetic low-temperature state of the undoped materials and the superconducting state that emerges upon doping, primarily the $d_{x^2-y^2}$ orbital state of the Cu^{2+} ions, suggest that electron-electron interactions are more significant than electron-phonon interactions in cuprates – making the superconductivity unconventional. Recent work on the Fermi surface has shown that nesting occurs at four points in the antiferromagnetic Brillouin zone where spin waves exist and that the superconducting energy gap is larger at these points. The weak isotope effects observed for most cuprates contrast with conventional superconductors that are well described by BCS theory.

Similarities and differences in the properties of hole-doped and electron doped cuprates:

- Presence of a pseudogap phase up to at least optimal doping.
- Different trends in the Uemura plot relating transition temperature to the superfluid density. The inverse square of the London penetration depth appears to

be proportional to the critical temperature for a large number of underdoped cuprate superconductors, but the constant of proportionality is different for hole- and electron-doped cuprates. The linear trend implies that the physics of these materials is strongly two-dimensional.

- Universal hourglass-shaped feature in the spin excitations of cuprates measured using inelastic neutron diffraction.
- Nernst effect evident in both the superconducting and pseudogap phases.

Iron-based superconductors

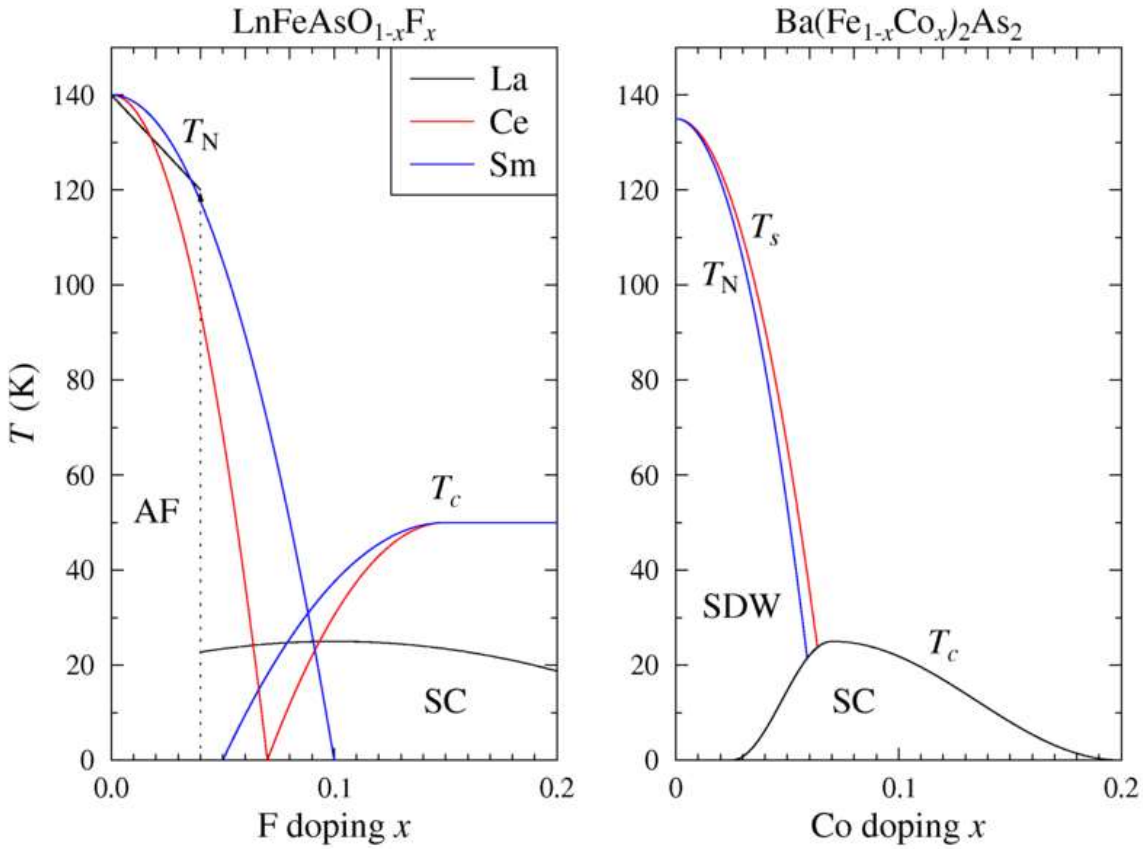

Simplified doping dependent phase diagrams of iron-based superconductors for both Ln-1111 and Ba-122 materials. The phases shown are the antiferromagnetic/spin density wave (AF/SDW) phase close to zero doping and the superconducting phase around optimal doping. The Ln-1111 phase diagrams for La and Sm were determined using muon spin spectroscopy, the phase diagram for Ce was determined using neutron diffraction. The Ba-122 phase diagram is based on.

Iron-based superconductors contain layers of iron and a pnictogen, such as arsenic, phosphorus, or chalcogens. This is currently the family with the second highest critical temperature, behind the cuprates. Interest in their superconducting properties began in 2006 with the discovery of superconductivity in LaFePO at 4 K and gained much greater

attention in 2008 after the analogous material LaFeAs(O,F) was found to superconduct at up to 43 K under pressure.

Since the original discoveries several families of iron-based superconductors have emerged:

- LnFeAs(O,F) or $LnFeAsO_{1-x}$ with T_c up to 56 K, referred to as 1111 materials. A fluoride variant of these materials was subsequently found with similar T_c values.
- $(Ba,K)Fe_2As_2$ and related materials with pairs of iron-arsenide layers, referred to as 122 compounds. T_c values range up to 38 K. These materials also superconduct when iron is replaced with cobalt
- LiFeAs and NaFeAs with T_c up to around 20 K. These materials superconduct close to stoichiometric composition and are referred to as 111 compounds.
- FeSe with small off-stoichiometry or tellurium doping.

Most undoped iron-based superconductors show a tetragonal-orthorhombic structural phase transition followed at lower temperature by magnetic ordering, similar to the cuprate superconductors. However, they are poor metals rather than Mott insulators and have five bands at the Fermi surface rather than one. The phase diagram emerging as the iron-arsenide layers are doped is remarkably similar, with the superconducting phase close to or overlapping the magnetic phase. Strong evidence that the T_c value varies with the As-Fe-As bond angles has already emerged and shows that the optimal Tc value is obtained with undistorted $FeAs_4$ tetrahedra. The symmetry of the pairing wavefunction is still widely debated, but an extended s-wave scenario is currently favoured.

Other materials sometimes referred to as high-temperature superconductors

Magnesium diboride is occasionally referred to as a high-temperature superconductor because its T_c value of 39 K is above that historically expected for BCS superconductors. However, it is more generally regarded as the highest T_c conventional superconductor, the increased T_c resulting from two separate bands being present at the Fermi energy.

Fulleride superconductors where alkali-metal atoms are intercalated into C_{60} molecules show superconductivity at temperatures of up to 38 K for Cs_3C_{60}.

Some organic superconductors and heavy fermion compounds are considered to be high-temperature superconductors because of their high T_c values relative to their Fermi energy, despite the T_c values being lower than for many conventional superconductors. This description may relate better to common aspects of the superconducting mechanism than the superconducting properties.

Theoretical work by Neil Ashcroft predicted that solid metallic hydrogen at extremely high pressure should become superconducting at approximately room-temperature because of its extremely high speed of sound and expected strong coupling between the

conduction electrons and the lattice vibrations. This prediction is yet to be experimentally verified.

All known high-T_c superconductors are Type-II superconductors. In contrast to Type-I superconductors, which expel all magnetic fields due to the Meissner Effect, Type-II superconductors allow magnetic fields to penetrate their interior in quantized units of flux, creating "holes" or "tubes" of normal metallic regions in the superconducting bulk. Consequently, high-T_c superconductors can sustain much higher magnetic fields.

Ongoing research

The question of how superconductivity arises in high-temperature superconductors is one of the major unsolved problems of theoretical condensed matter physics as of 2010. The mechanism that causes the electrons in these crystals to form pairs is not known. Despite intensive research and many promising leads, an explanation has so far eluded scientists. One reason for this is that the materials in question are generally very complex, multi-layered crystals (for example, BSCCO), making theoretical modelling difficult. Improving the quality and variety of samples also gives rise to considerable research, both with the aim of improved characterisation of the physical properties of existing compounds, and synthesizing new materials, often with the hope of increasing T_c. Technological research focusses on making HTS materials in sufficient quantities to make their use economically viable and optimizing their properties in relation to applications.

Possible mechanism

There have been two representative theories for HTS. Firstly, it has been suggested that the HTS emerges from antiferromagnetic spin fluctuations in a doped system. According to this theory, the pairing wave function of the cuprate HTS should have a $d_{x^2-y^2}$ symmetry. Thus, determining whether the pairing wave function has *d*-wave symmetry is essential to test the spin fluctuation mechanism. That is, if the HTS order parameter (pairing wave function) does not have *d*-wave symmetry, then a pairing mechanism related to spin fluctuations can be ruled out. (Similar arguments can be made for iron-based superconductors but the different material properties allow a different pairing symmetry.) Secondly, there was the **interlayer coupling model**, according to which a layered structure consisting of BCS-type (*s*-wave symmetry) superconductors can enhance the superconductivity by itself. By introducing an additional tunnelling interaction between each layer, this model successfully explained the anisotropic symmetry of the order parameter as well as the emergence of the HTS. Thus, in order to solve this unsettled problem, there have been numerous experiments such as photoemission spectroscopy, NMR, specific heat measurements, etc. But, unfortunately, the results were ambiguous, some reports supported the d symmetry for the HTS whereas others supported the s symmetry. This muddy situation possibly originated from the indirect nature of the experimental evidence, as well as experimental issues such as sample quality, impurity scattering, twinning, etc.

Junction experiment supporting the d symmetry

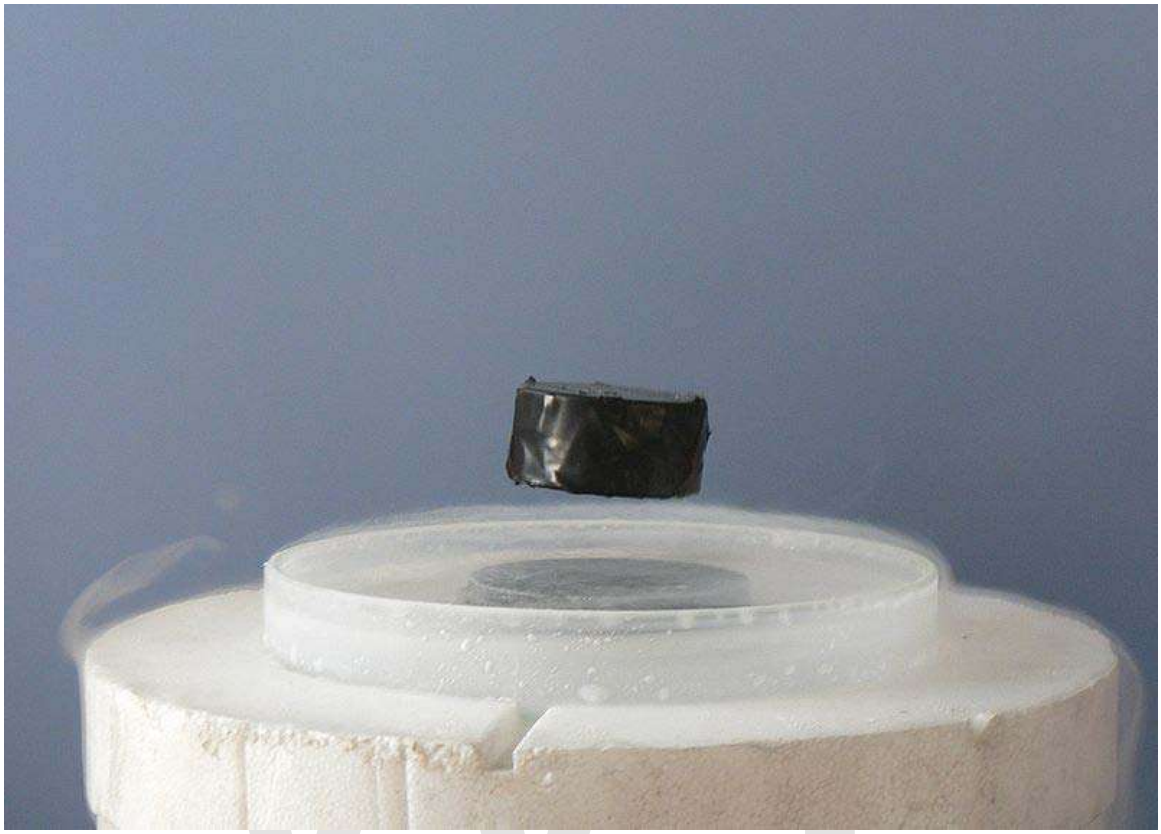

The Meissner effect or a magnet levitating above a superconductor (cooled by liquid nitrogen)

There was a clever experimental design to overcome the muddy situation. An experiment based on flux quantization of a three-grain ring of $YBa_2Cu_3O_7$ (YBCO) was proposed to test the symmetry of the order parameter in the HTS. The symmetry of the order parameter could best be probed at the junction interface as the Cooper pairs tunnel across a Josephson junction or weak link. It was expected that a half-integer flux, that is, a spontaneous magnetization could only occur for a junction of d symmetry superconductors. But, even if the junction experiment is the strongest method to determine the symmetry of the HTS order parameter, the results have been ambiguous. J. R. Kirtley and C. C. Tsuei thought that the ambiguous results came from the defects inside the HTS, so that they designed an experiment where both clean limit (no defects) and dirty limit (maximal defects) were considered simultaneously. In the experiment, the spontaneous magnetization was clearly observed in YBCO, which supported the d symmetry of the order parameter in YBCO. But, since YBCO is orthorhombic, it might inherently have an admixture of s symmetry. So, by tuning their technique further, they found that there was an admixture of s symmetry in YBCO within about 3%. Also, they found that there was a pure $d_{x^2-y^2}$ order parameter symmetry in the tetragonal $Tl_2Ba_2CuO_6$.

Qualitative explanation of the spin-fluctuation mechanism

While, despite all these years, the mechanism of high-T_c superconductivity is still highly controversial, this being due to mostly the lack of exact theoretical computations on such strongly interacting electron systems, most rigorous theoretical calculations, including phenomenological and diagrammatic approaches, converge on magnetic fluctuations as the pairing mechanism for these systems. The qualitative explanation is as follows. (Note that, in the following argument, one can replace “electron” with “hole” and vice versa depending on the actual material.)

In a normal conductor, a hole is created whenever an electron is moved. This causes a resistivity because charge neutrality must be conserved and as electrons move under an electric field, they drag holes behind them through defects and thermal oscillations in the system. In contrast, in a superconductor, one gets an unlimited supply of electrons without creating holes behind. This is through the creation of so-called Cooper pairs in a superconductor. Cooper pairs are pairs of electrons. In a normal conductor, creation of an electron leads to creation of a hole, which conserves the number of particles. But in a superconductor, it's possible to create a Cooper pair without creating holes and therefore not to conserve the number of particles, hence leading to the unlimited supply of electrons.

In a conventional superconductor, Cooper pairs are created as follows. When an electron moves through the system, it creates a depression in the atomic lattice through lattice vibrations known as phonons. If the depression of the lattice is strong enough, another electron can fall into the depression created by the first electron—the so-called water-bed effect—and a Cooper pair is formed. When this effect becomes strong enough, Cooper pairs win over the creation of holes behind the electrons, and the normal conductor turns into a superconductor through an unlimited supply of electrons by the creation of Cooper pairs.

In a high-T_c superconductor, the mechanism is extremely similar to a conventional superconductor. Except, in this case, phonons virtually play no role and their role is replaced by spin-density waves. As all conventional superconductors are strong phonon systems, all high-T_c superconductors are strong spin-density wave systems, within close vicinity of a magnetic transition to, for example, an antiferromagnet. When an electron moves in a high-T_c superconductor, its spin creates a spin-density wave around it. This spin-density wave in turn causes a nearby electron to fall into the spin depression created by the first electron (water-bed effect again). Hence, again, a Cooper pair is formed. Eventually, when the system temperature is lowered, more spin density waves and Cooper pairs are created and superconductivity begins when an unlimited supply of Cooper pairs, denoted as a phase transition, happens. Note that in high-T_c systems, as these systems are magnetic systems due to the Coulomb interaction, there is a strong Coulomb repulsion between electrons. This Coulomb repulsion prevents pairing of the Cooper pairs on the same lattice site. The pairing of the electrons occur at near-neighbor lattice sites as a result. This is the so-called *d*-wave pairing, where the pairing state has a node (zero) at the origin.

Chapter- 2

High-temperature Superconductors

Bismuth strontium calcium copper oxide

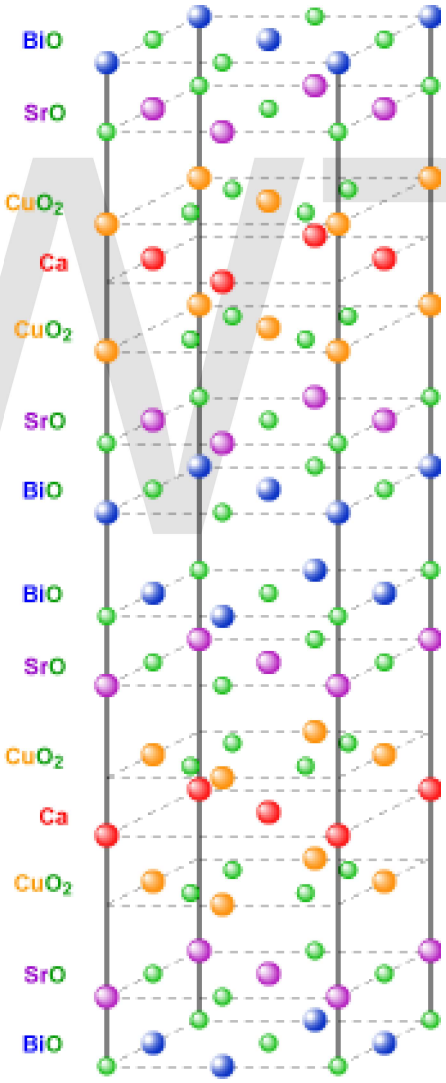

The unit cell of BSCCO-2212. The other BSCCO family members have very similar structures: 2201 has one less CuO_2 in its top and bottom half and no Ca layer, while 2223 has an extra CuO_2 and Ca layer in each half.

Bismuth strontium calcium copper oxide, or **BSCCO** (pronounced "bisko"), is a family of high-temperature superconductors having the generalized chemical formula $Bi_2Sr_2Ca_nCu_{n+1}O_{2n+6+x}$, with n=1 being the most commonly-studied compound (though n=0 and n=2 have also received significant attention). Discovered in 1988, BSCCO was the first high-temperature superconductor which did not contain a rare earth element. It is a cuprate superconductor, an important category of high-temperature superconductors sharing a two-dimensional layered (perovskite) structure (see figure above) with superconductivity taking place in a copper oxide plane. BSCCO and YBCO are the most studied cuprate superconductors.

Specific types of BSCCO are usually referred to using the sequence of the numbers of the metallic ions. Thus Bi-2201 is the n=1 compound ($Bi_2Sr_2CuO_{6+x}$), Bi-2212 is the n=2 compound ($Bi_2Sr_2CaCu_2O_{8+x}$) and Bi-2223 is the n=3 compound ($Bi_2Sr_2Ca_2Cu_3O_{10+x}$).

The BSCCO family is analogous to a thallium family of high-temperature superconductors referred to as TBCCO and having the general formula $Tl_2Ba_2Ca_{n-1}Cu_nO_{2n+4+x}$, and a mercury family HBCCO of formula $Hg_2Ba_2Ca_{n-1}Cu_nO_{2n+2+x}$. There are a number of other variants of these superconducting families. In general their critical temperature at which they become superconducting rises for the first few members then falls. Thus Bi-2201 has $T_c \approx 20$ K, Bi-2212 has $T_c \approx 95$ K, Bi-2223 has $T_c \approx 108$ K, and Bi-2234 has $T_c \approx 104$K. This last member is very difficult to synthesise

Discovery

BSCCO as a new class of superconductor was discovered by Maeda and coworkers at the National Research Institute for Metals in Japan, though at the time they were unable to determine its precise composition and structure. Almost immediately several groups, and most notably Subramanian *et al* at Dupont and Cava *et al* at AT&T Bell Labs, identified Bi-2212. The n=3 member proved quite elusive and was not identified until a month or so later by Tallon *et al* in a government research lab in New Zealand. There have been only minor improvements to these materials since. A key early development was to replace about 15% of the Bi by Pb which greatly accelerated the formation and quality of Bi-2223.

Properties

BSCCO needs to be hole-doped by an excess of oxygen atoms (δ in the formula) in order to superconduct. As in all high-temperature superconductors (HTS) T_c is sensitive to the exact doping level: the maximum Tc for Bi-2212 (as for most HTS) is achieved with an excess of about 0.16 holes per Cu atom. This is referred to as optimum doping. Samples with lower doping (and hence lower T_c) are generally referred to as underdoped while those with excess doping (also lower T_c) are overdoped. By changing the oxygen content T_c can thus be altered at will. By many measures, overdoped HTS are strong superconductors, even if their T_c is less than optimum, but underdoped HTS become extremely weak. The application of external pressure generally raises T_c in underdoped

samples to values that well exceed the maximum at ambient pressure. This is not fully understood though a secondary effect is that pressure increases the doping. Bi-2223 is complicated in that it has three distinct copper-oxygen planes. The two outer copper-oxygen layers are typically close to optimal doping while the remaining inner layer is markedly underdoped. Thus the application of pressure in Bi-2223 results in Tc rising to a maximum of about 123 K due to optimisation of the two outer planes. Following an extended decline, Tc then rises again towards 140 K due to optimisation of the inner plane. A key challenge therefore is to determine how to optimise all copper-oxygen layers simultaneously. Considerable improvements in superconducting properties could yet be achieved using such strategies.

BSCCO is a *Type II superconductor*. The upper critical field, H_{c2}, in Bi-2212 polycrystalline samples at 4.2 K has been measured as 200±25 T (cf 168±26 T for YBCO polycrystalline samples). In practise HTS are limited by the irreversibility field, H*, above which magnetic vortices melt or decouple. Even though BSCCO has a higher upper critical field than YBCO it has a much lower H* (typically smaller by a factor of 100) thus limiting its use for making high-field magnets. It is for this reason that conductors of YBCO are preferred to BSCCO though they are much more difficult to fabricate.

Wires and tapes

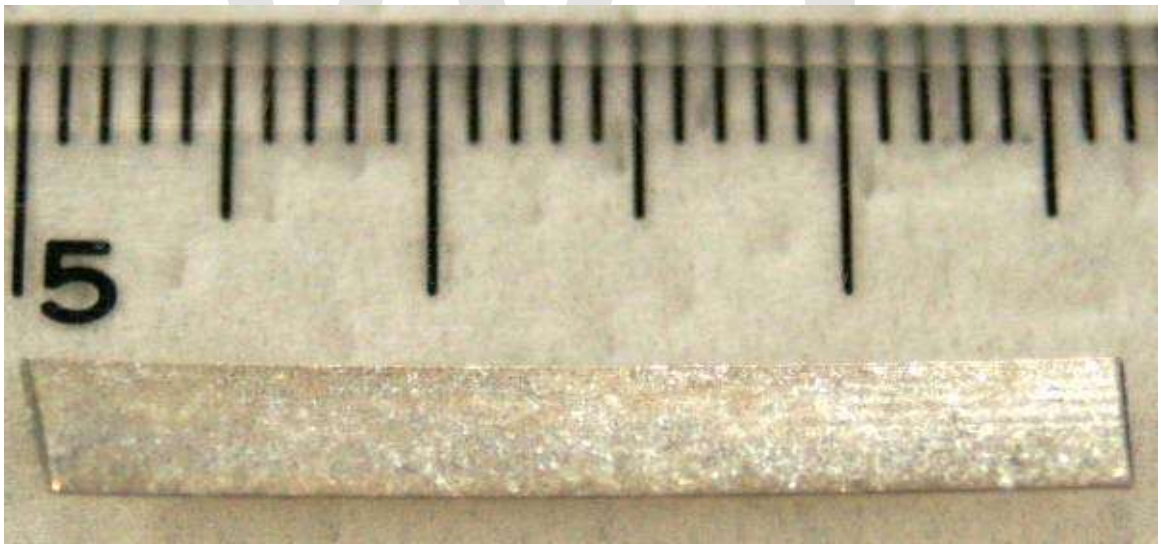

For practical applications, BSCCO is compressed with silver metal into tape via the PIT process

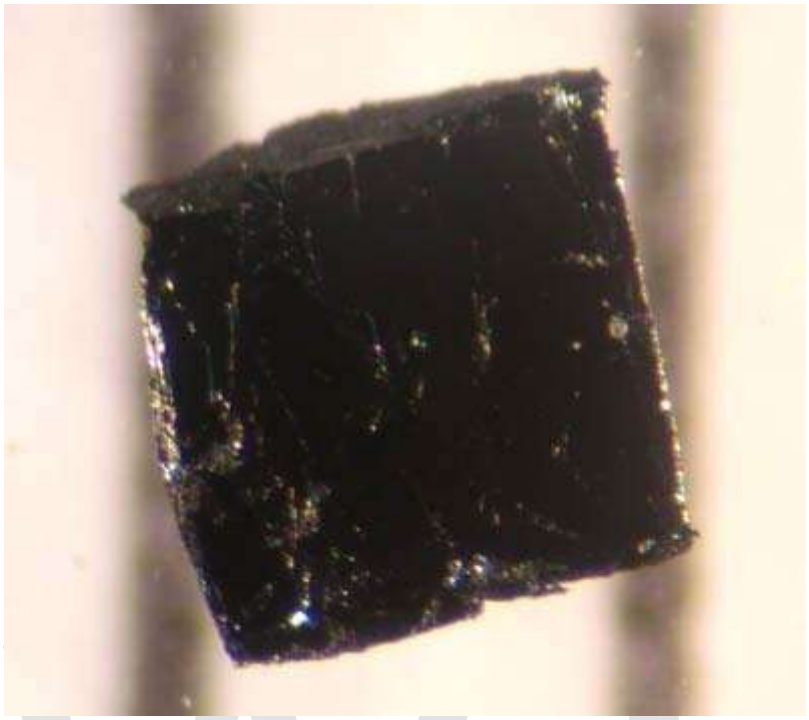

A piece of Bi2223. (The two lines in the background are 1 mm apart.)

BSCCO was the first HTS material to be used for making practical superconducting wires. All HTS have an extremely short coherence length, of the order of 1.6nm. This means that the grains in a polycrystalline wire must be extremely good contact – they must be atomically smooth. Further, because the superconductivity resides substantially only in the copper-oxygen planes the grains must be crystallographically aligned. BSCCO is therefore a good candidate because its grains can be aligned either by melt processing or by mechanical deformation. The double bismuth oxide layer is only weakly bonded by van der Waals forces. So like graphite or mica, deformation causes slip on these BiO planes and grains tend to deform into aligned plates. Further, because BSCCO has n=1, 2 and 3 members these naturally tend to accommodate low angle grain boundaries so that indeed they remain atomically smooth. Thus first-generation HTS wires (referred to as 1G) have been manufactured for many years now by companies such as American Superconductor Corporation (ASC) in the USA and Sumitomo in Japan – though ASC has now abandoned BSCCO wire in favour of 2G wire based on YBCO.

Typically, precursor powders are packed into a silver tube which is extruded down in diameter. These are then repacked as multiple tubes in a silver tube and again extruded down in diameter, then drawn down further in size and rolled into a flat tape. The last step ensures grain alignment. The tapes are then reacted at high temperature to form dense, crystallographically-aligned Bi-2223 multifilamentary conducting tape suitable for winding cables or coils for transformers, magnets, motors and generators. Typical tapes of 4mm width and 0.2mm thickness support a current at 77K of 200 A, giving a critical current density (maximal amperes per square metre of cross-sectional area) in the Bi-

2223 filaments of 5×10^5 Amps/cm2. This rises markedly with decreasing temperature so that many applications are implemented at 30-35 K, even though T_c is 108 K.

Thallium barium calcium copper oxide

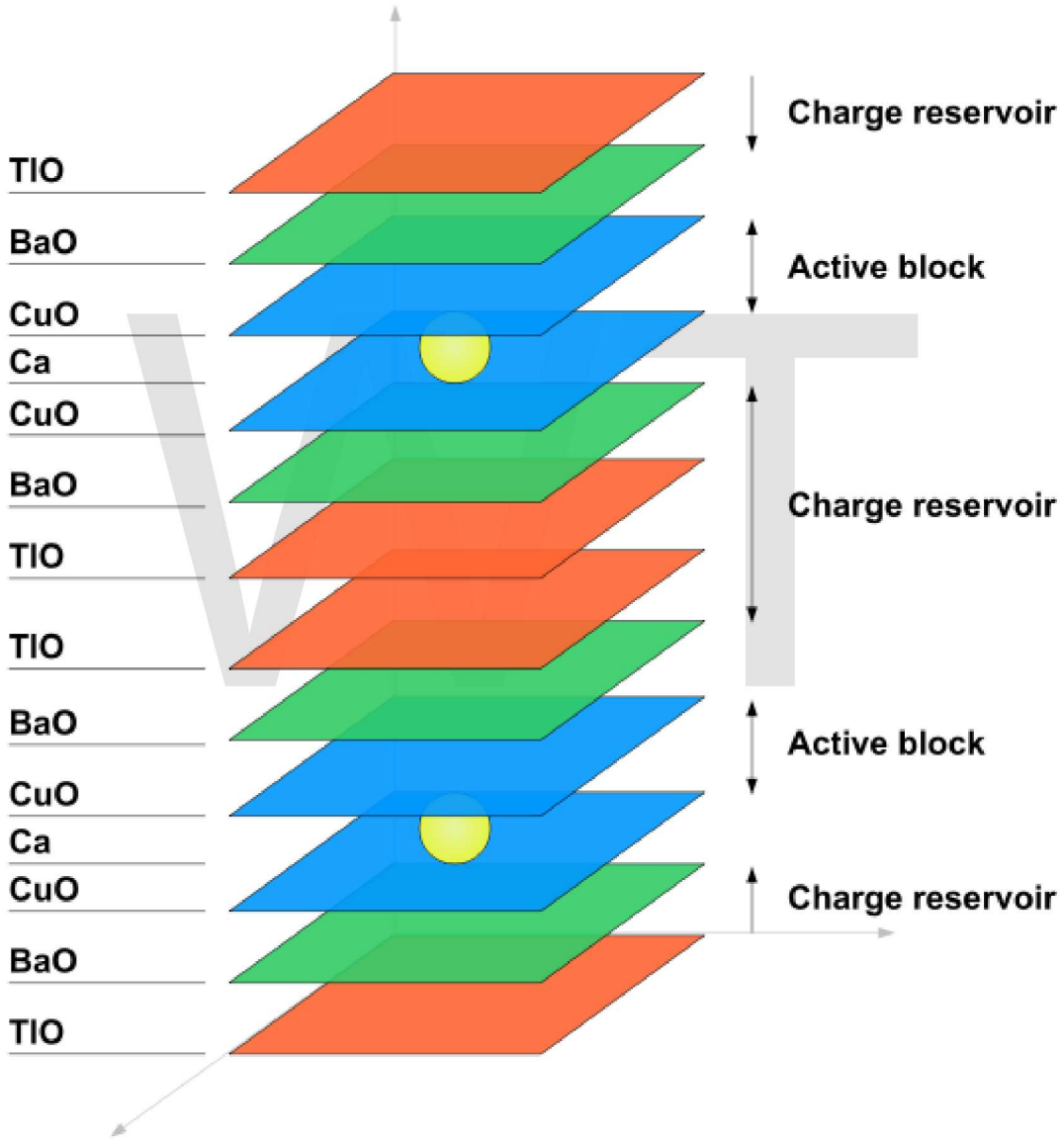

Schematic layered structure of TBCCO-2223

Thallium barium calcium copper oxide, or **TBCCO** (pronounced "tibco"), is a family of high-temperature superconductors having the generalized chemical formula $Tl_mBa_2Ca_{n-1}Cu_nO_{2n+m+2}$.

$Tl_2Ba_2Ca_2Cu_3O_{10}$ (TBCCO-2223) has a critical temperature (Tc) of 127 K, discovered in 1988.

Yttrium barium copper oxide

Yttrium barium copper oxide	
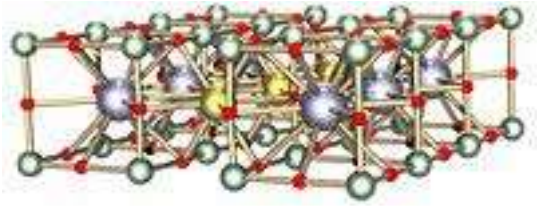	
IUPAC name barium copper yttrium oxide	
Other names YBCO, Y123, yttrium barium cuprate	
Identifiers	
CAS number	107539-20-8 ✓
Properties	
Molecular formula	$YBa_2Cu_3O_7$
Molar mass	666.19
Appearance	Black solid
Density	6.3 g/cm^3
Melting point	>1000 °C
Solubility in water	Insoluble
Structure	
Crystal structure	Based on the Perovskite structure.
Coordination geometry	Orthorhombic.
Hazards	
EU classification	Irritant (**Xi**).
Related compounds	
Related high-T_c superconductors	$BaLaO_{3-x}$
Related compounds	Yttrium(III) oxide Barium oxide Copper(II) oxide

Yttrium barium copper oxide, often abbreviated YBCO, is a crystalline chemical compound with the formula $YBa_2Cu_3O_7$. This material, a famous "high-temperature superconductor", achieved prominence because it was the first material to achieve superconductivity above the boiling point of nitrogen.

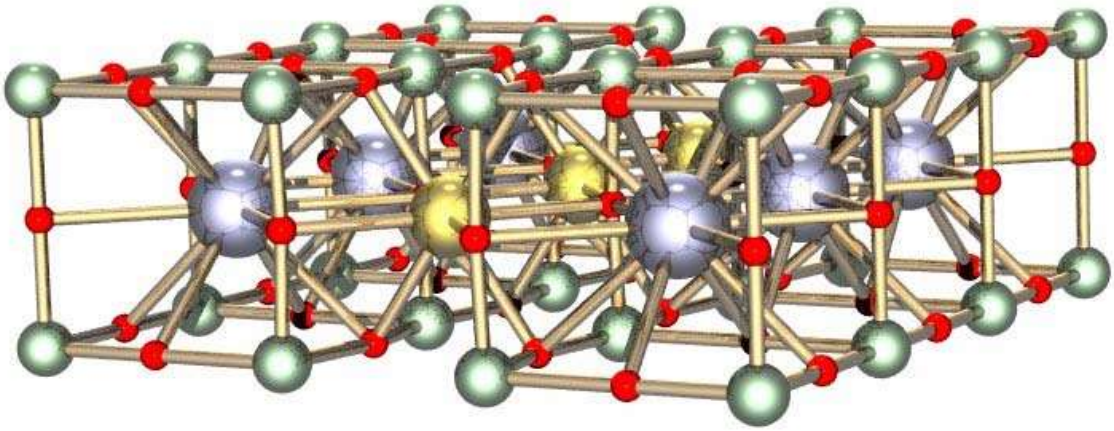

History

In April 1986 (seventy-five years after the discovery of superconductivity in 1911), Georg Bednorz and Karl Müller, working at IBM in Zurich, discovered that certain semiconducting oxides became superconducting at 35 K, then considered a relatively high temperature. In particular, the lanthanum barium copper oxides, an oxygen deficient perovskite-related material, proved promising. In 1987, Bednorz and Müller were jointly awarded the Nobel Prize in Physics for this work.

Building on that, Maw-Kuen Wu and his graduate students, Ashburn and Torng at the University of Alabama in Huntsville in 1987, and Paul Chu and his students at the University of Houston in 1987, discovered YBCO has a T_c of 93 K. (The first samples were $Y_{1.2}Ba_{0.8}CuO_4$.) Their work led to a rapid succession of new high temperature superconducting materials, ushering in a new era in material science and chemistry.

YBCO was the first material to become superconducting above 77 K, the boiling point of nitrogen. All materials developed before 1986 became superconducting only at temperatures near the boiling points of liquid helium or liquid hydrogen (T_b = 20.28 K) - the highest being Nb_3Ge at 23 K. The significance of the discovery of YBCO is the much lower cost of the refrigerant used to cool the material to below the critical temperature.

Synthesis

Relatively pure YBCO was first synthesized by heating a mixture of the metal carbonates at temperatures between 1000 to 1300 K.

$$4\ BaCO_3 + Y_2(CO_3)_3 + 6\ CuCO_3 + (1/2-x)\ O_2 \rightarrow 2\ YBa_2Cu_3O_{7-x} + 13\ CO_2$$

Modern syntheses of YBCO use the corresponding oxides and nitrates.

The superconducting properties of $YBa_2Cu_3O_{7-x}$ are sensitive to the value of x, its oxygen content. Only those materials with $0 \leq x \leq 0.65$ are superconducting below T_c, and when

$x \sim 0.07$ the material superconducts at the highest temperature of 95 K, or in highest magnetic fields: 120 T for **B** perpendicular and 250 T for **B** parallel to the CuO_2 planes.

In addition to being sensitive to the stoichiometry of oxygen, the properties of YBCO are influenced by the crystallization methods used. Care must be taken to sinter YBCO. YBCO is a crystalline material, and the best superconductive properties are obtained when crystal grain boundaries are aligned by careful control of annealing and quenching temperature rates.

Numerous other methods to synthesize YBCO have developed since its discovery by Wu and his coworkers, such as chemical vapor deposition (CVD), sol-gel, and aerosol methods. These alternative methods, however, still require careful sintering to produce a quality product.

However, new possibilities have been opened since the discovery that trifluoroacetic acid (TFA), a source of fluorine, prevents the formation of the undesired barium carbonate ($BaCO_3$). Routes such as CSD (chemical solution deposition) have opened a wide range of possibilities, particularly in the preparation of long length YBCO tapes. This route lowers the temperature necessary to get the correct phase to around 700 °C. This, and the lack of dependence on vacuum, makes this method a very promising way to get scalable YBCO tapes.

WT

Structure

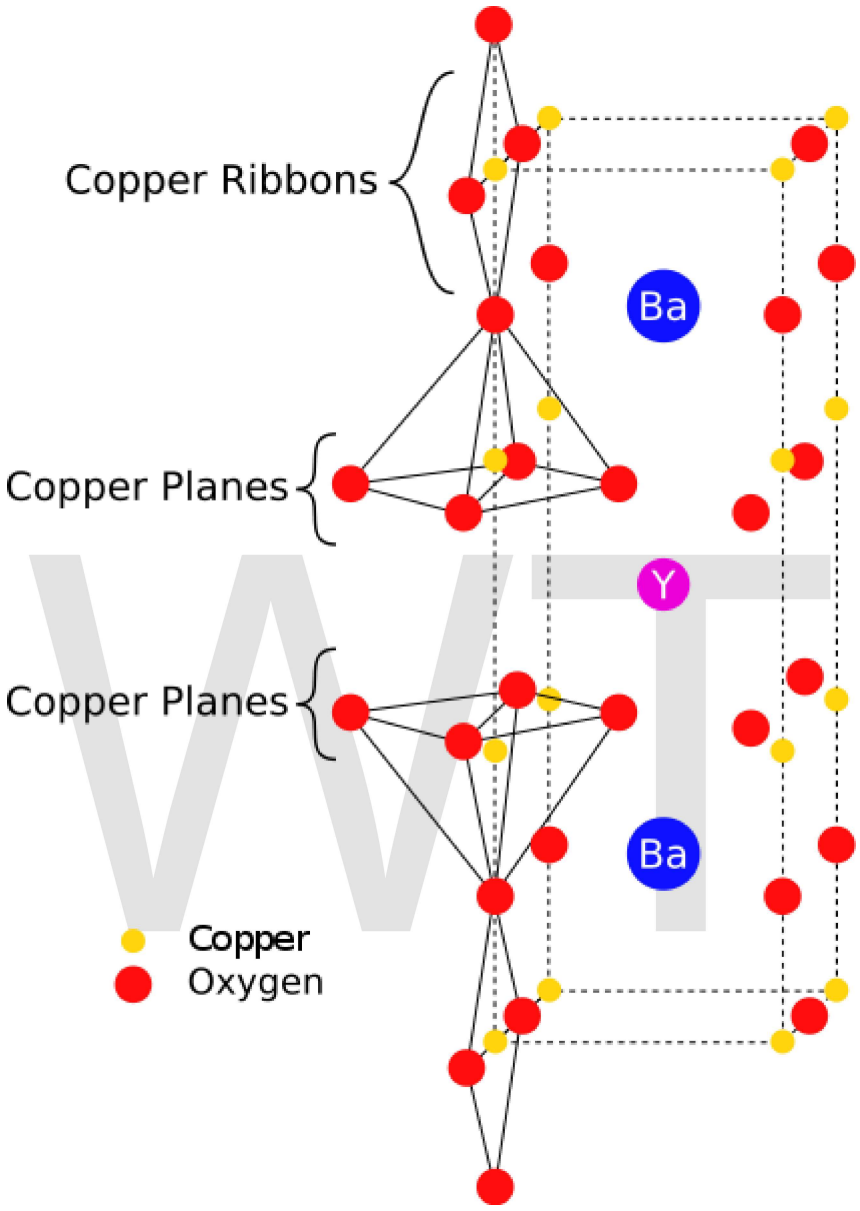

YBCO crystallises in a defect perovskite structure consisting of layers. The boundary of each layer is defined by planes of square planar CuO_4 units sharing 4 vertices. The planes can some times be slightly puckered. Perpendicular to these CuO_2 planes are CuO_4 ribbons sharing 2 vertices. The yttrium atoms are found between the CuO_2 planes, while the barium atoms are found between the CuO_4 ribbons and the CuO_2 planes. This structural feature is illustrated in the figure to the right.

More details

Although $YBa_2Cu_3O_7$ is a well-defined chemical compound with a specific structure and stoichiometry, materials with less than seven oxygen atoms per formula unit are non-stoichiometric compounds. The structure of these materials depends on the oxygen content. This non-stoichiometry is denoted by the $YBa_2Cu_3O_{7-x}$ in the chemical formula. When $x = 1$, the O(1) sites in the Cu(1) layer are vacant and the structure is tetragonal. The tetragonal form of YBCO is insulating and does not superconduct. Increasing the oxygen content slightly causes more of the O(1) sites to become occupied. For $x < 0.65$, Cu-O chains along the *b*-axis of the crystal are formed. Elongation of the *b*-axis changes the structure to orthorhombic, with lattice parameters of $a = 3.82$, $b = 3.89$, and $c = 11.68$ Å. Optimum superconducting properties occur when $x \sim 0.07$ and all of the O(1) sites are occupied with few vacancies.

In experiments where other elements are substituted at the Cu and Ba sites evidence has shown that conduction occurs in the Cu(2)O planes while the Cu(1)O(1) chains act as charge reservoirs, which provide carriers to the CuO planes. However, this model fails to address superconductivity in the homologue Pr123 (praseodymium instead of yttrium). This (conduction in the Copper planes) confines conductivity to the *a*-*b* planes and a large anisotropy in transport properties is observed. Along the *c*-axis, normal conductivity is 10 times smaller than in the *a*-*b* plane. For other cuprates in the same general class, the anisotropy is even greater and inter-plane transport is highly restricted.

Furthermore, the superconducting length scales show similar anisotropy, in both penetration depth ($\lambda_{ab} \approx 150$ nm $\lambda_c \approx 800$ nm) and coherence length, ($\xi_{ab} \approx 2$ nm, $\xi_c \approx 0.4$ nm). Although the coherence length in the *a*-*b* plane is 5 times greater than that along the *c*-axis it is quite small compared to classic superconductors such as niobium (where $\xi \approx 40$ nm). This modest coherence length means that the superconducting state is more susceptible to local disruptions from interfaces or defects on the order of a single unit cell, such as the boundary between twinned crystal domains. This sensitivity to small defects complicates fabricating devices with YBCO, and the material is also sensitive to degradation from humidity.

Superconductive properties

It is a Type-II superconductor.

Penetration depth: 120 nm in the *ab* plane, 800 nm along the *c* axis.

Coherence length: 2 nm in the *ab* plane, 0.4 nm along the *c* axis.

Properties of single crystals

The upper critical field is 120 T for **B** perpendicular and 250 T for **B** parallel to the CuO_2 planes.

Bulk properties

Bulk properties depend greatly on the manner of synthesis and treatment because of the effect on crystal size, alignment, and density and type of lattice defects.

Applications in technology

"The implementation of thin-film YBCO receiver coils has improved the signal-to-noise ratio of nuclear magnetic resonance (NMR) spectrometers by a factor of 3 compared to that achievable with conventional coils."

Several commercial applications of high temperature superconducting materials have been realized. For example, superconducting materials are finding use as magnets in magnetic resonance imaging, magnetic levitation, and Josephson junctions. (The most used material for power cables and magnets is BSCCO.)

YBCO has yet to be used in many applications involving superconductors for two primary reasons:

- First, while single crystals of YBCO have a very high critical current density, polycrystals have a very low critical current density: only a small current can be passed while maintaining superconductivity. This problem is due to crystal grain boundaries in the material. When the grain boundary angle is greater than about 5°, the supercurrent cannot cross the boundary. The grain boundary problem can be controlled to some extent by preparing thin films via CVD or by texturing the material to align the grain boundaries.
- A second problem limiting the use of this material in technological applications is associated with processing of the material. Oxide materials such as this are brittle, and forming them into wires by any conventional process does not produce a useful superconductor. (Unlike BSCCO, the powder-in-tube process does not give good results with YBCO.)

It should be noted that cooling materials to liquid nitrogen temperature (77 K) is often not practical on a large scale, although many commercial magnets are routinely cooled to liquid helium temperatures (4.2 K).

The most promising method developed to utilize this material involves deposition of YBCO on flexible metal tapes coated with buffering metal oxides. This is known as **coated conductor**. Texture (crystal plane alignment) can be introduced into the metal tape itself (the RABiTS process) or a textured ceramic buffer layer can be deposited, with the aid of an ion beam, on an untextured alloy substrate (the IBAD process). Subsequent oxide layers prevent diffusion of the metal from the tape into the superconductor while transferring the template for texturing the superconducting layer. Novel variants on CVD, PVD, and solution deposition techniques are used to produce long lengths of the final YBCO layer at high rates. Companies pursuing these processes include American Superconductor, Superpower (a division of Intermagnetics General Corp), Sumitomo,

Fujikura, Nexans Superconductors, and European Advanced Superconductors. A much larger number of research institutes have also produced YBCO tape by these methods.

Surface modification of YBCO

Surface modification of materials has often led to new and improved properties. Corrosion inhibition, polymer adhesion and nucleation, preparation of organic superconductor/ insulator/high-Tc superconductor trilayer structures, and the fabrication of metal/insulator/ superconductor tunnel junctions have been developed using surface modified YBCO.

These molecular layered materials are synthesized using cyclic voltammetry. Thus far, YBCO layered with alkylamines, arylamines, and thiols have been produced with varying stability of the molecular layer. It has been proposed that amines act as Lewis bases and bind to Lewis acidic Cu surface sites in $YBa_2Cu_3O_7$ to form stable coordination bonds.

Superstripes

Superstripes are metallic heterostructures at the atomic limit where the **shape resonance** in the energy gap parameters Δn is the driving mechanism for the amplification of the superconductivity critical temperature. These particular **heterostructures at atomic limit** are formed by a metallic superlattice of superconducting units (layers, or stripes, or wires, or spheres or balls) separated by an intercalated material like in cuprate materials. The **superstripes** show multiple superconducting gaps, i.e. different order parameters of the off diagonal superconducting order, therefore these materials are a particular case of the called **two-band** superconductor or **multiband** superconductor or **two-gap** superconductor, or multigap superconductor. A key particular feature of superstripes is that the different gaps are not only different in different portions of the k-space but also in different portions of the superlattice in the real space.

High Temperature Superconductivity in Superstripes

The prediction of high temperature superconductivity transition temperatures is rightly considered to be one of the most difficult problems in theoretical physics. The High Temperature Superconductivity in Superstripes is driven by a quantum mechanism that rises the critical temperature: a quantum interference effect in the Interband Pairing, that is a resonance in the exchange-like pair transfer between different condensates, providing a single critical temperature Tc. The quantum configuration interaction between different pairing channels is a particular case of shape resonance belonging to the group of Fano Feshbach resonances in atomic and nuclear physics. The quantum resonance is switched on when the chemical potential is tuned at an "electronic topological transition" (ETT) where one of the Fermi surfaces of the subbands appears or changes its dimensionality.

The tuning of the chemical potential at the shape resonance can be obtained by changing: the charge density and/or the superlattice structural parameters, and/or the superlattice misfit strain and/or the disorder.

The particular realizations of this type of unconventional superconductor made of superstripes are the cuprate materials made of CuO_2 layers intercalated by block layers, the magnesium diboride materials made of boron layers intercalated by Mg/Al/Sc layers and the oxypnictide materials made of FeAs layers intercalated by atomic or oxide layers.

Superstripes conferences

Superstripes has given the name to a series of conferences dedicated on this subject that started in 2008, "Superstripes 2008". The second "Superstripes 2010" meeting will be held in Erice, Italy July 19–25 (2010)

History

The name Superstripes has been introduced in 1999 for describing the intrinsic structural feature of materials showing High-temperature superconductivity: the structural modulation that coexists and favors high temperature superconductivity

WT

Chapter- 3

Superfluid

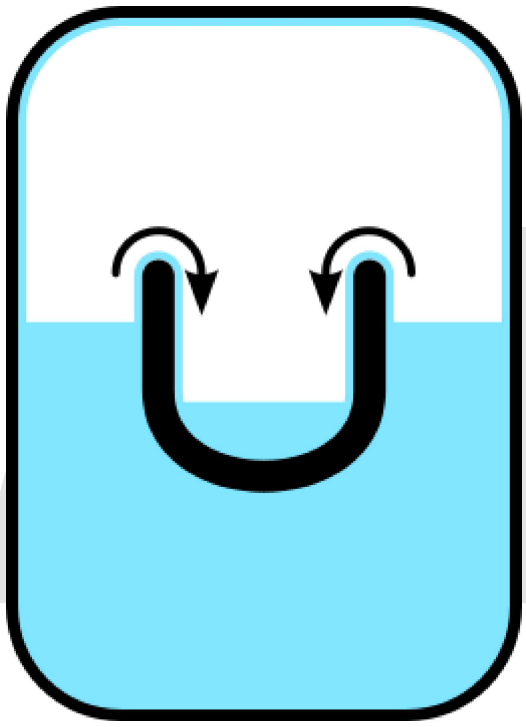

Helium II will "creep" along surfaces in order to find its own level - after a short while, the levels in the two containers will equalize. The Rollin film also covers the interior of the larger container; if it were not sealed, the helium II would creep out and escape.

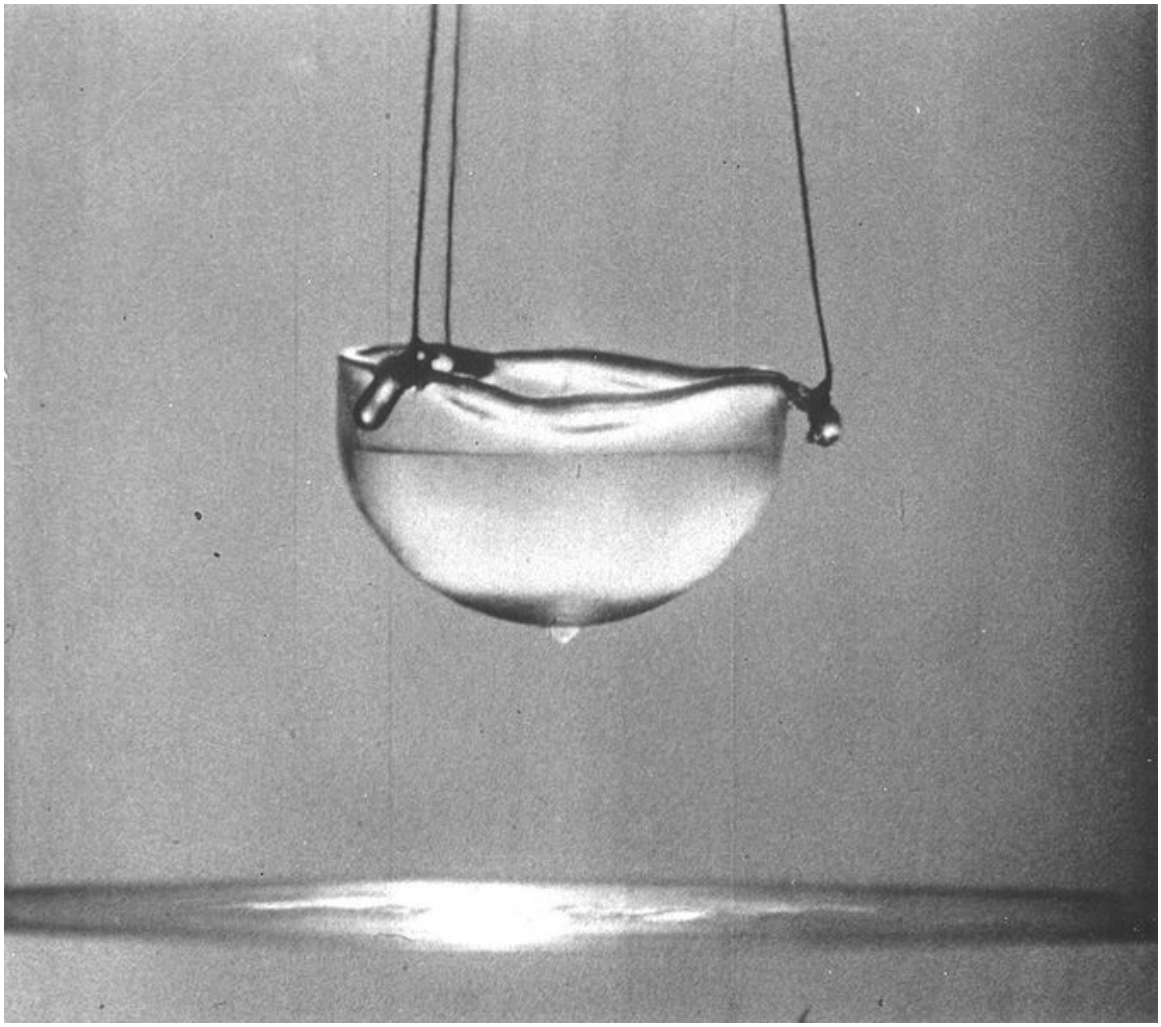

The liquid helium is in the superfluid phase. As long as it remains superfluid, it creeps up the inside wall of the cup as a thin film. It comes down on the outside, forming a drop which will fall into the liquid below. Another drop will form - and so on - until the cup is empty.

Superfluidity is a state of matter in which viscosity of a fluid vanishes, while thermal conductivity becomes infinite. These unusual effects are observed when liquids, typically of helium-4 or helium-3, overcome friction in surface interaction at a stage (known as the "lambda point", which is temperature and pressure, for helium-4) at which the liquid's viscosity becomes zero. Also known as a major facet in the study of quantum hydrodynamics, it was discovered by Pyotr Kapitsa, John F. Allen, and Don Misener in 1937 and has been described through phenomenological and microscopic theories. In the 1950s Hall and Vinen performed experiments establishing the existence of quantized vortex lines. In the 1960s, Rayfield and Reif established the existence of quantized vortex rings. Packard has observed the intersection of vortex lines with the free surface of the fluid, and Avenel and Varoquaux have studied the Josephson effect in superfluid ^{4}He.

Theories

L. D. Landau's phenomenological and semi-microscopic theory of superfluidity of ^{4}He earned him the Nobel Prize in Physics in 1962. Assuming that sound waves are the most important excitations in ^{4}He at low temperatures, he showed that ^{4}He flowing past a wall would not spontaneously create excitations if the flow velocity was less than the sound velocity. In this model, the sound velocity is the "critical velocity" above which superfluidity is destroyed.

(^{4}He has a lower flow velocity than the sound velocity, but this model is useful to illustrate the concept.) Landau also showed that the sound wave and other excitations could equilibrate with one another and flow separately from the rest of the ^{4}He called the "condensate".

From the momentum and flow velocity of the excitations he could then define a "normal fluid" density, which is zero at zero temperature and increases with temperature. At the so-called Lambda temperature, where the normal fluid density equals the total density, the ^{4}He is no longer superfluid.

To explain the early specific heat data on superfluid ^{4}He, Landau posited the existence of a type of excitation he called a "roton", but as better data became available he considered that the "roton" was the same as a high momentum version of sound.

Bijl in the 1940s, and Feynman around 1955, developed microscopic theories for the roton, which was shortly observed with inelastic neutron experiments by Palevsky.

Landau thought that vorticity entered superfluid ^{4}He by vortex sheets, but such sheets were shown to be unstable.

Lars Onsager and, later independently, Feynman showed that vorticity enters by quantized vortex lines. They also developed the idea of quantum vortex rings.

Background

Although the phenomenologies of the superfluid states of helium-4 and helium-3 are very similar, the microscopic details of the transitions are very different. Helium-4 atoms are bosons, and their superfluidity can be understood in terms of the Bose statistics that they obey. Specifically, the superfluidity of helium-4 can be regarded as a consequence of Bose-Einstein condensation in an interacting system. On the other hand, helium-3 atoms are fermions, and the superfluid transition in this system is described by a generalization of the BCS theory of superconductivity. In it, Cooper pairing takes place between atoms rather than electrons, and the attractive interaction between them is mediated by spin fluctuations rather than phonons. A unified description of superconductivity and superfluidity is possible in terms of gauge symmetry breaking.

Superfluids, such as supercooled helium-4, exhibit many unusual properties. Superfluid acts as if it were a mixture of a normal component, with all the properties associated with normal fluid, and a superfluid component. The superfluid component has zero viscosity, zero entropy, and infinite thermal conductivity. (It is thus impossible to set up a temperature gradient in a superfluid, much as it is impossible to set up a voltage difference in a superconductor.) Application of heat to a spot in superfluid helium results in a wave of heat conduction at the relatively high velocity of 20 m/s, called **second sound**.

One of the most spectacular results of these properties is known as the thermomechanical or "fountain effect". If a capillary tube is placed into a bath of superfluid helium and then heated, even by shining a light on it, the superfluid helium will flow up through the tube and out the top as a result of the Clausius-Clapeyron relation. A second unusual effect is that superfluid helium can form a layer, 30 nm thick, up the sides of any container in which it is placed.

A more fundamental property than the disappearance of viscosity becomes visible if superfluid is placed in a rotating container. Instead of rotating uniformly with the container, the rotating state consists of quantized vortices. That is, when the container is rotated at speed below the first critical velocity (related to the quantum numbers for the element in question) the liquid remains perfectly stationary. Once the first critical velocity (the speed of sound in the superfluid) is reached, the superfluid will very quickly begin spinning at the critical speed. The speed is quantized, that is, a superfluid can only spin at certain "allowed" or critical speed values. In simplified terms, if the container is rotated to a certain allowed speed, the superfluid will rotate very quickly along with the container, otherwise, if the speed is too slow, then the superfluid will not move at all. Rotation in a normal fluid like water is not quantized.

Properties

Theoretically, a normal fluid phase of non-zero entropy can coexist with a superfluidic phase with zero entropy. This leads to the strange phenomenon of a two-fluid model, in which there can be a transfer of mass without a transfer of energy: when such a fluid/superfluid system is introduced in a setup that would normally trap a fluid, the superfluid can flow out due to its zero-viscosity property, leaving the normal fluid behind. Thus, part of the fluid system's mass is transferred without any energy transfer (since the superfluid has zero entropy).

Applications

Recently in the field of chemistry, superfluid helium-4 has been successfully used in spectroscopic techniques as a quantum solvent. Referred to as Superfluid Helium Droplet Spectroscopy (SHeDS), it is of great interest in studies of gas molecules, as a single molecule solvated in a superfluid medium allows a molecule to have effective rotational freedom, allowing it to behave exactly as it would in the "gas" phase.

Superfluids are also used in high-precision devices such as gyroscopes, which allow the measurement of some theoretically predicted gravitational effects.

In 1999, one type of superfluid was used to trap light and greatly reduce its speed. In an experiment performed by Lene Hau, light was passed through a Bose-Einstein condensed gas of sodium (analogous to a superfluid) and found to be slowed to 17 m/s (61.2 km/h) from its normal speed of 299,792,458 metres per second in vacuum. This does not change the absolute value of c, nor is it completely new: any medium other than vacuum, such as water or glass, also slows down the propagation of light to c/n where n is the material's refractive index. The very slow speed of light and high refractive index observed in this particular experiment, moreover, is not a general property of all superfluids.

The Infrared Astronomical Satellite IRAS, launched in January 1983 to gather infrared data was cooled by 720 litres of superfluid helium, maintaining a temperature of 1.6 K (-271.4 °C).

21st century developments

In the early 2000s, physicists created a Fermionic condensate from pairs of ultra-cold fermionic atoms. Under certain conditions, fermion pairs form diatomic molecules and undergo Bose–Einstein condensation. At the other limit, the fermions (most notably superconducting electrons) form Cooper pairs which also exhibit superfluidity. This work with ultra-cold atomic gases has allowed scientists to study the region in between these two extremes, known as the BEC-BCS crossover.

Additionally, super*solids* may also have been discovered in 2004 by physicists at Penn State University. When helium-4 is cooled below about 200 mK under high pressures, a fraction (~1%) of the solid appears to become superfluid. By quench cooling or lengthening the annealing time, thus increasing or decreasing the defect density respectively, it was shown, via torsional oscillator experiment, that the supersolid fraction could be made to range from 20% to completely non-existent. This suggested that the supersolid nature of helium-4 is not intrinsic to helium-4 but a property of helium-4 and disorder. Some emerging theories posit that the supersolid signal observed in helium-4 was actually an observation of either a superglass state or intrinsically superfluid grain boundaries in the helium-4 crystal.

Chapter- 4

Carbon Nanotube

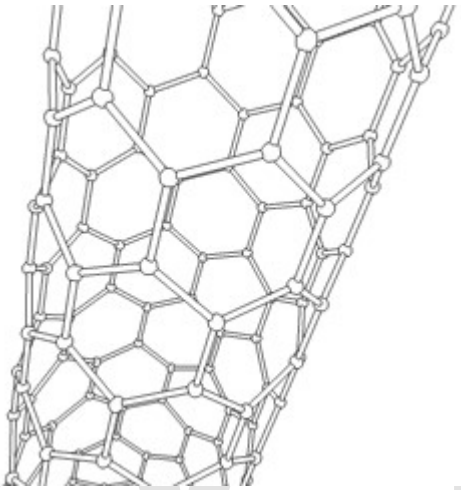

Carbon nanotubes (**CNTs**), are allotropes of carbon with a cylindrical nanostructure. Nanotubes have been constructed with length-to-diameter ratio of up to 132,000,000:1, significantly larger than any other material. These cylindrical carbon molecules have novel properties, making them potentially useful in many applications in nanotechnology, electronics, optics, and other fields of materials science, as well as potential uses in architectural fields. They may also have applications in the construction of body armor. They exhibit extraordinary strength and unique electrical properties, and are efficient thermal conductors.

Nanotubes are members of the fullerene structural family, which also includes the spherical buckyballs. The ends of a nanotube may be capped with a hemisphere of the buckyball structure. Their name is derived from their size, since the diameter of a nanotube is on the order of a few nanometers (approximately 1/50,000th of the width of a human hair), while they can be up to 18 centimeters in length (as of 2010). Nanotubes are categorized as single-walled nanotubes (SWNTs) and multi-walled nanotubes (MWNTs).

Applied quantum chemistry, specifically, orbital hybridization best describes chemical bonding in nanotubes. The chemical bonding of nanotubes is composed entirely of sp^2 bonds, similar to those of graphite. These bonds, which are stronger than the sp^3 bonds

found in alkanes, provide nanotubules with their unique strength. Moreover, nanotubes naturally align themselves into "ropes" held together by van der Waals forces.

Types of carbon nanotubes and related structures

Single-walled

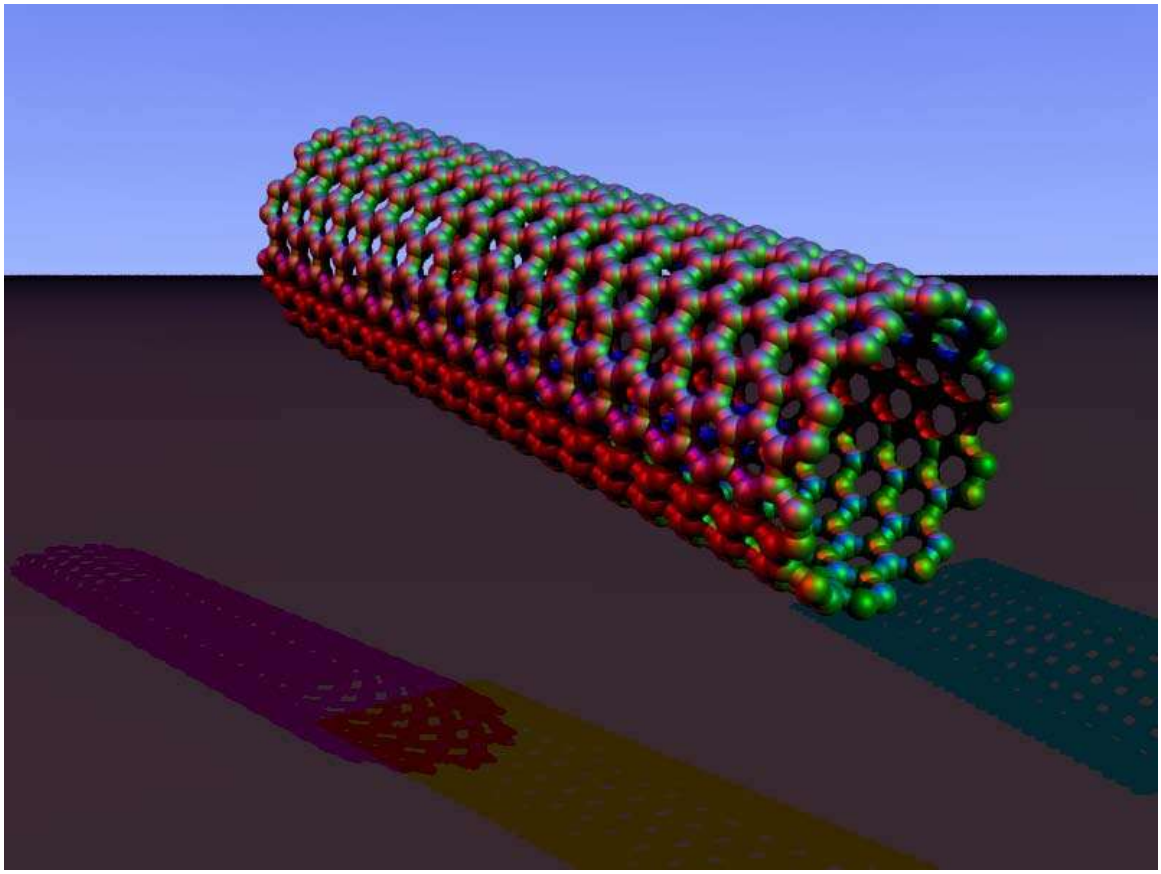

Armchair (*n*,*n*)

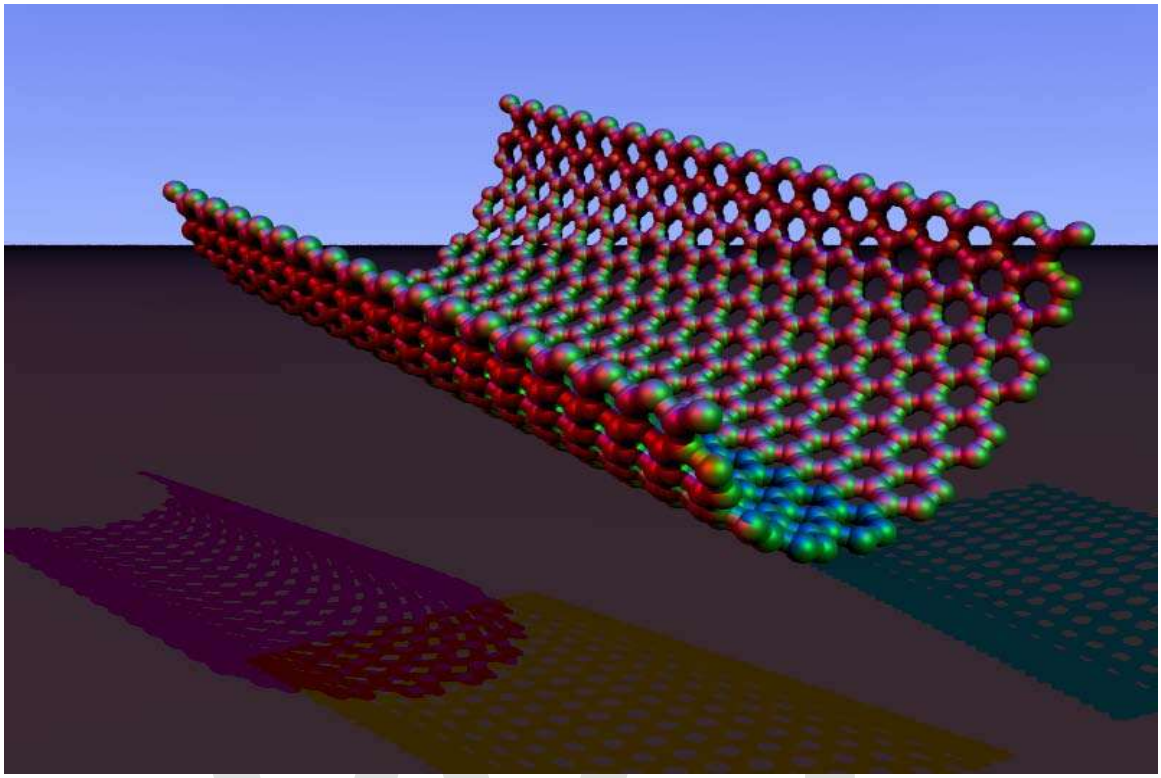

The chiral vector is bent, while the translation vector stays straight

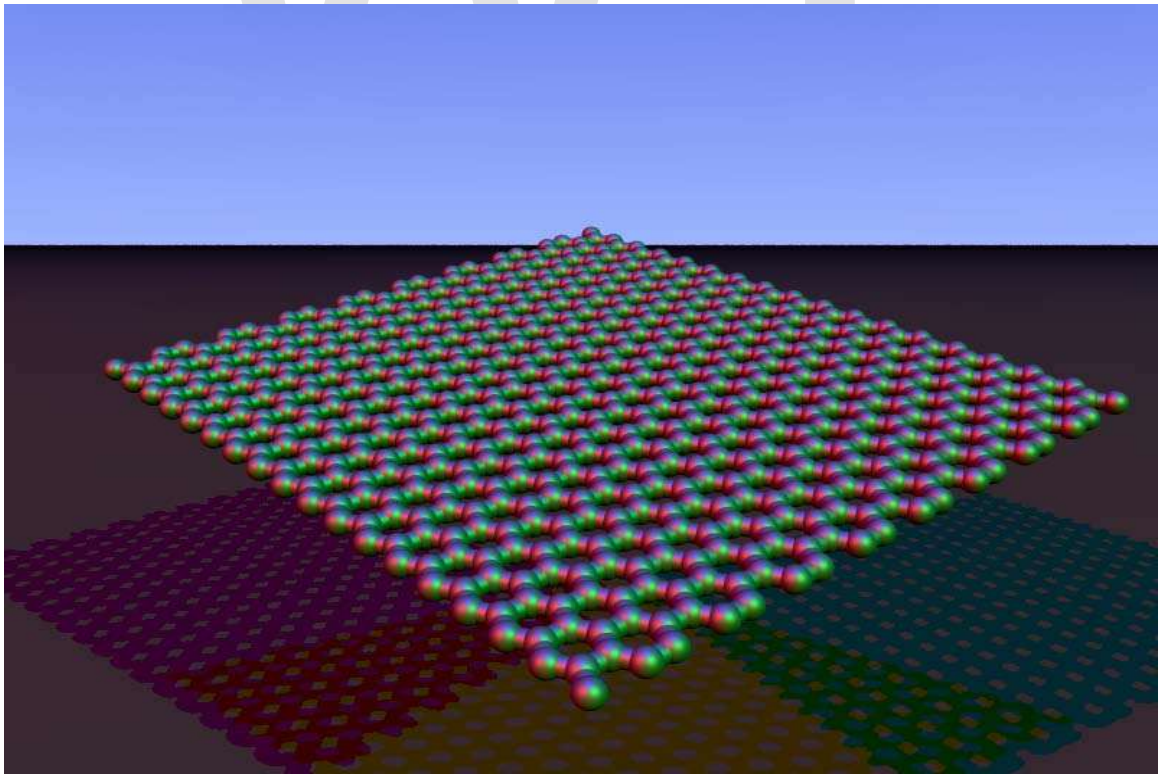

Graphene nanoribbon

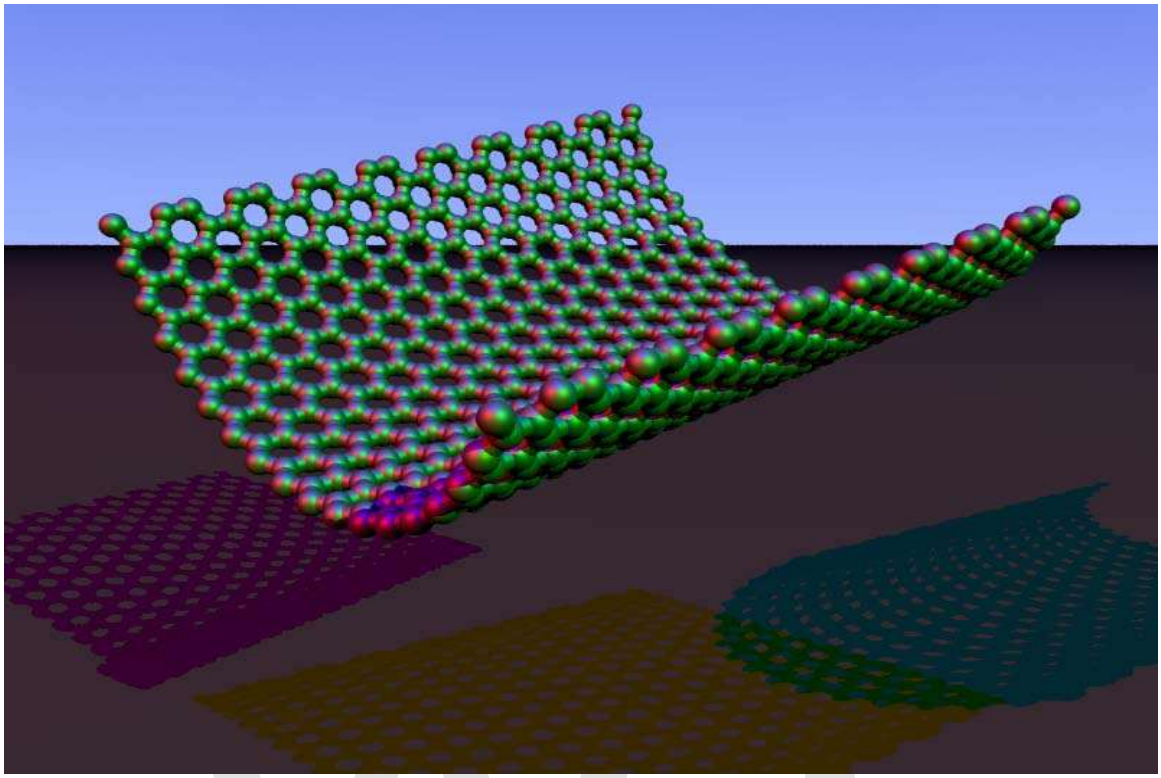

The chiral vector is bent, while the translation vector stays straight

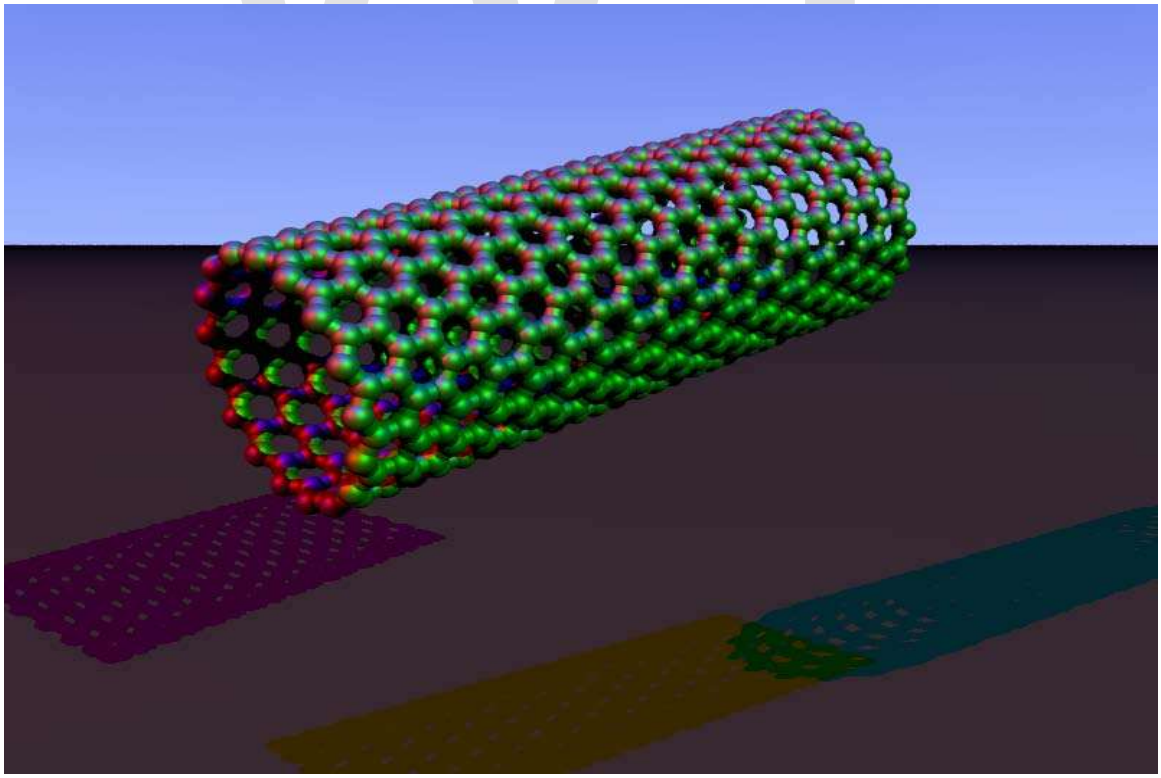

Zigzag (n,0)

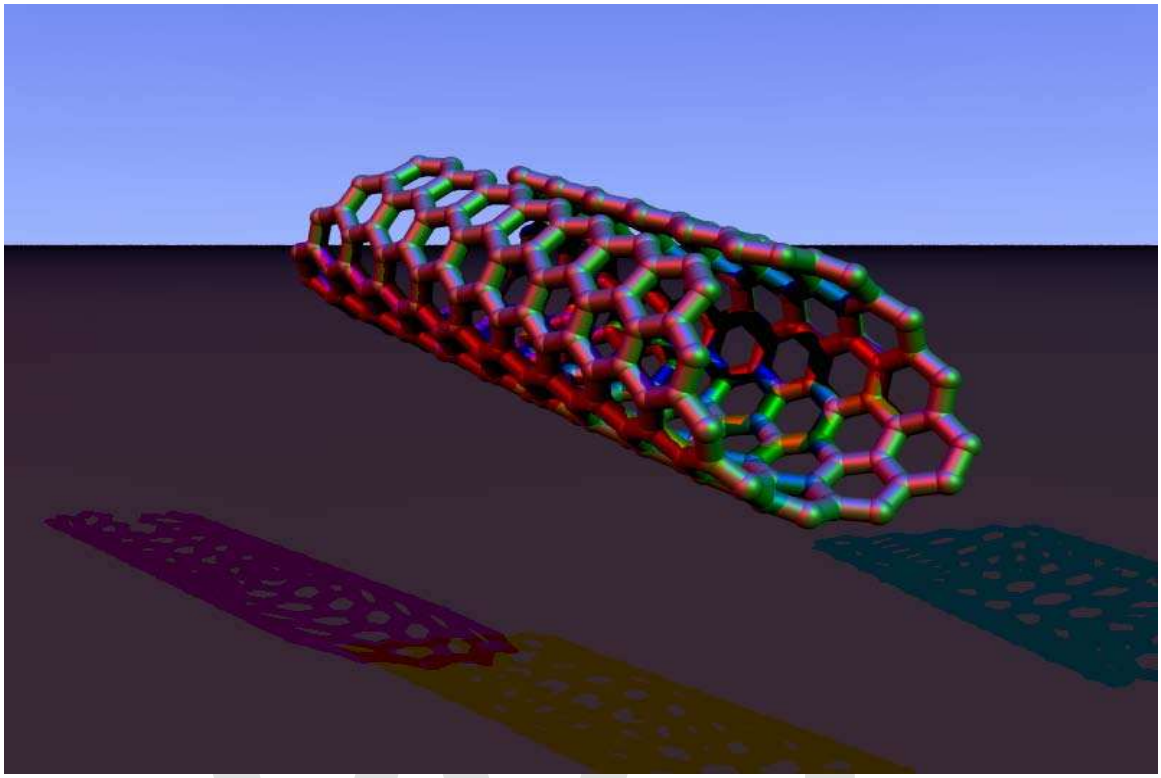

Chiral (*n*,*m*)

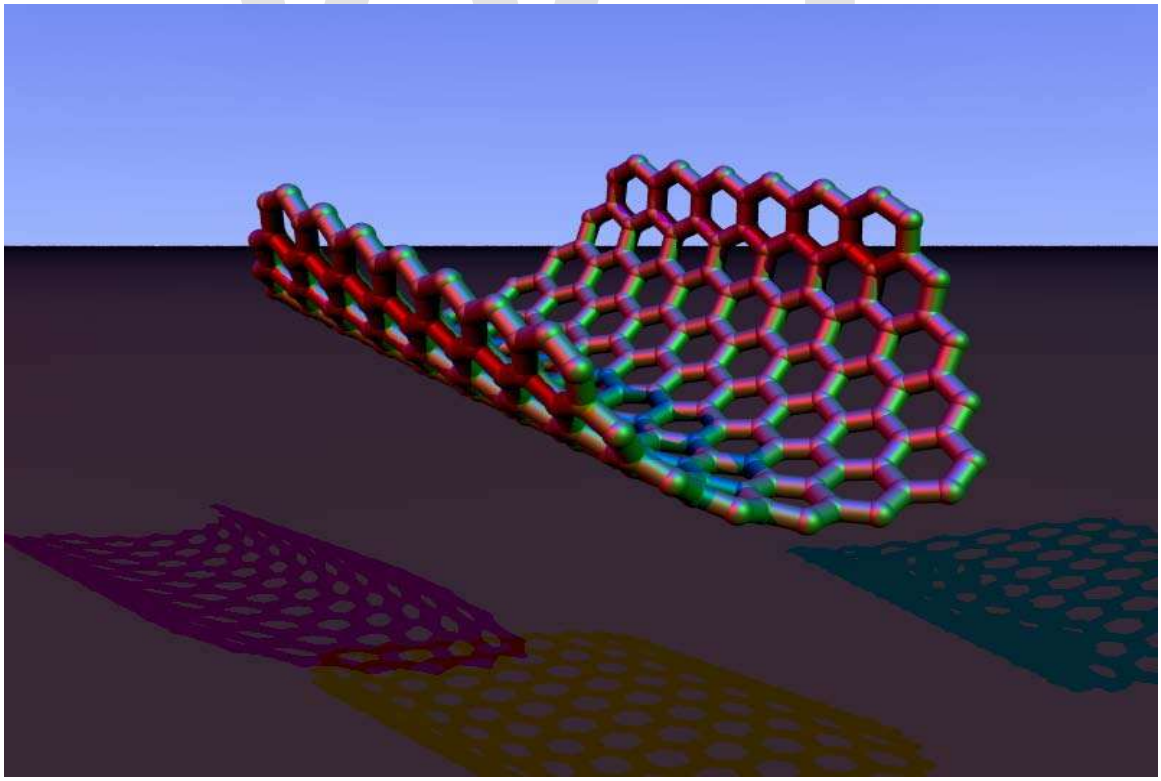

n and *m* can be counted at the end of the tube

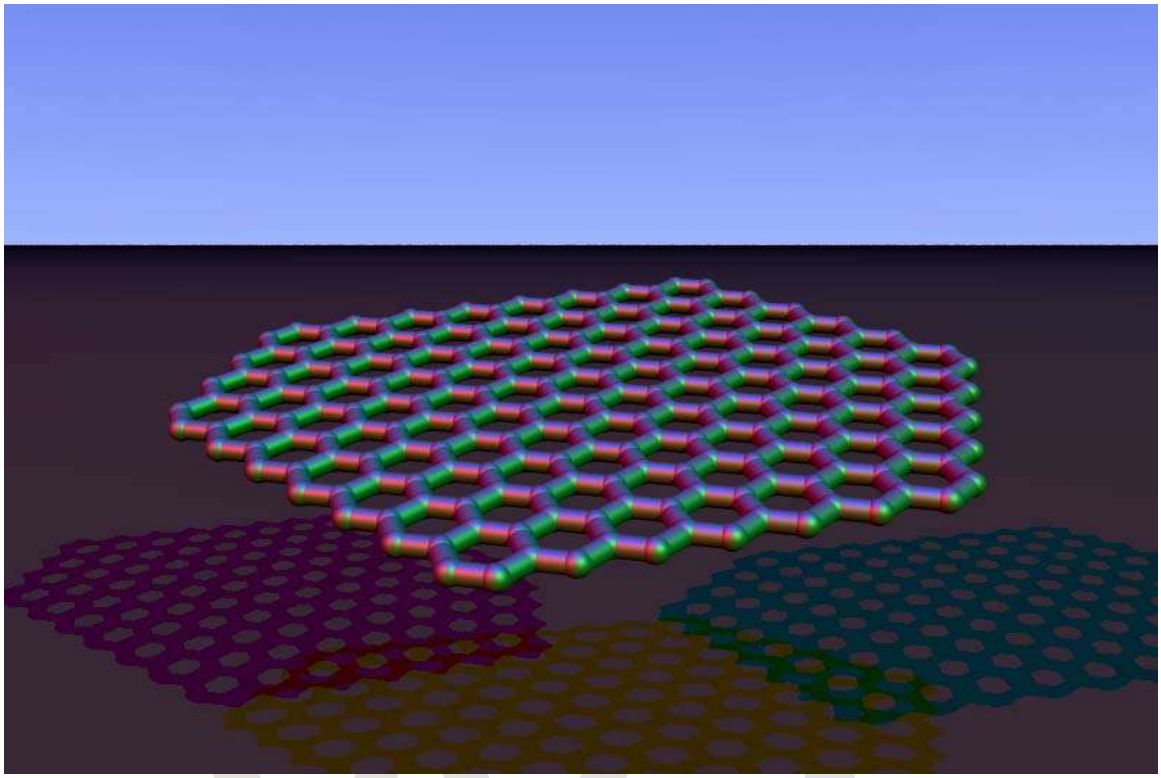

Graphene nanoribbon

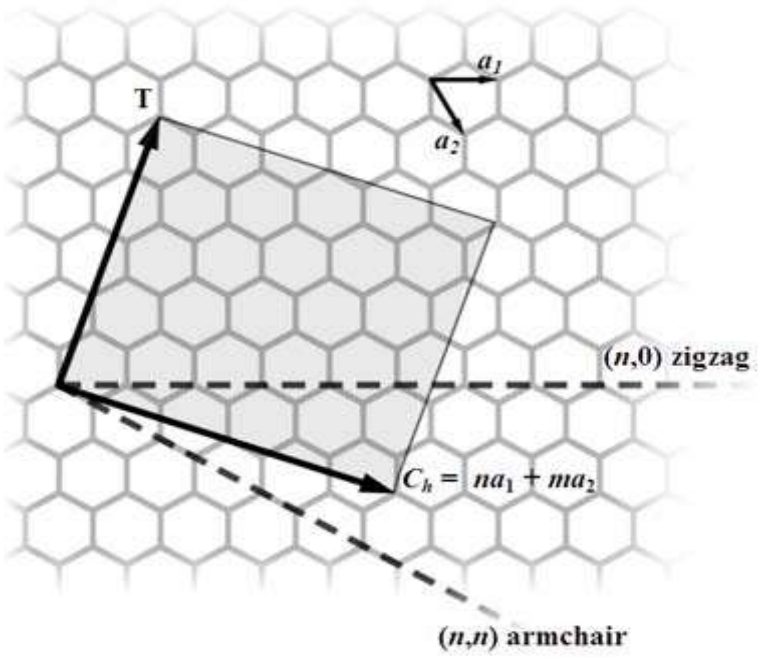

The (*n*,*m*) nanotube naming scheme can be thought of as a vector ($\mathbf{C}_h$) in an infinite graphene sheet that describes how to "roll up" the graphene sheet to make the nanotube. **T** denotes the tube axis, and $\mathbf{a}_1$ and $\mathbf{a}_2$ are the unit vectors of graphene in real space.

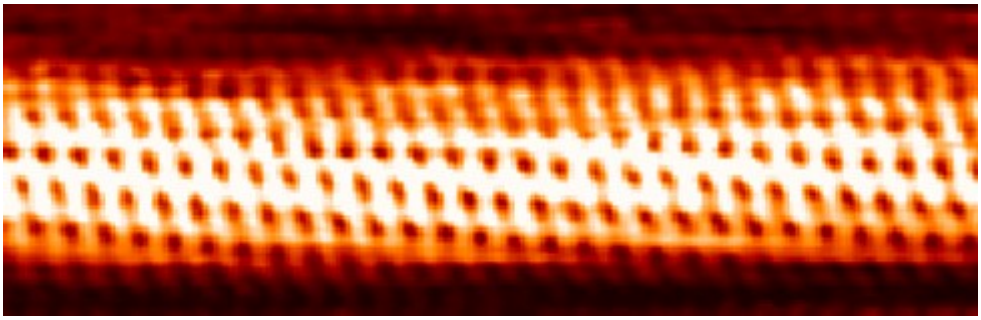

An STM image of single-walled carbon nanotube

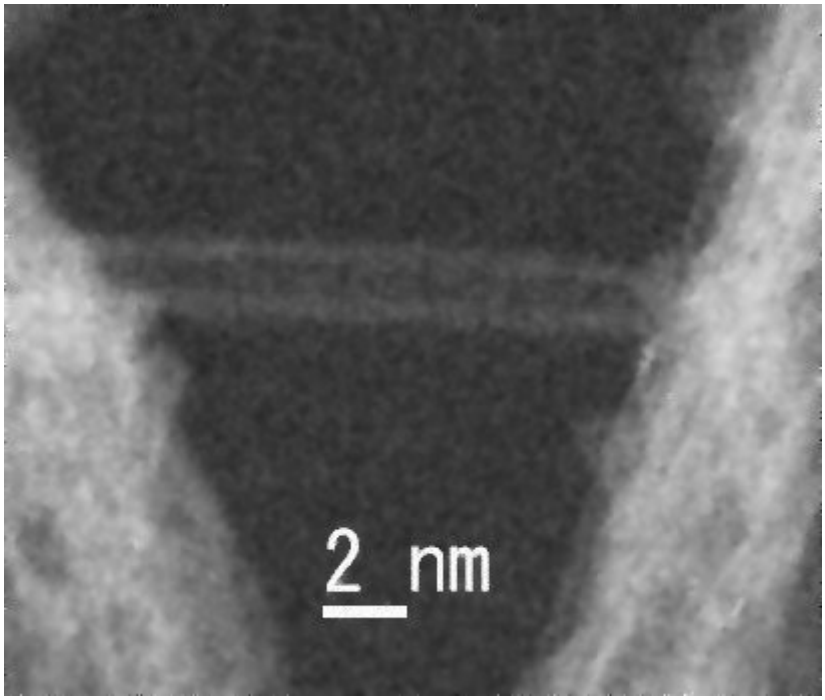

Transmission electron microscopy image showing a single-walled carbon nanotube

Most single-walled nanotubes (SWNT) have a diameter of close to 1 nanometer, with a tube length that can be many millions of times longer. The structure of a SWNT can be conceptualized by wrapping a one-atom-thick layer of graphite called graphene into a seamless cylinder. The way the graphene sheet is wrapped is represented by a pair of indices (*n*,*m*) called the chiral vector. The integers *n* and *m* denote the number of unit vectors along two directions in the honeycomb crystal lattice of graphene. If *m* = 0, the nanotubes are called "zigzag". If *n* = *m*, the nanotubes are called "armchair". Otherwise, they are called "chiral". The diameter of a nanotube can be calculated from its (n,m) indices as follows

$$d = \frac{a}{\pi}\sqrt{(n^2 + nm + m^2)}.$$

where a = 0.246 nm.

Single-walled nanotubes are an important variety of carbon nanotube because they exhibit electric properties that are not shared by the multi-walled carbon nanotube (MWNT) variants. In particular, their band gap can vary from zero to about 2 eV and their electrical conductivity can show metallic or semiconducting behavior, whereas MWNTs are zero-gap metals. Single-walled nanotubes are the most likely candidate for miniaturizing electronics beyond the micro electromechanical scale currently used in electronics. The most basic building block of these systems is the electric wire, and SWNTs can be excellent conductors. One useful application of SWNTs is in the development of the first intramolecular field effect transistors (FET). Production of the first intramolecular logic gate using SWNT FETs has recently become possible as well. To create a logic gate you must have both a p-FET and an n-FET. Because SWNTs are p-FETs when exposed to oxygen and n-FETs otherwise, it is possible to protect half of an SWNT from oxygen exposure, while exposing the other half to oxygen. This results in a single SWNT that acts as a NOT logic gate with both p and n-type FETs within the same molecule.

Single-walled nanotubes are dropping precipitously in price, from around $1500 per gram as of 2000 to retail prices of around $50 per gram of as-produced 40–60% by weight SWNTs as of March 2010.

Multi-walled

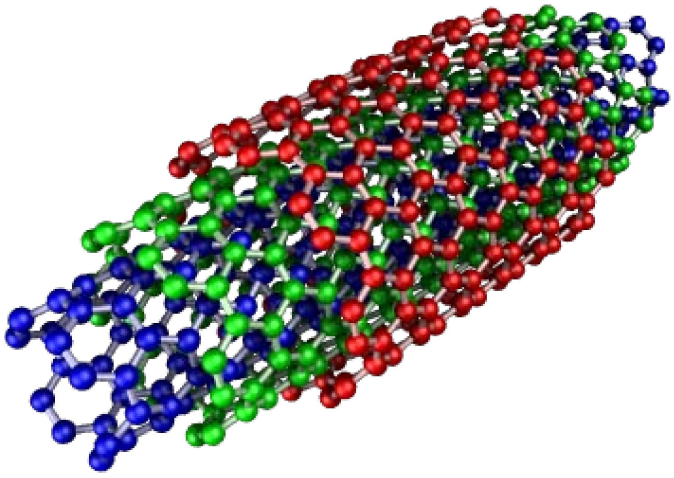

Triple-walled armchair carbon nanotube

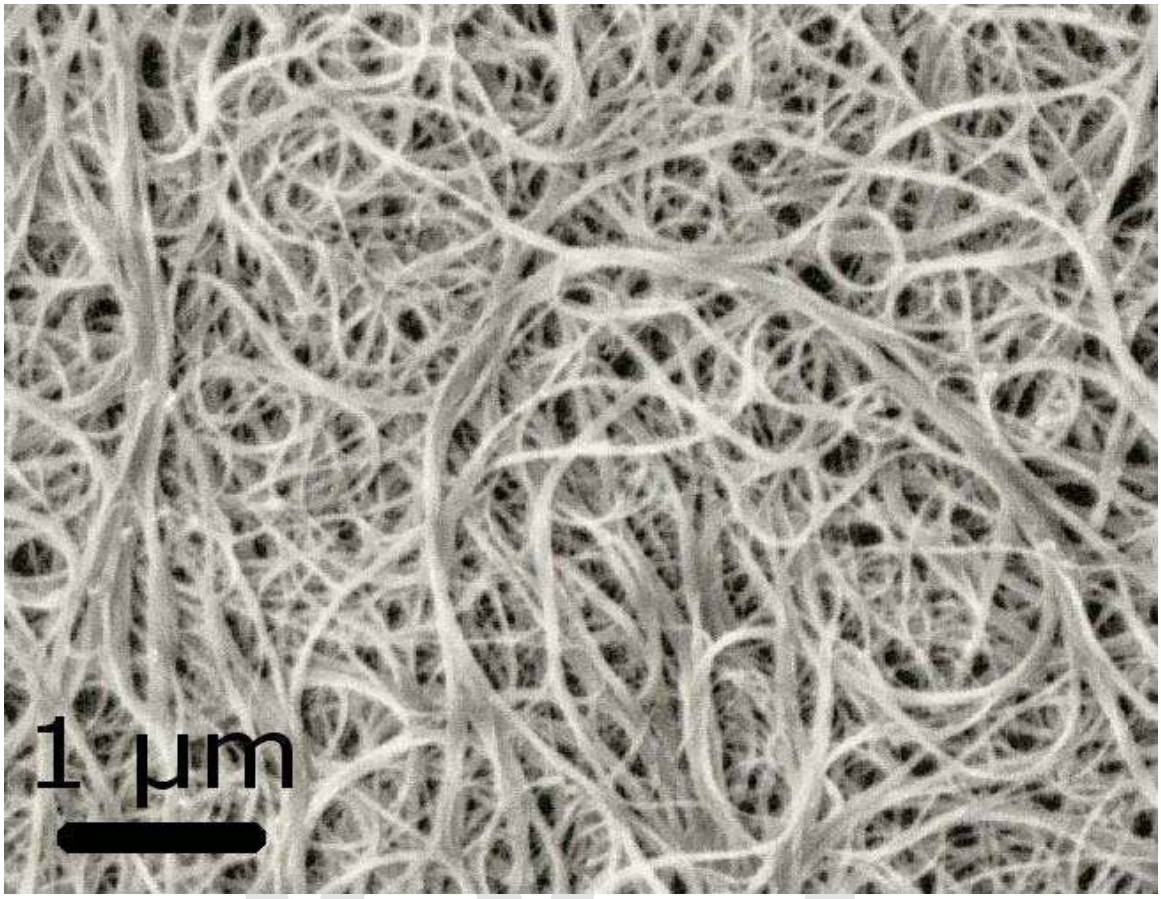

SEM image of carbon nanotubes bundles

Multi-walled nanotubes (MWNT) consist of multiple rolled layers (concentric tubes) of graphite. There are two models which can be used to describe the structures of multi-walled nanotubes. In the *Russian Doll* model, sheets of graphite are arranged in concentric cylinders, e.g. a (0,8) single-walled nanotube (SWNT) within a larger (0,17) single-walled nanotube. In the *Parchment* model, a single sheet of graphite is rolled in around itself, resembling a scroll of parchment or a rolled newspaper. The interlayer distance in multi-walled nanotubes is close to the distance between graphene layers in graphite, approximately 3.4 Å.

The special place of double-walled carbon nanotubes (DWNT) must be emphasized here because their morphology and properties are similar to SWNT but their resistance to chemicals is significantly improved. This is especially important when functionalization is required (this means grafting of chemical functions at the surface of the nanotubes) to add new properties to the CNT. In the case of SWNT, covalent functionalization will break some C=C double bonds, leaving "holes" in the structure on the nanotube and thus modifying both its mechanical and electrical properties. In the case of DWNT, only the outer wall is modified. DWNT synthesis on the gram-scale was first proposed in 2003 by the CCVD technique, from the selective reduction of oxide solutions in methane and hydrogen.

Torus

A stable nanobud structure

In theory, a nanotorus is a carbon nanotube bent into a torus (doughnut shape). Nanotori are predicted to have many unique properties, such as magnetic moments 1000 times larger than previously expected for certain specific radii. Properties such as magnetic moment, thermal stability, etc. vary widely depending on radius of the torus and radius of the tube.

Nanobud

Carbon nanobuds are a newly created material combining two previously discovered allotropes of carbon: carbon nanotubes and fullerenes. In this new material, fullerene-like "buds" are covalently bonded to the outer sidewalls of the underlying carbon nanotube. This hybrid material has useful properties of both fullerenes and carbon nanotubes. In particular, they have been found to be exceptionally good field emitters. In composite materials, the attached fullerene molecules may function as molecular anchors preventing slipping of the nanotubes, thus improving the composite's mechanical properties.

Cup stacked carbon nanotubes

Cup-stacked carbon nanotubes (CSCNTs) differ from other quasi-1D carbon structures, which normally behave as quasi-metallic conductors of electrons. CSCNTs exhibit semiconducting behaviors due to the stacking microstructure of graphene layers.

Extreme carbon nanotubes

Cycloparaphenylene

The observation of the *longest* carbon nanotubes (18.5 cm long) was reported in 2009. These nanotubes were grown on Si substrates using an improved chemical vapor deposition (CVD) method and represent electrically uniform arrays of single-walled carbon nanotubes.

The *shortest* carbon nanotube is the organic compound cycloparaphenylene which was synthesized in early 2009.

The *thinnest* carbon nanotube is armchair (2,2) CNT with a diameter of 3 Å. This nanotube was grown inside a multi-walled carbon nanotube. Assigning of carbon nanotube type was done by combination of high-resolution transmission electron microscopy (HRTEM), Raman spectroscopy and density functional theory (DFT) calculations.

The *thinnest freestanding* single-walled carbon nanotube is about 4.3 Å in diameter. Researchers suggested that it can be either (5,1) or (4,2) SWCNT, but exact type of carbon nanotube remains questionable. (3,3), (4,3) and (5,1) carbon nanotubes (all about 4 Å in diameter) were unambiguously identified using more precise aberration-corrected high-resolution transmission electron microscopy. However, they were found inside of double-walled carbon nanotubes.

Properties

Strength

Carbon nanotubes are the strongest and stiffest materials yet discovered in terms of tensile strength and elastic modulus respectively. This strength results from the covalent sp^2 bonds formed between the individual carbon atoms. In 2000, a multi-walled carbon nanotube was tested to have a tensile strength of 63 gigapascals (GPa). (This, for illustration, translates into the ability to endure tension of a weight equivalent to 6422 kg on a cable with cross-section of 1 mm^2.) Since carbon nanotubes have a low density for a solid of 1.3 to 1.4 $g \cdot cm^{-3}$, its specific strength of up to 48,000 $kN \cdot m \cdot kg^{-1}$ is the best of known materials, compared to high-carbon steel's 154 $kN \cdot m \cdot kg^{-1}$.

Under excessive tensile strain, the tubes will undergo plastic deformation, which means the deformation is permanent. This deformation begins at strains of approximately 5% and can increase the maximum strain the tubes undergo before fracture by releasing strain energy.

CNTs are not nearly as strong under compression. Because of their hollow structure and high aspect ratio, they tend to undergo buckling when placed under compressive, torsional or bending stress.

Comparison of mechanical properties

Material	Young's modulus (TPa)	Tensile strength (GPa)	Elongation at break (%)
SWNT	~1 (from 1 to 5)	13–53[E]	16
Armchair SWNT	0.94[T]	126.2[T]	23.1
Zigzag SWNT	0.94[T]	94.5[T]	15.6–17.5
Chiral SWNT	0.92		
MWNT	0.27[E]–0.8[E]–0.95[E]	11[E]–63[E]–150[E]	
Stainless steel	0.186[E]–0.214[E]	0.38[E]–1.55[E]	15–50
Kevlar–29&149	0.06[E]–0.18[E]	3.6[E]–3.8[E]	~2

[E]Experimental observation; [T]Theoretical prediction

The above discussion referred to axial properties of the nanotube, whereas simple geometrical considerations suggest that carbon nanotubes should be much softer in the radial direction than along the tube axis. Indeed, TEM observation of radial elasticity suggested that even the van der Waals forces can deform two adjacent nanotubes. Nanoindentation experiments, performed by several groups on multiwalled carbon nanotubes, indicated Young's modulus of the order of several GPa confirming that CNTs are indeed rather soft in the radial direction.

Hardness

Standard single walled carbon nanotubes can withstand a pressure up to 24GPa without deformation. They then under go a transformation to superhard phase nanotubes. Maximum pressures measured using current experimental techniques are around 55GPa. However, these new superhard phase nanotubes collapse at an even higher, albeit unknown, pressure.

The bulk modulus of superhard phase nanotubes is 462 to 546 GPa, even higher than that of diamond (420 GPa for single diamond crystal).

Kinetic

Multi-walled nanotubes are multiple concentric nanotubes precisely nested within one another. These exhibit a striking telescoping property whereby an inner nanotube core may slide, almost without friction, within its outer nanotube shell, thus creating an atomically perfect linear or rotational bearing. This is one of the first true examples of molecular nanotechnology, the precise positioning of atoms to create useful machines. Already, this property has been utilized to create the world's smallest rotational motor. Future applications such as a gigahertz mechanical oscillator are also envisaged.

Electrical

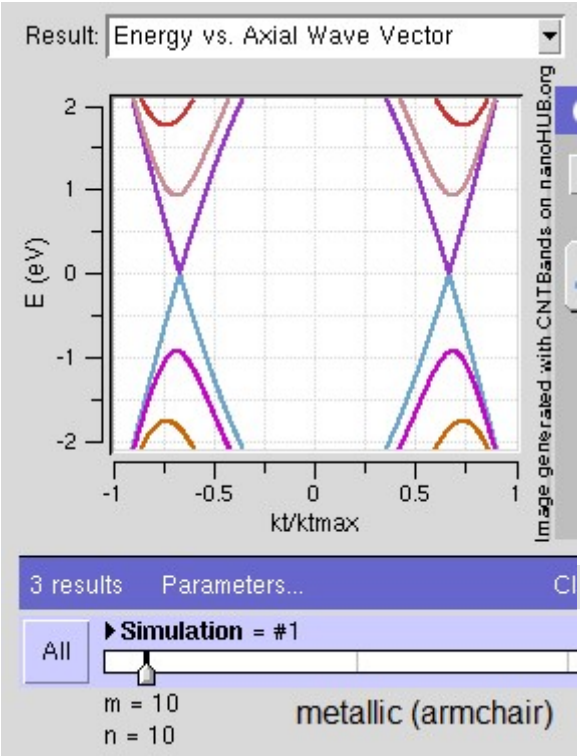

Band structures computed using tight binding approximation for (6,0) CNT (zigzag, metallic) (10,2) CNT (semiconducting) and (10,10) CNT (armchair, metallic).

Because of the symmetry and unique electronic structure of graphene, the structure of a nanotube strongly affects its electrical properties. For a given (n,m) nanotube, if $n = m$, the nanotube is metallic; if $n - m$ is a multiple of 3, then the nanotube is semiconducting with a very small band gap, otherwise the nanotube is a moderate semiconductor. Thus all armchair ($n = m$) nanotubes are metallic, and nanotubes (6,4), (9,1), etc. are semiconducting.

However, this rule has exceptions, because curvature effects in small diameter carbon nanotubes can influence strongly electrical properties. Thus, a (5,0) SWCNT that should be semiconducting in fact is metallic according to the calculations. Likewise, *vice versa*--zigzag and chiral SWCNTs with small diameters that should be metallic have finite gap (armchair nanotubes remain metallic). In theory, metallic nanotubes can carry an electric current density of 4×10^9 A/cm^2 which is more than 1,000 times greater than metals such as copper, where for copper interconnects current densities are limited by electromigration.

Multiwalled carbon nanotubes with interconnected inner shells show superconductivity with a relatively high transition temperature $T_c = 12$ K. In contrast, the T_c value is an order of magnitude lower for ropes of single-walled carbon nanotubes or for MWNTs with usual, non-interconnected shells.

Thermal

All nanotubes are expected to be very good thermal conductors along the tube, exhibiting a property known as "ballistic conduction", but good insulators laterally to the tube axis. Measurements show that a SWNT has a room-temperature thermal conductivity along its axis of about 3500 $W \cdot m^{-1} \cdot K^{-1}$; compare this to copper, a metal well-known for its good thermal conductivity, which transmits 385 $W \cdot m^{-1} \cdot K^{-1}$. A SWNT has a room-temperature thermal conductivity across its axis (in the radial direction) of about 1.52 $W \cdot m^{-1} \cdot K^{-1}$, which is about as thermally conductive as soil. The temperature stability of carbon nanotubes is estimated to be up to 2800 °C in vacuum and about 750 °C in air.

Defects

As with any material, the existence of a crystallographic defect affects the material properties. Defects can occur in the form of atomic vacancies. High levels of such defects can lower the tensile strength by up to 85%. Another form of carbon nanotube defect is the Stone Wales defect, which creates a pentagon and heptagon pair by rearrangement of the bonds. Because of the very small structure of CNTs, the tensile strength of the tube is dependent on its weakest segment in a similar manner to a chain, where the strength of the weakest link becomes the maximum strength of the chain.

Crystallographic defects also affect the tube's electrical properties. A common result is lowered conductivity through the defective region of the tube. A defect in armchair-type tubes (which can conduct electricity) can cause the surrounding region to become semiconducting, and single monoatomic vacancies induce magnetic properties.

Crystallographic defects strongly affect the tube's thermal properties. Such defects lead to phonon scattering, which in turn increases the relaxation rate of the phonons. This reduces the mean free path and reduces the thermal conductivity of nanotube structures. Phonon transport simulations indicate that substitutional defects such as nitrogen or boron will primarily lead to scattering of high-frequency optical phonons. However, larger-scale defects such as Stone Wales defects cause phonon scattering over a wide range of frequencies, leading to a greater reduction in thermal conductivity.

One-dimensional transport

Because of the nanoscale dimensions, electrons propagate only along the tube's axis and electron transport involves many quantum effects. Because of this, carbon nanotubes are frequently referred to as “one-dimensional”.

Toxicity

Determining the toxicity of carbon nanotubes has been one of the most pressing questions in nanotechnology. Unfortunately, such research has only just begun. Thus, the data are still fragmentary and subject to criticism. Preliminary results highlight the difficulties in evaluating the toxicity of this heterogeneous material. Parameters such as structure, size

distribution, surface area, surface chemistry, surface charge, and agglomeration state as well as purity of the samples, have considerable impact on the reactivity of carbon nanotubes. However, available data clearly show that, under some conditions, nanotubes can cross membrane barriers, which suggests that if raw materials reach the organs they can induce harmful effects such as inflammatory and fibrotic reactions.

A study led by Alexandra Porter from the University of Cambridge shows that CNTs can enter human cells and accumulate in the cytoplasm, causing cell death.

Results of rodent studies collectively show that regardless of the process by which CNTs were synthesized and the types and amounts of metals they contained, CNTs were capable of producing inflammation, epithelioid granulomas (microscopic nodules), fibrosis, and biochemical/toxicological changes in the lungs. Comparative toxicity studies in which mice were given equal weights of test materials showed that SWCNTs were more toxic than quartz, which is considered a serious occupational health hazard when chronically inhaled. As a control, ultrafine carbon black was shown to produce minimal lung responses.

The needle-like fiber shape of CNTs, similar to asbestos fibers, raises fears that widespread use of carbon nanotubes may lead to mesothelioma, cancer of the lining of the lungs often caused by exposure to asbestos. A recently-published pilot study supports this prediction. Scientists exposed the mesothelial lining of the body cavity of mice, as a surrogate for the mesothelial lining of the chest cavity, to long multiwalled carbon nanotubes and observed asbestos-like, length-dependent, pathogenic behavior which included inflammation and formation of lesions known as granulomas. Authors of the study conclude:

> "This is of considerable importance, because research and business communities continue to invest heavily in carbon nanotubes for a wide range of products under the assumption that they are no more hazardous than graphite. Our results suggest the need for further research and great caution before introducing such products into the market if long-term harm is to be avoided."

According to co-author Dr. Andrew Maynard:

> "This study is exactly the kind of strategic, highly focused research needed to ensure the safe and responsible development of nanotechnology. It looks at a specific nanoscale material expected to have widespread commercial applications and asks specific questions about a specific health hazard. Even though scientists have been raising concerns about the safety of long, thin carbon nanotubes for over a decade, none of the research needs in the current U.S. federal nanotechnology environment, health and safety risk research strategy address this question."

Although further research is required, results presented today clearly demonstrate that, under certain conditions, especially those involving chronic exposure, carbon nanotubes can pose a serious risk to human health.

Synthesis

Powder of carbon nanotubes

Techniques have been developed to produce nanotubes in sizeable quantities, including arc discharge, laser ablation, high pressure carbon monoxide (HiPco), and chemical vapor deposition (CVD). Most of these processes take place in vacuum or with process gases. CVD growth of CNTs can occur in vacuum or at atmospheric pressure. Large quantities of nanotubes can be synthesized by these methods; advances in catalysis and continuous growth processes are making CNTs more commercially viable.

Arc discharge

Nanotubes were observed in 1991 in the carbon soot of graphite electrodes during an arc discharge, by using a current of 100 amps, that was intended to produce fullerenes. However the first macroscopic production of carbon nanotubes was made in 1992 by two researchers at NEC's Fundamental Research Laboratory. The method used was the same as in 1991. During this process, the carbon contained in the negative electrode sublimates because of the high discharge temperatures. Because nanotubes were initially discovered using this technique, it has been the most widely-used method of nanotube synthesis.

The yield for this method is up to 30 percent by weight and it produces both single- and multi-walled nanotubes with lengths of up to 50 micrometers with few structural defects.

Laser ablation

In the laser ablation process, a pulsed laser vaporizes a graphite target in a high-temperature reactor while an inert gas is bled into the chamber. Nanotubes develop on the cooler surfaces of the reactor as the vaporized carbon condenses. A water-cooled surface may be included in the system to collect the nanotubes.

This process was developed by Dr. Richard Smalley and co-workers at Rice University, who at the time of the discovery of carbon nanotubes, were blasting metals with a laser to produce various metal molecules. When they heard of the existence of nanotubes they replaced the metals with graphite to create multi-walled carbon nanotubes. Later that year the team used a composite of graphite and metal catalyst particles (the best yield was from a cobalt and nickel mixture) to synthesize single-walled carbon nanotubes.

The laser ablation method yields around 70% and produces primarily single-walled carbon nanotubes with a controllable diameter determined by the reaction temperature. However, it is more expensive than either arc discharge or chemical vapor deposition.

Chemical vapor deposition (CVD)

Nanotubes being grown by plasma enhanced chemical vapor deposition

The catalytic vapor phase deposition of carbon was first reported in 1959, but it was not until 1993 that carbon nanotubes were formed by this process. In 2007, researchers at the University of Cincinnati (UC) developed a process to grow aligned carbon nanotube arrays of 18 mm length on a FirstNano ET3000 carbon nanotube growth system.

During CVD, a substrate is prepared with a layer of metal catalyst particles, most commonly nickel, cobalt, iron, or a combination. The metal nanoparticles can also be produced by other ways, including reduction of oxides or oxides solid solutions. The diameters of the nanotubes that are to be grown are related to the size of the metal

particles. This can be controlled by patterned (or masked) deposition of the metal, annealing, or by plasma etching of a metal layer. The substrate is heated to approximately 700°C. To initiate the growth of nanotubes, two gases are bled into the reactor: a process gas (such as ammonia, nitrogen or hydrogen) and a carbon-containing gas (such as acetylene, ethylene, ethanol or methane). Nanotubes grow at the sites of the metal catalyst; the carbon-containing gas is broken apart at the surface of the catalyst particle, and the carbon is transported to the edges of the particle, where it forms the nanotubes. This mechanism is still being studied. The catalyst particles can stay at the tips of the growing nanotube during the growth process, or remain at the nanotube base, depending on the adhesion between the catalyst particle and the substrate. Thermal catalytic decomposition of hydrocarbon has become an active area of research and can be a promising route for the bulk production of CNTs. Fluidised bed reactor is the most widely used reactor for CNT preparation. Scale-up of the reactor is the major challenge.

CVD is a common method for the commercial production of carbon nanotubes. For this purpose, the metal nanoparticles are mixed with a catalyst support such as MgO or Al_2O_3 to increase the surface area for higher yield of the catalytic reaction of the carbon feedstock with the metal particles. One issue in this synthesis route is the removal of the catalyst support via an acid treatment, which sometimes could destroy the original structure of the carbon nanotubes. However, alternative catalyst supports that are soluble in water have proven effective for nanotube growth.

If a plasma is generated by the application of a strong electric field during the growth process (plasma enhanced chemical vapor deposition*), then the nanotube growth will follow the direction of the electric field. By adjusting the geometry of the reactor it is possible to synthesize vertically aligned carbon nanotubes (i.e., perpendicular to the substrate), a morphology that has been of interest to researchers interested in the electron emission from nanotubes. Without the plasma, the resulting nanotubes are often randomly oriented. Under certain reaction conditions, even in the absence of a plasma, closely spaced nanotubes will maintain a vertical growth direction resulting in a dense array of tubes resembling a carpet or forest.

Of the various means for nanotube synthesis, CVD shows the most promise for industrial-scale deposition, because of its price/unit ratio, and because CVD is capable of growing nanotubes directly on a desired substrate, whereas the nanotubes must be collected in the other growth techniques. The growth sites are controllable by careful deposition of the catalyst. In 2007, a team from Meijo University demonstrated a high-efficiency CVD technique for growing carbon nanotubes from camphor. Researchers at Rice University, until recently led by the late Richard Smalley, have concentrated upon finding methods to produce large, pure amounts of particular types of nanotubes. Their approach grows long fibers from many small seeds cut from a single nanotube; all of the resulting fibers were found to be of the same diameter as the original nanotube and are expected to be of the same type as the original nanotube.

Super-growth CVD

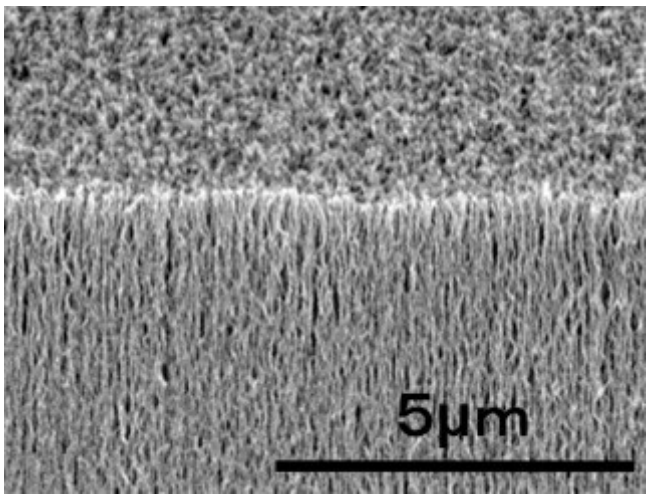

SEM photo of SWNT forests produced by super-growth

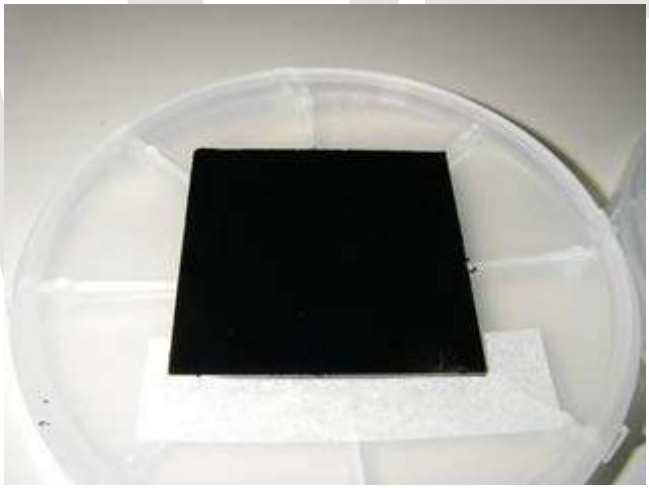

A small SWNT sample produced by super-growth

Super-growth CVD (water-assisted chemical vapour deposition) process was developed by Kenji Hata, Sumio Iijima and co-workers at AIST, Japan. In this process, the activity and lifetime of the catalyst are enhanced by addition of water into the CVD reactor. Dense millimeter-tall nanotube "forests", aligned normal to the substrate, were produced. The forests growth rate could be expressed, as

$$H(t) = \beta\tau_o(1 - e^{-t/\tau_o}).$$

In this equation, β is the initial growth rate and τ_o is the characteristic catalyst lifetime.

Their specific surface exceeds 1,000 m^2/g (capped) or 2,200 m^2/g (uncapped), surpassing the value of 400–1,000 m^2/g for HiPco samples. The synthesis efficiency is about 100

times higher than for the laser ablation method. The time required to make SWNT forests of the height of 2.5 mm by this method was 10 minutes in 2004. Those SWNT forests can be easily separated from the catalyst, yielding clean SWNT material (purity >99.98%) without further purification. For comparison, the as-grown HiPco CNTs contain about 5-35% of metal impurities; it is therefore purified through dispersion and centrifugation that damages the nanotubes. The super-growth process avoids this problem. Patterned highly organized single-walled nanotube structures were successfully fabricated using the super-growth technique.

The mass density of super-growth CNTs is about 0.037 g/cm^3. It is much lower than that of conventional CNT powders (~1.34 g/cm^3), probably because the latter contain metals and amorphous carbon.

The super-growth method is basically a variation of CVD. Therefore, it is possible to grow material containing SWNT, DWNTs and MWNTs, and to alter their ratios by tuning the growth conditions. Their ratios change by the thinness of the catalyst. Many MWNTs are included so that the diameter of the tube is wide.

The vertically aligned nanotube forests originate from a "zipping effect" when they are immersed in a solvent and dried. The zipping effect is caused by the surface tension of the solvent and the van der Waals forces between the carbon nanotubes. It aligns the nanotubes into a dense material, which can be formed in various shapes, such as sheets and bars, by applying weak compression during the process. Densification increases the Vickers hardness by about 70 times and density is 0.55 g/cm^3. The packed carbon nanotubes are more than 1 mm long and have a carbon purity of 99.9% or higher; they also retain the desirable alignment properties of the nanotubes forest.

Natural, incidental, and controlled flame environments

Fullerenes and carbon nanotubes are not necessarily products of high-tech laboratories; they are commonly formed in such mundane places as ordinary flames, produced by burning methane, ethylene, and benzene, and they have been found in soot from both indoor and outdoor air. However, these naturally occurring varieties can be highly irregular in size and quality because the environment in which they are produced is often highly uncontrolled. Thus, although they can be used in some applications, they can lack in the high degree of uniformity necessary to satisfy the many needs of both research and industry. Recent efforts have focused on producing more uniform carbon nanotubes in controlled flame environments. Such methods have promise for large-scale, low-cost nanotube synthesis, though they must compete with rapidly developing large scale CVD production.

Application related issues

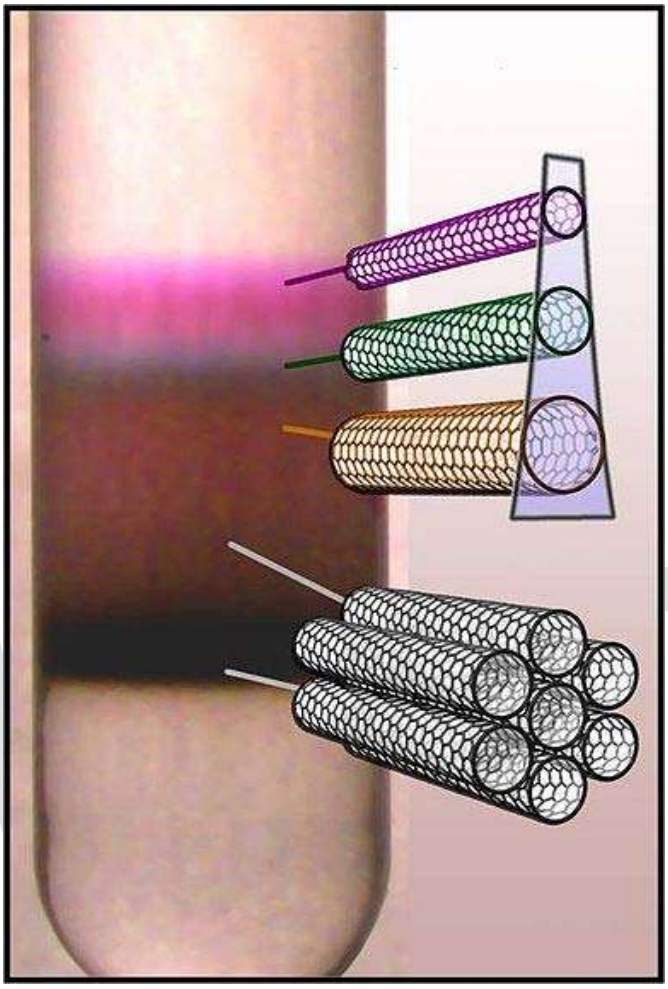

Centrifuge tube with a solution of carbon nanotubes, which were sorted by diameter using density-gradient ultracentrifugation.

Many electronic applications of carbon nanotubes crucially rely on techniques of selectively producing either semiconducting or metallic CNTs, preferably of a certain chirality. Several methods of separating semiconducting and metallic CNTs are known, but most of them are not yet suitable for large-scale technological processes. The most efficient method relies on density-gradient ultracentrifugation which separates surfactant-wrapped nanotubes by the minute difference in their density. This density difference often translates into difference in the nanotube diameter and (semi)conducting properties. Another method of separation uses a sequence of freezing, thawing, and compression of SWNTs embedded in agarose gel. This process results in a solution containing 70% metallic SWNTs and leaves a gel containing 95% semiconducting SWNTs. The diluted solutions separated by this method show various colors. Moreover, SWNTs can be separated by the column chromatography method. Yield is 95% in semiconductor type SWNT and 90% in metallic type SWNT.

In addition to separation of semiconducting and metallic SWNTs, it is possible to sort SWNTs by length, diameter, and chirality. The highest resolution length sorting, with length variation of <10%, has thus far been achieved by size exclusion chromatography (SEC) of DNA-dispersed carbon nanotubes (DNA-SWNT). SWNT diameter separation has been achieved by density-gradient ultracentrifugation (DGU) using surfactant-dispersed SWNTs and by ion-exchange chromatography (IEC) for DNA-SWNT. Purification of individual chiralities has also been demonstrated with IEC of DNA-SWNT: specific short DNA oligomers can be used to isolate individual SWNT chiralities. Thus far, 12 chiralities have been isolated at purities ranging from 70% for (8,3) and (9,5) SWNTs to 90% for (6,5), (7,5) and (10,5)SWNTs. There have been successful efforts to integrate these purified nanotubes into devices, e. g. FETs.

An alternative to separation is development of a selective growth of semiconducting or metallic CNTs. Recently, a new CVD recipe was announced which involves a combination of ethanol and methanol gases and quartz substrates resulting in horizontally aligned arrays of 95–98% semiconducting nanotubes.

Nanotubes are usually grown on nanoparticles of magnetic metal (Fe, Co), which facilitates production of electronic (spintronic) devices. In particular control of current through a field-effect transistor by magnetic field has been demonstrated in such a single-tube nanostructure.

Current applications

Current use and application of nanotubes has mostly been limited to the use of bulk nanotubes, which is a mass of rather unorganized fragments of nanotubes. Bulk nanotube materials may never achieve a tensile strength similar to that of individual tubes, but such composites may nevertheless yield strengths sufficient for many applications. Bulk carbon nanotubes have already been used as composite fibers in polymers to improve the mechanical, thermal and electrical properties of the bulk product.

- Easton-Bell Sports, Inc. have been in partnership with Zyvex Performance Materials, using CNT technology in a number of their bicycle components—including flat and riser handlebars, cranks, forks, seatposts, stems and aero bars.
- Zyvex Performance Materials has also built a 54' maritime vessel, the Piranha Unmanned Surface Vessel, as a technology demonstrator for what is possible using CNT technology. CNTs help improve the structural performance of the vessel, resulting in a lightweight 8,000 lb boat that can carry a payload of 15,000 lb over a range of 2,500 miles.
- Amroy Europe Oy manufactures Hybtonite carbon nanoepoxy resins where carbon nanotubes have been chemically bond to epoxy, resulting composite material that is 20% to 30% stronger than other composite materials. It has been used for wind turbines, marine paints and variety of sports gear such as skis, ice hockey sticks, baseball bats, hunting arrows and surfboards.

Other current applications include:

- tips for atomic force microscope probes
- in tissue engineering, carbon nanotubes can act as scaffolding for bone growth
- in the Kanzius cancer therapy, single-walled carbon nanotubes are inserted around cancerous cells, then excited with radio waves, which causes them to heat up and kill the surrounding cells

Potential applications

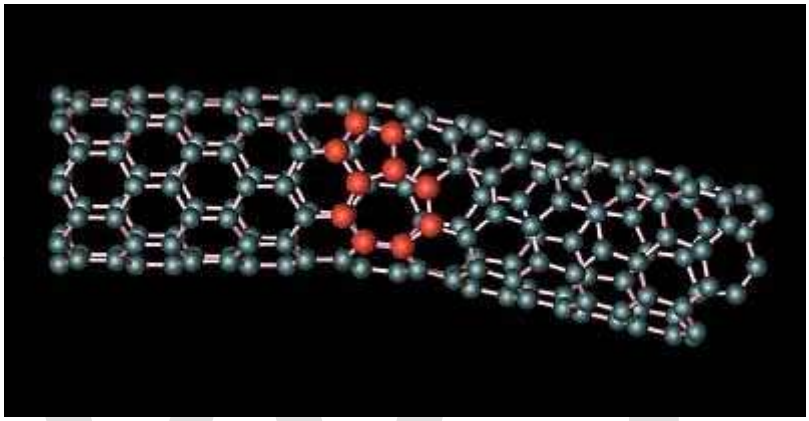

The joining of two carbon nanotubes with different electrical properties to form a diode has been proposed. L Chico et al. Phys Rev Lett 76, 971 (1996)

The strength and flexibility of carbon nanotubes makes them of potential use in controlling other nanoscale structures, which suggests they will have an important role in nanotechnology engineering. The highest tensile strength of an individual multi-walled carbon nanotube has been tested to be is 63 GPa. Carbon nanotubes were found in Damascus steel from the 17th century, possibly helping to account for the legendary strength of the swords made of it.

Structural

Because of the carbon nanotube's superior mechanical properties, many structures have been proposed ranging from everyday items like clothes and sports gear to combat jackets and space elevators. However, the space elevator will require further efforts in refining carbon nanotube technology, as the practical tensile strength of carbon nanotubes can still be greatly improved.

For perspective, outstanding breakthroughs have already been made. Pioneering work led by Ray H. Baughman at the NanoTech Institute has shown that single and multi-walled nanotubes can produce materials with toughness unmatched in the man-made and natural worlds.

Because of the high mechanical strength of carbon nanotubes, research is being made into weaving them into clothes to create stab-proof and bulletproof clothing. The nanotubes would effectively stop the bullet from penetrating the body, although the bullet's kinetic energy would likely cause broken bones and internal bleeding.

In electrical circuits

Nanotube-based transistors, also known as carbon nanotube field-effect transistors (CNFETs), have been made that operate at room temperature and that are capable of digital switching using a single electron. However, one major obstacle to realization of nanotubes has been the lack of technology for mass production. In 2001 IBM researchers demonstrated how metallic nanotubes can be destroyed, leaving semiconducting ones behind for use as transistors. Their process is called "constructive destruction" which includes the automatic destruction of defective nanotubes on the wafer. This process, however, only gives control over the electrical properties on a statistical scale.

The potential of carbon nanotubes was demonstrated in 2003 when room-temperature ballistic transistors with ohmic metal contacts and high-k gate dielectric were reported, showing 20–30x higher ON current than state-of-the-art Si MOSFETs. This presented an important advance in the field as CNT was shown to potentially outperform Si. At the time, a major challenge was ohmic metal contact formation. In this regard, palladium, which is a high work function metal was shown to exhibit Schottky barrier-free contacts to semiconducting nanotubes with diameters >1.7 nm.

The first nanotube integrated memory circuit was made in 2004. One of the main challenges has been regulating the conductivity of nanotubes. Depending on subtle surface features a nanotube may act as a plain conductor or as a semiconductor. A fully automated method has however been developed to remove non-semiconductor tubes.

Another way to make carbon nanotube transistors has been to use random networks of them. By doing so one averages all of their electrical differences and one can produce devices in large scale at the wafer level. This approach was first patented by Nanomix Inc.(date of original application June 2002). It was first published in the academic literature by the United States Naval Research Laboratory in 2003 through independent research work. This approach also enabled Nanomix to make the first transistor on a flexible and transparent substrate.

Large structures of carbon nanotubes can be used for thermal management of electronic circuits. An approximately 1 mm–thick carbon nanotube layer was used as a special material to fabricate coolers, this materials has very low density, ~20 times lower weight than a similar copper structure, while the cooling properties are similar for the two materials.

Overall, incorporating carbon nanotubes as transistors into logic-gate circuits with densities comparable to modern CMOS technology has not yet been demonstrated.

As paper batteries

A paper battery is a battery engineered to use a paper-thin sheet of cellulose (which is the major constituent of regular paper, among other things) infused with aligned carbon nanotubes. The nanotubes act as electrodes; allowing the storage devices to conduct electricity. The battery, which functions as both a lithium-ion battery and a supercapacitor, can provide a long, steady power output comparable to a conventional battery, as well as a supercapacitor's quick burst of high energy—and while a conventional battery contains a number of separate components, the paper battery integrates all of the battery components in a single structure, making it more energy efficient.

Solar cells

Solar cells developed at the New Jersey Institute of Technology use a carbon nanotube complex, formed by a mixture of carbon nanotubes and carbon buckyballs (known as fullerenes) to form snake-like structures. Buckyballs trap electrons, although they can't make electrons flow. Add sunlight to excite the polymers, and the buckyballs will grab the electrons. Nanotubes, behaving like copper wires, will then be able to make the electrons or current flow.

Ultracapacitors

MIT Laboratory for Electromagnetic and Electronic Systems uses nanotubes to improve ultracapacitors. The activated charcoal used in conventional ultracapacitors has many small hollow spaces of various size, which create together a large surface to store electric charge. But as charge is quantized into elementary charges, i.e. electrons, and each such elementary charge needs a minimum space, a significant fraction of the electrode surface is not available for storage because the hollow spaces are not compatible with the charge's requirements. With a nanotube electrode the spaces may be tailored to size—few too large or too small—and consequently the capacity should be increased considerably.

Other applications

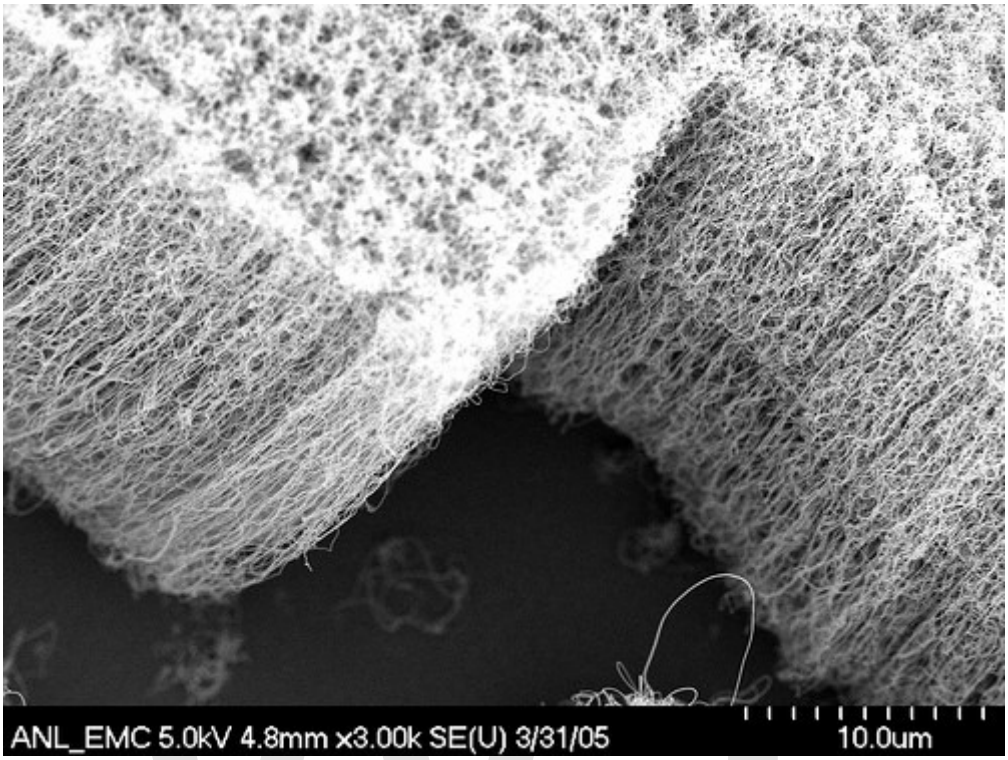

Aligned nanotubes are preferred for many applications

Carbon nanotubes have been implemented in nanoelectromechanical systems, including mechanical memory elements (NRAM being developed by Nantero Inc.) and nanoscale electric motors.

In May 2005, Nanomix Inc placed on the market a hydrogen sensor which integrated carbon nanotubes on a silicon platform. Since then Nanomix has been patenting many such sensor applications such as in the field of carbon dioxide, nitrous oxide, glucose, DNA detection, etc.

Research at University of California, Riverside has shown that carbon nanotubes are suitable scaffold materials for osteoblast proliferation and bone formation.

Eikos Inc of Franklin, Massachusetts and Unidym Inc. of Silicon Valley, California are developing transparent, electrically conductive films of carbon nanotubes to replace indium tin oxide (ITO). Carbon nanotube films are substantially more mechanically robust than ITO films, making them ideal for high-reliability touchscreens and flexible displays. Printable water-based inks of carbon nanotubes are desired to enable the production of these films to replace ITO. Nanotube films show promise for use in displays for computers, cell phones, PDAs, and ATMs.

A nanoradio, a radio receiver consisting of a single nanotube, was demonstrated in 2007. In 2008 it was shown that a sheet of nanotubes can operate as a loudspeaker if an alternating current is applied. The sound is not produced through vibration but thermoacoustically.

A flywheel made of carbon nanotubes could be spun at extremely high velocity on a floating magnetic axis in a vacuum, and potentially store energy at a density approaching that of conventional fossil fuels. Since energy can be added to and removed from flywheels very efficiently in the form of electricity, this might offer a way of storing electricity, making the electrical grid more efficient and variable power suppliers (like wind turbines) more useful in meeting energy needs. The practicality of this depends heavily upon the cost of making massive, unbroken nanotube structures, and their failure rate under stress.

Ultra-short SWNTs (US-tubes) have been used as nanoscaled capsules for delivering MRI contrast agents in vivo.

Nitrogen-doped carbon nanotubes may replace platinum catalysts used to reduce oxygen in fuel cells. A forest of vertically-aligned nanotubes can reduce oxygen in alkaline solution more effectively than platinum, which has been used in such applications since the 1960s. The nanotubes have the added benefit of not being subject to carbon monoxide poisoning.

Discovery

A 2006 editorial written by Marc Monthioux and Vladimir Kuznetsov in the journal *Carbon* described the interesting and often misstated origin of the carbon nanotube. A large percentage of academic and popular literature attributes the discovery of hollow, nanometer-size tubes composed of graphitic carbon to Sumio Iijima of NEC in 1991.

In 1952 L. V. Radushkevich and V. M. Lukyanovich published clear images of 50 nanometer diameter tubes made of carbon in the Soviet *Journal of Physical Chemistry*. This discovery was largely unnoticed, as the article was published in the Russian language, and Western scientists' access to Soviet press was limited during the Cold War. It is likely that carbon nanotubes were produced before this date, but the invention of the transmission electron microscope (TEM) allowed direct visualization of these structures.

Carbon nanotubes have been produced and observed under a variety of conditions prior to 1991. A paper by Oberlin, Endo, and Koyama published in 1976 clearly showed hollow carbon fibers with nanometer-scale diameters using a vapor-growth technique. Additionally, the authors show a TEM image of a nanotube consisting of a single wall of graphene. Later, Endo has referred to this image as a single-walled nanotube.

In 1979 John Abrahamson presented evidence of carbon nanotubes at the 14th Biennial Conference of Carbon at Pennsylvania State University. The conference paper described carbon nanotubes as carbon fibers which were produced on carbon anodes during arc

discharge. A characterization of these fibers was given as well as hypotheses for their growth in a nitrogen atmosphere at low pressures.

In 1981 a group of Soviet scientists published the results of chemical and structural characterization of carbon nanoparticles produced by a thermocatalytical disproportionation of carbon monoxide. Using TEM images and XRD patterns, the authors suggested that their “carbon multi-layer tubular crystals” were formed by rolling graphene layers into cylinders. They speculated that by rolling graphene layers into a cylinder, many different arrangements of graphene hexagonal nets are possible. They suggested two possibilities of such arrangements: circular arrangement (armchair nanotube) and a spiral, helical arrangement (chiral tube).

In 1987, Howard G. Tennett of Hyperion Catalysis was issued a U.S. patent for the production of "cylindrical discrete carbon fibrils" with a "constant diameter between about 3.5 and about 70 nanometers..., length 10^2 times the diameter, and an outer region of multiple essentially continuous layers of ordered carbon atoms and a distinct inner core...."

Iijima's discovery of multi-walled carbon nanotubes in the insoluble material of arc-burned graphite rods in 1991 and Mintmire, Dunlap, and White's independent prediction that if single-walled carbon nanotubes could be made, then they would exhibit remarkable conducting properties helped create the initial buzz that is now associated with carbon nanotubes. Nanotube research accelerated greatly following the independent discoveries by Bethune at IBM and Iijima at NEC of *single-walled* carbon nanotubes and methods to specifically produce them by adding transition-metal catalysts to the carbon in an arc discharge. The arc discharge technique was well-known to produce the famed Buckminster fullerene on a preparative scale, and these results appeared to extend the run of accidental discoveries relating to fullerenes. The original observation of fullerenes in mass spectrometry was not anticipated, and the first mass-production technique by Krätschmer and Huffman was used for several years before realizing that it produced fullerenes.

The discovery of nanotubes remains a contentious issue. Many believe that Iijima's report in 1991 is of particular importance because it brought carbon nanotubes into the awareness of the scientific community as a whole.

Chapter- 5

Metamaterial

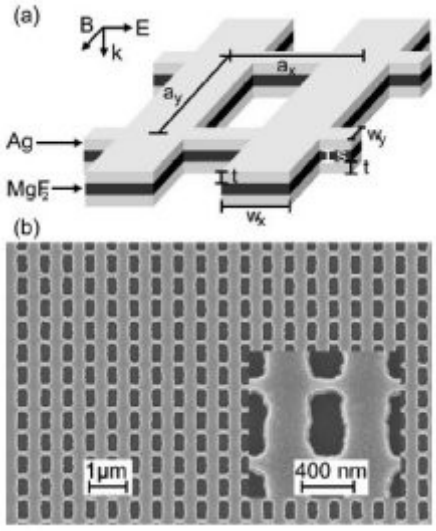

Schematic diagram for light bending metamaterial, at 1.5 micron wavelength. Courtesy of G. Dolling et al., Opt. Lett. 31, 1800 (2006).

Metamaterials are artificial materials engineered to have properties that may not be found in nature. Metamaterials usually gain their properties from structure rather than composition, using small inhomogeneities to create effective macroscopic behavior.

The primary research in metamaterials investigates materials with negative refractive index. Negative refractive index materials appear to permit the creation of superlenses which can have a spatial resolution below that of the wavelength. In other work, a form of 'invisibility' has been demonstrated at least over a narrow wave band with gradient-index materials. Although the first metamaterials were electromagnetic, acoustic and seismic metamaterials are also areas of active research.

Potential applications of metamaterials are diverse and include remote aerospace applications, sensor detection and infrastructure monitoring, smart solar power management, public safety, radomes, high-frequency battlefield communication and lenses for high-gain antennas, improving ultrasonic sensors, and even shielding structures from earthquakes.

The research in metamaterials is interdisciplinary and involves such fields as electrical engineering, electromagnetics, solid state physics, microwave and antennae engineering, optoelectronics, classic optics, material sciences, semiconductor engineering, nanoscience and others.

Electromagnetic metamaterials

Metamaterials have become a new subdiscipline within physics and electromagnetism (especially optics and photonics).

They show promise for optical and microwave applications such as new types of beam steerers, modulators, band-pass filters, lenses, microwave couplers, and antenna systems. Metamaterials consist of periodic structures.

An electromagnetic metamaterial affects electromagnetic waves by having structural features smaller than the wavelength of light. In addition, if a metamaterial is to behave as a homogeneous material accurately described by an effective refractive index, its features must be much smaller than the wavelength. To date, subwavelength structures have shown only a few questionable results at visible wavelengths.

For microwave radiation, the structures need only be on the order of few centimeters. Microwave frequency metamaterials are usually synthetic, constructed as arrays of electrically conductive elements (such as loops of wire) which have suitable inductive and capacitive characteristics. These are known as split-ring resonators.

Another structure which can exhibit subwavelength characteristics are frequency selective surfaces (FSS) known as Artificial Magnetic Conductors (AMC) or alternately called High Impedance Surfaces (HIS). These also have inductive and capacitive characteristics, which are directly related to its subwavelength structure.

Photonic crystals and frequency-selective surfaces such as diffraction gratings, dielectric mirrors, and optical coatings do have apparent similarities to subwavelength structured metamaterials. However, these are usually considered distinct from subwavelength structures, as their features are structured for the wavelength at which they function, and thus cannot be approximated as a homogeneous material.

However, novel-material structures such as photonic crystals are effective with the visible light spectrum. The middle of the visible spectrum has a wavelength of approximately 560 nm (for sunlight), the photonic crystal structures are generally half this size or smaller, that is <280 nm.

Winston E. Kock developed materials that had similar characteristics to metamaterials in the late 1940s. Materials, which exhibited reversed physical characteristics were first described theoretically by Victor Veselago in 1967. A little over 30 years later, in the year 2000, Smith et al. reported the experimental demonstration of functioning electromagnetic metamaterials by horizontally stacking, periodically, split-ring resonators

and thin wire structures. Later, a method was provided in 2002 to realize negative index metamaterials using artificial lumped-element loaded transmission lines in microstrip technology. At microwave frequencies, the first real invisibility cloak was realized in 2006. However, only a very small object was imperfectly hidden.

In 2007, one researcher stated that for metamaterial applications to be realized, several goals must be achieved. Reducing energy loss, which is a major limiting factor, keep developing three-dimensional isotropic materials instead of planar structures, then finding ways to mass produce.

Negative refractive index

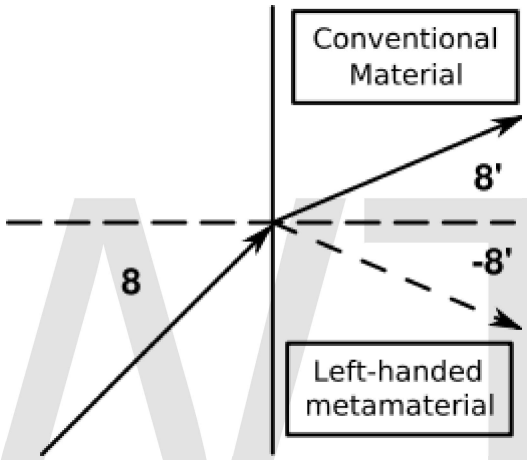

A comparison of refraction in a left-handed metamaterial to that in a normal material

The greatest potential of metamaterials is the possibility to create a structure with a negative refractive index, since this property is not found in any non-synthetic material. Almost all materials encountered in optics, such as glass or water, have positive values for both permittivity ε and permeability μ. However, many metals (such as silver and gold) have negative ε at visible wavelengths. A material having either (but not both) ε or μ negative is opaque to electromagnetic radiation.

Although the optical properties of a transparent material are fully specified by the parameters ε and μ, refractive index *n* is often used in practice, which can be determined from $n=\pm\sqrt{\epsilon\mu}$. All known non-metamaterial transparent materials possess positive ε and μ. By convention the positive square root is used for *n*.

However, some engineered metamaterials have $\varepsilon < 0$ and $\mu < 0$. Because the product εμ is positive, *n* is real. Under such circumstances, it is necessary to take the negative square root for *n*. Physicist Victor Veselago proved that such substances can transmit light.

The foregoing considerations are simplistic for actual materials, which must have complex-valued ε and μ. The real parts of both ε and μ do not have to be negative for a

passive material to display negative refraction. Metamaterials with negative n have numerous interesting properties:

- Snell's law ($n_1 \sin\theta_1 = n_2 \sin\theta_2$), but as n_2 is negative, the rays will be refracted on the *same* side of the normal on entering the material.
- The Doppler shift is reversed: that is, a light source moving toward an observer appears to reduce its frequency.
- Cherenkov radiation points the other way.
- The time-averaged Poynting vector is antiparallel to phase velocity. This means that unlike a normal right-handed material, the wave fronts are moving in the opposite direction to the flow of energy.

For plane waves propagating in electromagnetic metamaterials, the electric field, magnetic field and wave vector follow a left-hand rule. This is a reversal of direction when compared to the behavior of conventional optical materials.

Negative refractive index is an important characteristic in metamaterial design and fabrication. As reverse-refraction media, these occur when both permittivity ε and permeability μ are negative. Furthermore, this condition occurs mathematically from the vector triplet **E**, **H** and **k**.

In ordinary, everyday materials - solid, liquid, or gas; transparent or opaque; conductor or insulator - the conventional refractive index dominates. This means that permittivity and permeability are both positive resulting in an ordinary index of refraction. However, metamaterials have the capability to exhibit a state where both permittivity and permeability are negative, resulting in an extraordinary, index of negative refraction.

Different classes of electromagnetic metamaterials

With metamaterials, the lower density of materials means that components, devices, and systems can be lightweight and small, while at the same time enhancing system and component performance.

The border between synthetic materials and metamaterials is vague and novel properties are being discovered in natural materials. This is because unusual properties are also produced in conventional materials by processing them at nanoscales. However, a distinguishing feature of metamaterials is that they can be specifically fabricated to fulfill a certain objective and to fit the desired application. The size and spacing of elements in the material are created smaller than the radiated wavelength. Consequently, incident radiation cannot distinguish the collection of elements from a homogeneous material.

Electromagnetic metamaterials have also been synthesized by embedding various constituents/inclusions with novel geometric shapes and forms in some host media. In this type of composite media electromagnetic waves interact with the designed inclusions, inducing electric and magnetic moments, which in turn affect the macroscopic effective permittivity and permeability of this, bulk composite "medium".

Since electromagnetic metamaterials can be synthesized by embedding artificially fabricated inclusions (as large-scale artificial atoms) in a specified host medium, or on a host surface, this provides the designer with a large set of available, independent parameters. Those parameters define how the metamaterial is to be engineered. They include the properties of the host materials, and the size, shape, and composition of the inclusions. Other parameters to consider are the density, arrangement, and alignment of these inclusions. By defining all these parameters during fabrication, a metamaterial is engineered for specific electromagnetic responses. Additionally, these responses are not found in the individual constituents. All these design parameters can play a key role in the final outcome of the synthesis process.

Various types of composite material, both electromagnetic and other types are being studied by various research groups worldwide. Electromagnetic metamaterials are represented by different classes, as follows:

Negative index materials

In ***negative index metamaterials*** (NIM), both permittivity and permeability are negative resulting in a negative index of refraction. Hence, because of the double negative parameters these are also known as Double Negative Metmaterials or double negative materials (DNG) Other terminologies for NIMs are "left-handed media", "media with a negative refractive index", and "backward-wave media", along with other nomenclatures.

In optical materials, if both permittivity $\boldsymbol{\varepsilon}$ and permeability $\boldsymbol{\mu}$ are positive this results in propagation in the *forward* direction. If both ε and μ are negative, a *backward* wave is produced. If ε and μ have different polarities, then this does not result in wave propagation. Mathematically, quadrant II and quadrant IV have coordinates (0,0) in a coordinate plane where ε is the horizontal axis, and μ is the vertical axis.

In 1968 Victor Veselago published a paper theorizing plane wave propagation in a material whose permittivity and permeability were assumed to be simultaneously negative. In such a material, he showed that the phase velocity would be anti-parallel to the direction of poynting vector. This is contrary to wave propagation in natural occurring materials. In the years 2000 and 2001, papers were published about the first demonstrations of an artificial material that produced a negative index of refraction. By 2007, research experiments which involved negative refractive index had been conducted by many groups.

To date, materials exhibiting a negative index of refraction have only been demonstrated as artificially constructed materials.

Single negative metamaterials

In single negative (SNG) metamaterials either permittivity or permeability are negative, but not both. These are ENG metamaterials and MNG metamaterials discussed below. Interesting experiments have been conducted by combining two SNG layers into one

metamaterial. These effectively create another form of DNG metamaterial. A slab of ENG material and slab of MNG material have been joined to conduct wave reflection experiments. This resulted in the exhibition of properties such as resonances, anomalous tunneling, transparency, and zero reflection. Like Negative index materials, SNGs are innately dispersive, so their permittivity ε, permeability μ, and refraction index n, will alter with changes in frequency.

- Epsilon negative media (ENG) – permittivity ε is negative while permeability μ is positive. Many plasmas exhibit this characteristic. For example noble metals such as gold or silver will exhibit this characteristic in the infrared and visible spectrums.
- Mu-negative media (MNG) – permittivity ε is positive while permeability μ is negative. A material, which called *gyrotropic* or *gyromagnetic* exhibits this characteristic. A *gyrotropic* material is a medium that has been altered by the presence of a quasistatic magnetic field. This results in the *magneto-optic effect*. A *magneto-optic effect* is any one of a number of phenomena in which an electromagnetic wave propagates through a medium that has been altered by the presence of a quasistatic magnetic field. In such a material, left- and right-rotating elliptical polarizations can propagate at different speeds, leading to a number of important phenomena. When light is transmitted through a layer of magneto-optic material, the result is called the Faraday effect: the plane of polarization can be rotated, forming a Faraday rotator. The results of reflection from a magneto-optic material are known as the magneto-optic Kerr effect. Two gyrotropic materials with reversed rotation directions of the two principal polarizations are called optical isomers.

Electromagnetic bandgap metamaterials

Electromagnetic bandgap metamaterials control the propagation of light. This is accomplished with either a class of metamaterial known as photonic crystals (PC), or another class known as left-handed materials (LHM) Both are a novel class of artificially engineered structure, and both control and manipulate the propagation of electromagnetic waves (light). PCs can prohibit light propagation altogether. However, both the PC and LHM are capable of allowing it to propagate in certain, designed directions, and both can be designed to have electromagnetic bandgaps at desired frequencies.

In addition, metamaterials such as Photonic crystals (PC) are complex, periodic, materials and are considered to be electromagnetic bandgap material. However, a PC is at first distinguished from sub-wavelength structures, such as tunable metamaterials, because the PC derives its properties from its band gap characteristics. In addition the PC operates at the wavelength of light, compared to other metamaterials which operate as a sub-wavelength structure. Furthermore, the complex response of photonic crystals functions by diffracting light. In contrast, a permittivity and permeability defines metamaterials (also a complex response), which is derived from their sub-wavelength structure and diffraction must be eliminated.

The PC is also a material in which periodic inclusions inhibit wave propagation due to destructive interference from scattering from the periodic repetition. The photonic bandgap property of PCs makes them the EM analog of the electronic semi-conductor crystals.

Intended material fabrication of EBGs has the goal of creating periodic, dielectric structures, with low loss, and that are of high quality. An EBG affects the properties of the photon in the same way semiconductor materials affect the properties of the electron. So, it happens that the PC is the perfect bandgap material, because it allows no propagation of light. Each unit of the prescribed periodic structure acts like large scale atoms.

Electromagnetic bandgap structured (EBG) metamaterials are designed to prevent the propagation of an allocated bandwidth of frequencies, for certain arrival angles and polarizations. With *EBG materials* new methods utilize the properties of various dielectrics to achieve better performance. A variety of geometries and structures have been proposed to fabricate the special *EBG metamaterial* properties. However, in practice it is impossible to build a flawless EBG device. Factors such as advances in ideas, research, testing and development, along with the prospects of significant technological solutions, have driven the development of EBG applied science.

Commercial production of dielectric EBG devices has lagged, because commercial rewards are not readily apparent. However, start-up companies are cropping up solely focused on exploiting EBG metamaterials. These metamaterials have been manufactured for frequencies ranging from a few gigahertz (GHz) up to several terahertz (THz). In other words, applications have achieved fabricated media for radio frequency, microwave and mid-infrared regions. "It now appears that EBG concepts can, in many cases act as improved replacements for conventional solutions to electromagnetic problems." Applicable developments include an EBG transmission line, fabricated utilizing the special properties of metamaterials, EBG woodpiles made of square dielectric bars, and several different types of low gain antennas.

An EBG is a result of a metamaterial that functions in the regime where the period is an appreciable amount of the wavelength, and constructive and destructive interference occur.

Double positive medium

Double positive mediums (DPS) do occur in nature such as naturally occurring dielectrics. Permittivity and magnetic permeability are both positive and wave propagation is in the forward direction. Artificial materials have been fabricated which have DPS, ENG, and MNG properties combined.

Bi-isotropic and bianisotropic metamaterials

Categorizing metamaterials into double or single negative, or double positive, is normally done based on the assumption that the metamaterial has independent electric and magnetic responses described by the parameters ε and μ. However in many examples of electromagnetic metamaterials, the electric field causes magnetic polarization, and the magnetic field induces an electrical polarization, i.e., magnetoelectric coupling. Such media are denoted as being bi-isotropic. Media which are exhibit magneto-electric coupling, and which are also anisotropic (which is the case for many commonly used metamaterial structures), are referred to as bi-anisotropic. are denoted as bi-anisotropic.

Intrinsic to magnetoelectric coupling of *bi-isotropic media*, are four material parameters interacting with the electric (**E**) and magnetic (**H**) field strengths, and electric (**D**) and magnetic (**B**) flux densities. These four material parameters are ε, μ, κ and χ or permittivity, permeability, strength of chirality, and the Tellegen parameter respectively. Furthermore, in this type of media, the material parameters do not vary with changes along a rotated coordinate system of measurements. In this way they are also defined as invariant or scalar.

The intrinsic magnetoelectric parameters, κ and χ, affect the phase of the wave. Furthermore, the effect of the chirality parameter is to split the refractive index. In *isotropic media* this results in wave propagation only if ε and μ have the same sign. In bi-isotropic media with χ assumed to be zero, and κ a non-zero value, different results are shown. Both a backward wave and a forward wave can occur. Alternatively, two forward waves or two backward waves can occur, depending on the strength of the chirality parameter.

Chiral metamaterials

When a metamaterial is constructed from chiral elements then it is considered to be a chiral metamaterial, and the effective parameter k will be non-zero. This is a potential source of confusion as *within the metamaterial literature there are two conflicting uses of the terms left and right-handed*. The first refers to one of the two circularly polarized waves which are the propagating modes in chiral media. The second relates to the triplet of electric field, magnetic field and Poynting vector which arise in negative refractive index media, which in most cases are not chiral.

Some of the earliest structures which may be considered metamaterials date back to Jagadish Chandra Bose who in 1898 researched substances with chiral properties and to studies by Karl Ferdinand Lindman on wave interaction with metallic helices as artificial chiral media in the early twentieth century. In the 1950s and 1960s, artificial dielectrics were studied for lightweight microwave antennas. Microwave radar absorbers moved into the research arena in the 1980s and 1990s as applications for artificial chiral media.

Wave propagation properties in chiral metamaterials demonstrate that negative refraction can be realized in chiral metamaterials with a strong chirality, with neither negative ε nor

μ as a requirement. This is because the refractive index of the medium has distinct values for the left and right, given by

$$n = \sqrt{\epsilon\mu} \pm \kappa$$

It can be seen that a negative index will occur *for one polarization* if $\kappa > \sqrt{\varepsilon\mu}$. In this case, it is not necessary that either or both ε and μ be negative for *backward* wave propagation.

Split-ring resonators

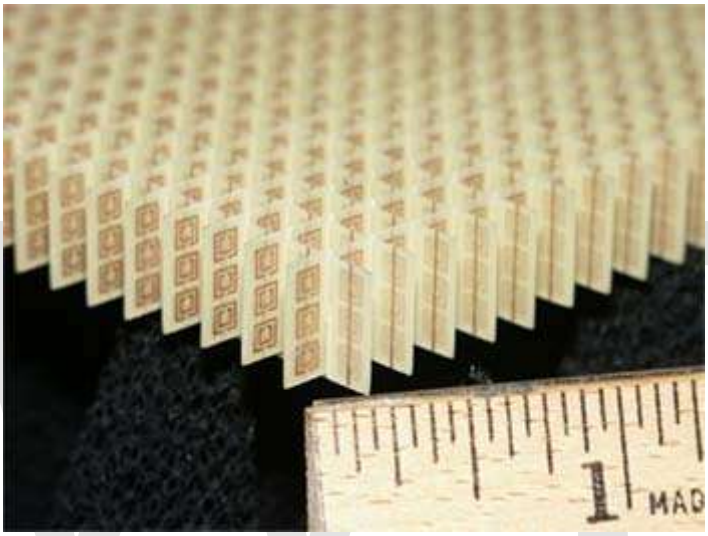

Left-handed metamaterial array configuration, which was constructed of copper split-ring resonators and wires mounted on interlocking sheets of fiberglass circuit board. The total array consists of 3 by 20×20 unit cells with overall dimensions of 10×100×100 mm.

A *split-ring resonator (SRR)* is a component part of a negative index metamaterial (NIM), also known as double negative metamaterials (DNG). They are also component parts of other types of metamaterial such as Single Negative metamaterial (SNG). SRR's are also used for research in Terahertz metamaterials, Acoustic metamaterials, and Metamaterial antennas. SRRs are a pair of concentric annular rings with splits in them at opposite ends. The rings are made of nonmagnetic metal like copper and have small gap between them.

A magnetic flux penetrating the metal rings will induce rotating currents in the rings, which produce their own flux to enhance or oppose the incident field (depending on the SRR's resonant properties). This field pattern is dipolar. Because of splits in the rings, the structure can support resonant wavelengths much larger than the diameter of the rings. This would not happen in closed rings. The small gaps between the rings produces large capacitance values which lower the resonating frequency, as the time constant is large. The dimensions of the structure are small compared to the resonant wavelength. This results in low radiative losses, and very high quality factors.

At frequencies below the resonant frequency, the real part of the magnetic permeability of the SRR becomes large (positive), and at frequencies higher than resonance it will become negative. This negative permeability can be used with the negative dielectric constant of another structure to produce negative refractive index materials.

Application of metamaterials

Below are applications of metamaterials (or types of metamaterials), which are at different stages of research. *Metamaterial antennas* (see below) are commercially available.

Terahertz metamaterials

Terahertz radiation lies at the far end of the infrared band, just before the start of the microwave band.

Terahertz metamaterials are metamaterials which interact at terahertz frequencies. For research or applications of the terahertz range for metamaterials and other materials, the frequency range is usually defined as 0.1 to 10 THz. This corresponds to the millimeter and submillimeter wavelengths between 3 mm (EHF band) and 0.03 mm (long-wavelength edge of far-infrared light).

Photonic metamaterials

A *Photonic metamaterial* is an artificially fabricated, sub-wavelength, periodic structure, designed to interact with optical frequencies (mid-infrared). The sub-wavelength period distinguishes the photonic metamaterial from photonic band gap structures.

Tunable metamaterials

A *tunable metamaterial* is a metamaterial which has the capability to arbitrarily adjust frequency changes in the refractive index at will. A tunable metamaterial encompasses the development of expanding beyond the bandwidth limitations in left-handed materials by constructing various types of metamaterials.

Frequency selective surface (FSS) based metamaterials

FSS based metamaterials have become an alternative to the fixed frequency metamaterial. The former allow for optional changes of frequencies in a single medium (metamaterial), rather than the restrictive limitations of a fixed frequency response. Other applications are also being explored.

Nonlinear metamaterials

Metamaterials may also be fabricated which include some form of nonlinear media - materials which have properties which change with the power of the incident wave. Nonlinear media are essential for nonlinear optics. However most optical materials have a relatively weak nonlinear response, meaning that their properties only change by a small amount for large changes in the intensity of the electromagnetic field. *Nonlinear metamaterials* can overcome this limitation, since the local electromagnetic fields of the inclusions in the metamaterial can be much larger than the average value of the field. In addition, exotic properties such as a negative refractive index, open up opportunities to tailor the phase matching conditions, which must be satisfied in any nonlinear optical structure.

Metamaterial absorber

A **metamaterial absorber** manipulates the loss components of the complex effective parameters, permittivity and magnetic permeability of metamaterials, to create a high electromagnetic absorber. Loss components are often noted in applications of negative refractive index (photonic metamaterials, antenna systems metamaterials) or transformation optics (metamaterial cloaking, celestial mechanics), but often not utilized in these applications.

Superlens

A *superlens* uses metamaterials to achieve resolution beyond the capabilities of ordinary lenses (beyond the diffraction limit). The diffraction limit is inherent in conventional optical devices or lenses.

Cloaking devices

Metamaterials are a basis for attempting to build a practical cloaking device. The possibility of a working invisibility cloak was demonstrated on October 19, 2006. According to the article, a team led by scientists at Pratt School of Engineering, Duke University has demonstrated the first working "invisibility cloak." The cloak deflects microwave beams so they flow around a "hidden" object inside with little distortion, making it appear almost as if nothing were there at all. Such a device typically involves surrounding the object to be cloaked with a shell which affects the passage of light near it. The associated report was published in the journal *Science*.

In related research, it may eventually be possible to use plasmons to cancel out visible light or electromagnetic radiation emanating from an object. This plasmonic cover would work by suppressing the scattering of light by resonating with illuminated light, which could render objects "nearly invisible to an observer." The plasmonic screen would have

to be tuned to the object being hidden, and would only suppress a specific wavelength—an object made invisible in red light would still be visible in multicolored daylight.

In October 2006, a US-British team of scientists created a metamaterial which rendered an object invisible to microwave radiation. As the visible spectrum is one of the bands of electromagnetic radiation, this was considered the first step toward a cloaking device for visible light, although more advanced nanoengineering techniques would be needed due to light's short wavelengths.

On 2 April 2007, Vladimir Shalaev at Purdue University announced a theoretical design for an optical cloaking device based on the 2006 British concept. The design deploys an array of tiny needles projecting from a central spoke that would render an object within the cloak invisible for red light (wavelength of 632.8 nanometers).

In 2009, at Duke University the latest advance—a series of algorithms were developed, to guide the design and fabrication of new metamaterials. David Smith of the Duke Engineering department, comparing the 2006 device, is quoted: "The difference between the original device and the latest model is like night and day. The new device can cloak a much wider spectrum of waves—nearly limitless—and will scale far more easily to infrared and visible light. The approach we used should help us expand and improve our abilities to cloak different types of waves." The article also noted that "once the algorithm was developed, the latest cloaking device was completed from conception to fabrication in nine days, compared to the four months required to create the original, and more rudimentary, device."

Metamaterial antennas

Metamaterial antennas are a class of antennas which use metamaterials to improve the performance of the antenna systems. Applying metamaterials to increase performance of antennas has garnered much interest. Demonstrations have shown that metamaterials could enhance the radiated power of an antenna. Materials which can attain negative permeability could possibly allow for properties such as an electrically small antenna size, high directivity, and tunable operational frequency.

Acoustic metamaterials

Acoustic metamaterials are artificially fabricated materials designed to control, direct, and manipulate sound in the form of sonic, infrasonic, or ultrasonic waves, as these might occur in gases, liquids, and solids. The hereditary line into acoustic metamaterials follows from theory and research in electromagnetic metamaterials. Furthermore, with acoustic metamaterials, sonic waves can now be extended to the negative refraction domain.

Control of the various forms of sound waves is mostly accomplished through the bulk modulus β, mass density ρ, and Chirality. The bulk modulus and density are analogies of the electromagnetic parameters, permittivity and permeability, in electromagnetic

metamaterials. Related to this is the mechanics of sound wave propagation in a lattice structure. Also materials have mass, and instrinsic degrees of stiffness. Together, these form a resonant system, and the mechanical (sonic) resonance may be excited by appropriate sonic frequencies (for example pulses at audio frequencies).

Seismic metamaterials

Seismic metamaterials, are metamaterials which are designed to counteract the adverse effects of seismic waves on man-made structures, which exist on or near the surface of the earth.

Other uses

Metamaterials have been proposed for designing agile antennas. Research at the National Institute of Standards and Technology has demonstrated that thin metamaterial films can greatly reduce the size of resonating circuits that generate microwaves, potentially enabling even smaller cell phones and other microwave devices. It has been theorized that metamaterials could be built to bend matter around them because of the subatomic properties of matter. Such a matter cloak could for example bend a bullet around a person rather than absorb the impact as traditional bulletproof vests do.

Theoretical models

Left-handed materials were first described theoretically by Victor Veselago in 1967.

John Pendry was the first to theorize a practical way to make a left-handed metamaterial. Left-handed in this context means a material in which the right-hand rule is not followed, allowing an electromagnetic wave to convey energy (have a group velocity) in the lode against its phase velocity. Pendry's initial idea was that metallic wires aligned along the direction of propagation could provide a metamaterial with negative permittivity ($\varepsilon < 0$). Note however that natural materials (such as ferroelectrics) were already known to exist with negative permittivity; the challenge was to construct a material which also showed negative permeability ($\mu < 0$). In 1999 Pendry demonstrated that a split ring (C shape) with its axis placed along the direction of wave propagation could provide a negative permeability. In the same paper, he showed that a periodic array of wires and ring could give rise to a negative refractive index. A related negative-permeability particle, which was also proposed by Pendry, is the Swiss roll.

The analogy is as follows: All materials are made of atoms, which are dipoles. These dipoles modify the light velocity by a factor *n* (the refractive index). The ring and wire units play the role of atomic dipoles: the wire acts as a ferroelectric atom, while the ring acts as an inductor *L* and the open section as a capacitor *C*. The ring as a whole therefore acts as an LC circuit. When the electromagnetic field passes through the ring, an induced current is created and the generated field is perpendicular to the magnetic field of the light. The magnetic resonance results in a negative permeability; the index is negative as

well. (The lens is not truly flat, since the capacitance of the structure imposes a slope for the electric induction.)

In peer reviewed journal articles, there are several (mathematical) material models which describe frequency response in DNGs. One of these is the Lorentz model. This describes electron motion in terms of a driven-damped, harmonic oscillator. When the acceleration component of the Lorentz mathematical model is small compared to the other components of the equation, then the Debye model is applied. When the restoring force component is negligible, and the coupling coefficient is generally the plasma frequency, then the Drude model is applied. There are other component distinctions that call for the use of one of these models, depending on its polarity, or purpose.

Institutional networks engaged in metamaterial research

Novel electromagnetic materials

The number of groups studying metamaterials is continuously increasing. For example, Duke University has initiated an umbrella organization researching metamaterials under the banner "*Novel Electromagnetic Materials*" and became a leading metamaterials research center. The center is a part of an international team, which also includes California Institute of Technology, Harvard University, UCLA, Max Planck Institute of Germany, and the FOM Institute of the Netherlands. In addition, there are currently six groups connected to this umbrella organization, which are conducting intense metamaterial research:

MURI

MURI stands for Multidisciplinary University Research Initiative. Tens of Universities and a few government organizations participate in the *MURI* program. A *MURI* Metamaterials web page can be found at UC Berkeley. A few other Universities which participate in MURI are UC Los Angeles, UC San Diego, Massachusetts Institute of Technology, and Imperial College in London, UK. The sponsors are Office of Naval Research (ONR) and the Defense Advanced Research Project Agency (DARPA).

The **MURI** program supports research by teams of research investigators that intersect more than one traditional science and engineering discipline in order to accelerate both research progress and transition of research results to application. Most MURI efforts involve researchers from multiple academic institutions and academic departments. Based on the proposals selected in the fiscal 2009, a total of 69 academic institutions are expected to participate in 41 research efforts.

Metamorphose

The Virtual Institute for Artificial Electromagnetic Materials and Metamaterials ”*Metamorphose VI AISBL*” is a non-profit international association whose purposes are the research, the study and the promotion of artificial electromagnetic materials and metamaterials. Some of their stated main tasks are to spread excellence in this field, in particular, by organizing scientific conferences and creating specialized journals in this field; create and manage research programs in this field; activate and manage training programs (including PhD and training programs for students and industrial partners); and transfer new technology in this field to the European Industry.

WT

Chapter- 6

Negative Index Metamaterials

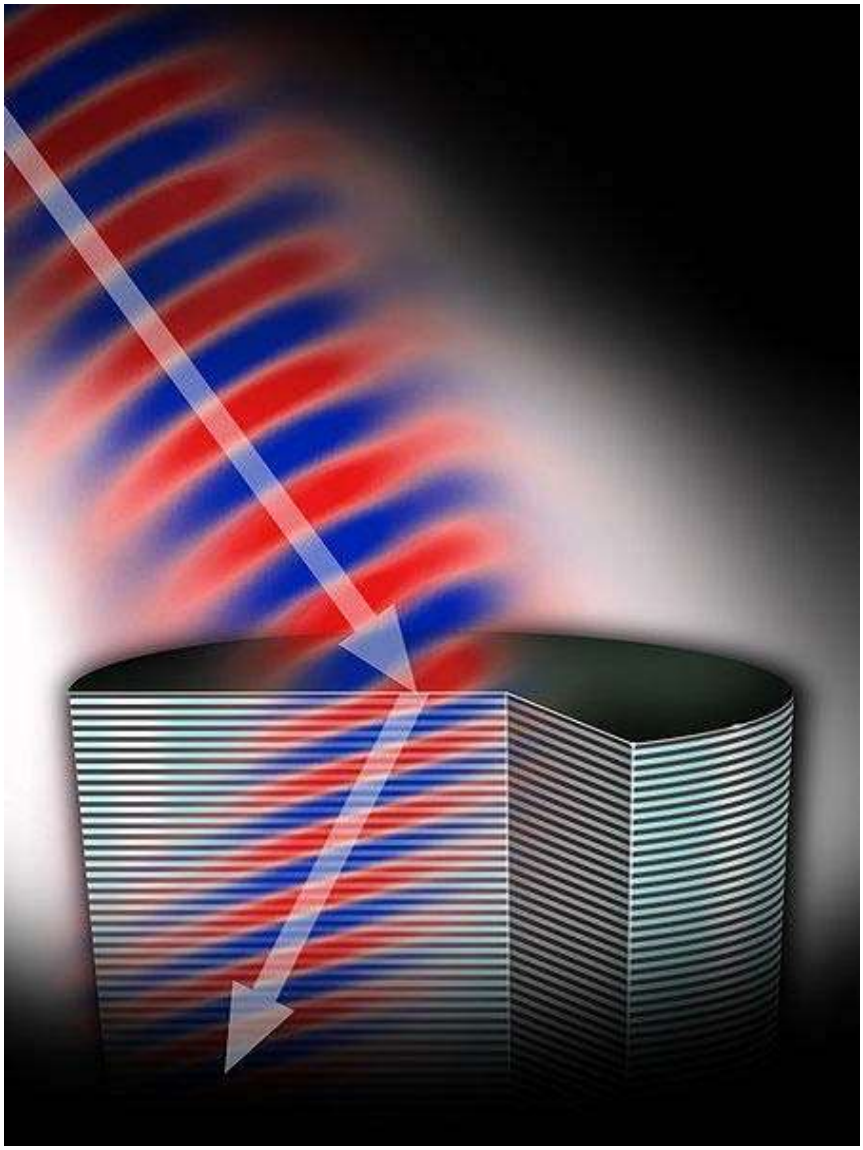

A negative index metamaterial causes light to refract, or bend, in a manner that wouldn't occur naturally

Negative index metamaterials (NIMs) are artificial structures where the refractive index has a negative value over some frequency range. This does not occur in any known natural materials, and thus is only achievable with engineered structures known as *metamaterials*. Metamaterial broadly refers to any synthetic material with unusual refractive properties, among other descriptions.

Metamaterials which exhibit a negative value for the refractive index (NIM) are often referred to by any of several names and terminologies: "left-handed media (LHM), backward wave media (BW media), media with negative refractive index, double negative (DNG) metamaterials, and other similar names.

Overview

Metamaterials are incarnations of materials first proposed by a Russian theorist Victor Veselago in 1967. Also known as left-handed or negative index materials, the proposed materials were theorized to exhibit optical properties opposite to those of glass, air, and the other right-handed—or positive index—materials of our everyday world. In particular, energy is transported in a direction opposite to that of propagating wave fronts, rather than traveling in lockstep, as is the case in positive index materials. As a result, when juxtaposed with a positive index material, negative index materials were predicted to exhibit counter intuitive properties, like bending, or refracting, light in unnatural ways. The system exploits the bulk materials properties of each component, but the collective result is an outsize response to light. The composition of the materials are ordered in geometric arrangements with dimensions that are fractions of the wavelength of interest - microwave, infrared, or terahertz frequencies.

Furthermore, metamaterials are tailor-made composites--combinations of materials designed to achieve optical properties not seen in nature. The properties stem from the unique structure of the composites, with features smaller than the wavelength of light separated by sub-wavelength distances. By fabricating such metamaterials, researchers are attempting to overcome fundamental limits tied to the wavelength of light. Light hitting a metamaterial is transformed into electromagnetic waves of a different variety, which are shorter in wavelength than the incident light. This transformation leads to unusual and counter intuitive properties that might be harnessed for practical use.

Manipulating permittivity and permeability

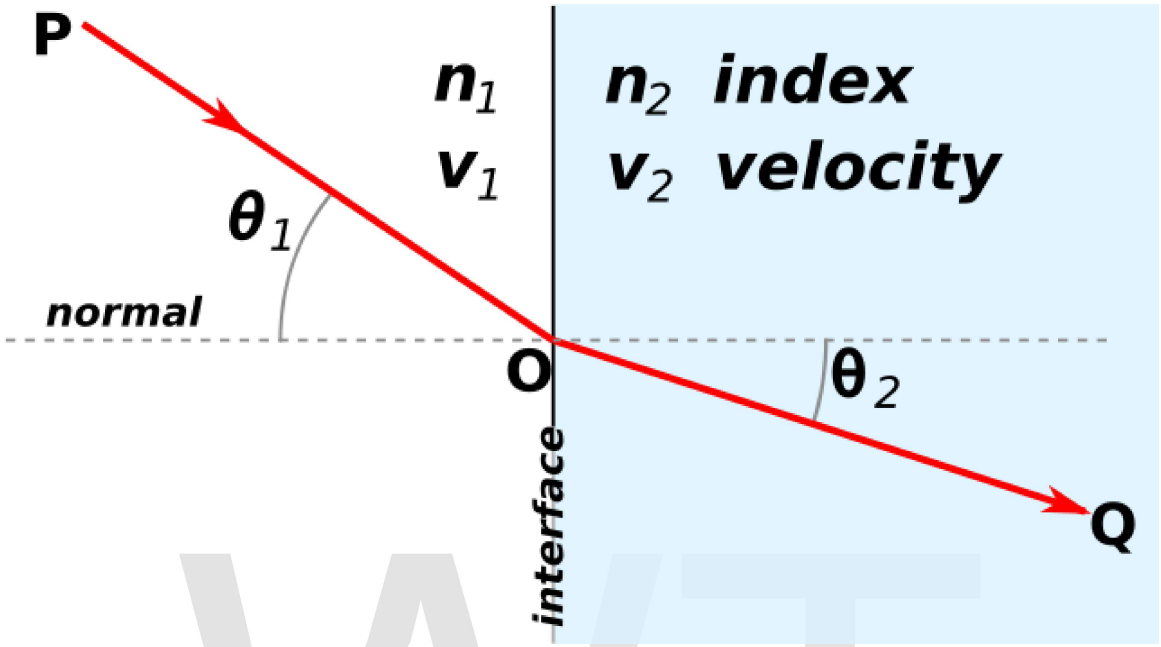

Refraction of light at the interface between two media of different refractive indices, with $n_2 > n_1$. Since the velocity is lower in the second medium ($v_2 < v_1$), the angle of refraction θ_2 is less than the angle of incidence θ_1; that is, the ray in the higher-index medium is closer to the normal.

To describe any electromagnetic properties of a given material such as an optical lens, two significant parameters should be noted. These are permittivity, **ε**, and permeability, **μ**, which could allow for accurate prediction of light waves traveling of within materials, and electromagnetic phenomena that occur at the surface between two materials (interface).

For example, refractive index is an electromagnetic phenomenon which occurs at the surface (or interface) between two materials. Snell's law states that the relationship between the radiated angle of incidence, and the resulting refracted angle of transmission, rests on the refractive index, *n*, of the two media (materials). Mathematics provides a visualization with $n=\pm\sqrt{\epsilon\mu}$. Hence, it can be seen that the behavior of the refractive index is dependent on the association of these two parameters, as well as their quantitative values. Therefore, if designed or arbitrarily modified values can be inputs for ε, and, μ then the behavior of propagating electromagnetic waves inside the material can be manipulated at will. This capability then allows for intentional determination of the refractive index.

For example, in 1967, Victor Veselago analytically determined that light will refract in the reverse direction (negatively) at the interface between a material with negative refractive index and a material exhibiting conventional refractive index. This extraordinary material was realized, on paper, with simultaneous negative values for ε,

and, μ, and could be termed a double negative material. However, in Veselago's day, a material which exhibits double negative parameters simultaneously seemed impossible, because no natural materials exist which can produce this effect. Therefore his work was ignored for three decades.

In general, the physical properties of natural materials cause limitations. Most dielectrics only have positive permittivities, $\varepsilon > 0$. Metals will exhibit negative permittivity, $\varepsilon < 0$ at optical frequencies, and plasmas exhibit negative permittivity values in certain frequency bands. Pendry et al. demonstrated that the plasma frequency can be made to occur in the lower microwave frequencies for metals, with an effective medium of metal rods that replaces the bulk metal. However, in each of these cases permeability remains always positive. At microwave frequencies, it is possible for negative μ to occur in some ferromagnetic materials. But, the inherent drawback is they are difficult to find above terahertz frequencies. In any case, a natural material that can achieve negative values for permittivity and permeability simultaneously has not been found, or discovered. Hence, all of this has led to constructing artificial composite materials known as metamaterials to achieve desired results.

Physical properties never before produced in nature

Theoretical articles were published in 1996 and 1999 which showed that artificially fabricated materials could be constructed to purposely exhibit an effective permittivity and permeability, respectively. These papers, along with Veselago's 1967 theoretical analysis of the properties of negative index materials, provided the background when finally fabricating a metamaterial with simultaneous effective permittivity and permeability, for the first time.

Essentially, a metamaterial developed to exhibit negative index behavior is typically formed from individual components. Each component responds independently to a radiated electromagnetic wave as it travels through the material. Each component has its own response to the electric and magnetic fields of the radiated source. Since these components are smaller than the radiated wavelength it is understood that a macroscopic view includes an effective value for both permittivity and permeability.

Composite material

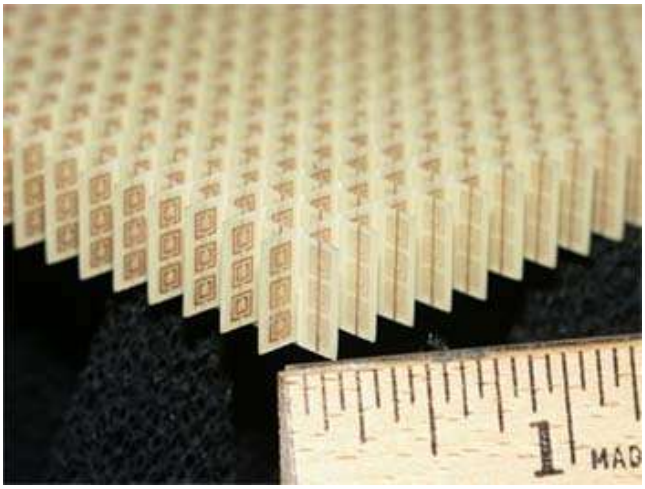

A split-ring resonator array is configured as a material that produces negative index of refraction. It was constructed of copper split-ring resonators and wires mounted on interlocking sheets of fiberglass circuit board. The total array consists of 3 by 20×20 unit cells with overall dimensions of 10×100×100 mm.

In the year 2000 a team of UCSD researchers produced a new class of composite materials which exhibited unusual physical properties that were never before produced in nature. These materials obey the laws of physics, but behave differently from normal materials. In essence these *negative index metamaterials* were noted for having the ability to reverse many of the physical properties that govern the behavior of ordinary optical materials. One of those unusual properties is the capability to reverse, for the first time, the Snell's law of refraction. Until this year 2000 demonstration by the UCSD team, the material was unavailable. Advances during the 1990s in fabrication and computation capabilities allowed these first metamaterials to be constructed. Thus, the "new" metamaterial was tested for the effects described by Victor Veselago 30 years earlier, but only at first in the microwave frequency domain. Reversal of phase velocity was established during this first test. Studies of this experiment, which followed shortly thereafter, announced that other effects had occurred.

To date (March 2010) these materials have only been commonly demonstrated at wavelengths longer those in the visible spectrum. In addition, NIMs are fabricated from opaque materials, and usually made of non-magnetic constituents. However, as an illustration – if these materials could be demonstrated at visible frequencies, and a flashlight is shone on a NIM slab, the material should focus the light at a point on the other side. This is not possible with a sheet of ordinary opaque material.

When first demonstrated this composite material (NIM) was limited to transmitting microwave radiation at frequencies of 4 to 7 gigahertz. This is approximated to be the range of operating frequencies between household microwave ovens(2.45 GHz) and military radars (10 GHz). At demonstrated frequencies, pulses of electromagnetic

radiation moving through the material in one direction are composed of constituent waves moving in the opposite direction.

The metamaterial was constructed as a periodic array of copper conducting elements. The design was such that the cells, and the lattice spacing between the cells, were much smaller than the radiated electromagnetic wavelength. Hence, it behaves as an effective medium. The material has become notable because its range of (effective) permittivity ε_{eff} and permeability μ_{eff} values have exceeded those found in any ordinary material. Furthermore, the characteristic of negative (effective) permeability evinced by this medium is particularly notable, because it has *not* been found in ordinary materials. In addition, the negative values for the magnetic component is directly related to its left-handed nomenclature, and properties (discussed in a section below). The split-ring resonator (SRR), based on the prior 1999 theoretical article, is the tool employed to achieve negative permeability. This first composite *metamaterial* is then composed of split-ring resonators and electrical conducting posts.

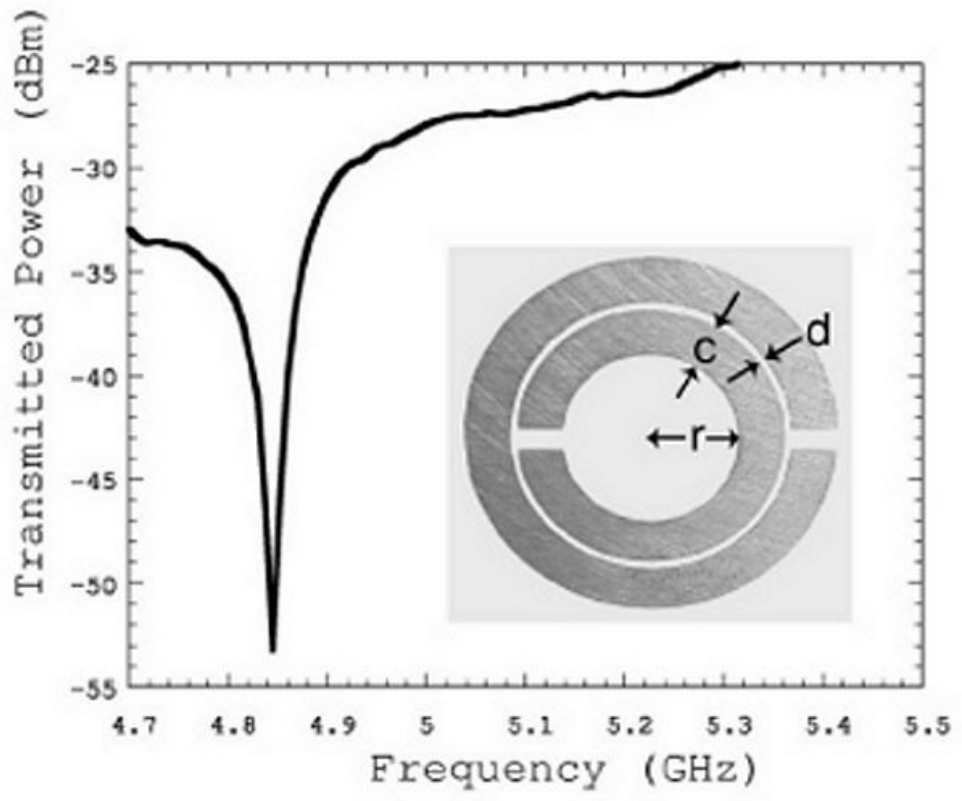

A single copper split-ring resonator (SRR) and the mapped resonance curve to the left. The dimensions of the SRR are: c = 0.8 mm, d = 0.2 mm, and r = 1.5 mm. Quality factor at around 600. The SRR has its resonance at about 4.845 GHz.

With antiferromagnets and certain types of insulating ferromagnets, effective negative magnetic permeability is achievable when polariton resonance exists. However, to achieve a negative index of refraction, permittivity with negative values must occur within the same frequency range. The artificially fabricated split-ring resonator is a design that accomplishes this, along with the promise of dampening high losses. With this first introduction of the metamaterial, it appears that the losses incurred were smaller than antiferromagnetic, or ferromagnetic materials.

Simultaneous negative permittivity and permeability

Negative permittivity $\varepsilon_{eff} < 0$ had already been discovered and realized in metals for frequencies all the way up to the plasma frequency, before the first metamaterial. There are two requirements to achieve a negative value for refraction. First, is to fabricate a material which can produce negative permeability $\mu_{eff} < 0$. Second, negative values for both permittivity and permeability must occur simultaneously over a common range of frequencies.

Therefore, for the first metamaterial, the nuts and bolts are one split-ring resonator electromagnetically combined with one (electric) conducting post. These are designed to resonate at designated frequencies to achieve the desired values. Looking at the make-up of the split ring, the associated magnetic field pattern from the SRR is dipolar. This dipolar behavior is notable because this means it mimics nature's atom, but on a much larger scale, such as in this case at 2.5 millimeters. Atoms exist on the scale of picometers.

The splits in the rings create a dynamic where the SRR unit cell can be made resonant at radiated wavelengths *much larger* than the diameter of the rings. If the rings were closed, a half wavelength boundary would be electromagnetically imposed as a requirement for resonance.

The split in the second ring is oriented opposite the split in the first ring. It is there to generate a large capacitance, which occurs in the small gap. This capacitance substantially decreases the resonant frequency while concentrating the electric field. The individual SRR depicted on the right had a resonant frequency of 4.845 GHz, and the resonance curve, inset in the graph, is also shown. The radiative losses from absorption and reflection are noted to be small, because the unit dimensions are much smaller than the free space, radiated wavelength.

When these units or cells, are combined into a periodic arrangement the magnetic coupling between the resonators is strengthened, and a *strong magnetic coupling occurs*. Properties unique in comparison to ordinary or conventional materials begin to emerge. For one thing, this periodic strong coupling creates a material which now has an effective magnetic permeability μ_{eff} in response to the radiated-incident magnetic field.

One fundamental limitation was demonstrated theoretically and is unavoidable in practice. Dispersion with frequency is a necessary but not sufficient condition for a negative index. As all materials are dispersive to some degree, this is not truly a problem.

Composite material passband

Graphing the general dispersion curve, a region of propagation occurs from zero up to a lower band edge, followed by a gap, and then an upper passband. The presence of a 400 MHz gap between 4.2 GHz and 4.6 GHz implies a band of frequencies where $\mu_{eff} < 0$ occurs.

Furthermore, when wires are added symmetrically between the split rings, a passband occurs within the previously forbidden band of the split ring dispersion curves. That this passband occurs within a previously forbidden region indicates that the negative ε_{eff} for this region has combined with the negative μ_{eff} to allow propagation. This fit with theoretical predictions. Mathematically, the dispersion relation leads to a band with negative group velocity everywhere, and a bandwidth that is independent of the plasma frequency, within the stated conditions.

Mathematical modeling and experiment have both shown that periodically arrayed conducting elements (non-magnetic by nature) respond predominately to the magnetic component of incident electromagnetic fields. The result is an effective medium and negative μ_{eff} over a band of frequencies. The permeability was verified to be the region of the forbidden band, where the gap in propagation occurred - from a finite section of material. This was combined with a negative permittivity material, $\varepsilon_{eff} < 0$, to form a "left-handed" medium, which formed a propagation band with negative group velocity where previously there was only attenuation. This validated predictions. In addition, a later work determined that this first metamaterial had a range of frequencies over which the refractive index was predicted to be negative for one direction of propagation. Other predicted electrodynamic effects were to be investigated in other research.

Describing a left-handed material

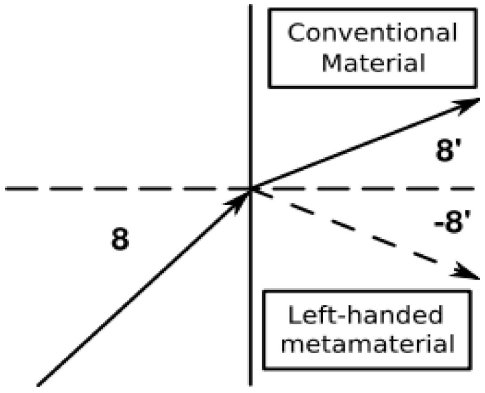

A comparison of refraction in a negative index metamaterial to that in a conventional material having the same, but positive refractive index. The incident beam 8 enters from air and refracts in a normal (8') or metamaterial (-8').

From the conclusions in the above section a left-handed material (LHM) can be defined. It is a material which exhibits simultaneous negative values for permittivity, ε, and permeability, μ, in an overlapping frequency region. Since the values are derived from the effects of the composite medium system as a whole, these are defined as effective permittivity, ε_{eff}, and effective permeability, μ_{eff}. Real values are then derived to denote the value of negative index of refraction, and wave vectors. This means that in practice losses will occur for a given medium used to transmit electromagnetic radiation such as microwave, or infrared frequencies, or visible light - for example. In this instance, real values describe either the amplitude or the intensity of a transmitted wave relative to an incident wave, while ignoring the negligible loss values.

Isotropic, negative index in two dimensions

In sections above, the first fabricated metamaterial was constructed with resonating elements, which exhibited one direction of incidence and polarization. In other words, this structure exhibited left-handed propagation in one dimension. This was discussed in relation to Veselago's seminal work 33 years earlier (1967). He predicted that intrinsic to a material which manifests negative values of effective permittivity and permeability, are several types of reversed physics phenomena. Hence, there was then a critical need for a higher dimensional LHMs to confirm Veselago's theory, as expected. The confirmation would include reversal of Snell's law (index of refraction), along with other reversed phenomena.

In the beginning of 2001 the existence of a higher dimensional structure was reported. It was two dimensional and demonstrated by both experiment and numerical confirmation. It was an LHM, a composite constructed of wire strips mounted behind the split-ring resonators (SRRs) in a periodic configuration. It was created for the express purpose of being suitable for further experiments to produce the Veselago predicted effects.

Experimental verification of a negative index of refraction

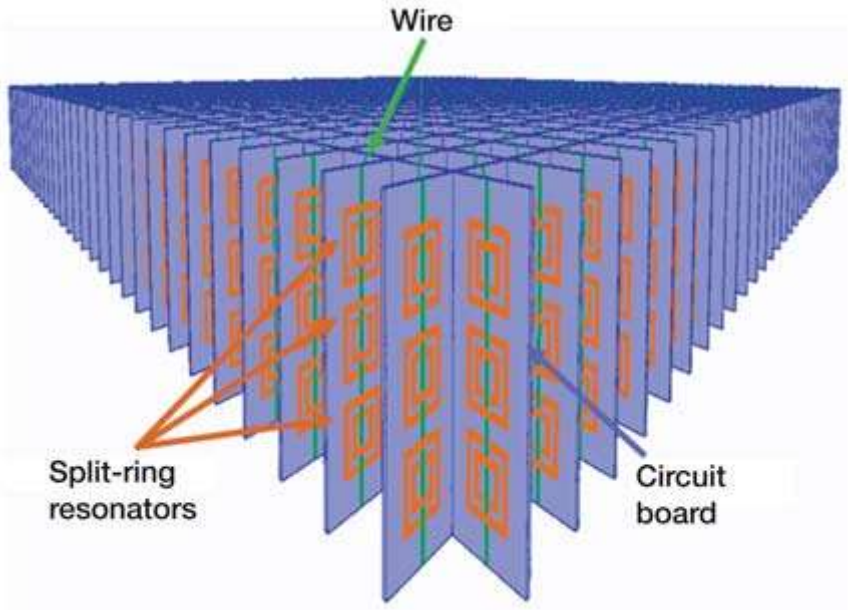

Split-ring resonator consisting of an inner square with a split on one side embedded in an outer square with a split on the other side. Split-ring resonators are on the front and right surfaces of the square grid, and single vertical wires are on the back and left surfaces.

According to Snell's law, when refraction of light is measured or observed for ordinary materials surrounded by air, the value is always greater than one, $n > 1$. A refracted ray entering a material from air will be bent towards, but never end up on the same side as the normal. In addition, the science and practice of optical lensing and imaging is based on the knowledge that any material with a refractive index different from its environment will alter the direction of incoming rays which do not arrive in a straight line in relation to the interface (of the material surface and air). Also, lenses have been designed focus and steer the various spectra of light (EM radiation) in frequency ranges from radio to the visible spectra. Furthermore, all known natural occurring materials demonstrate refractive indices that are positive. However, a theoretical work in 1967 showed that a refractive index with negative values is possible and that this does not violate the laws of physics. As discussed previously (above), the first metamaterial had a range of frequencies over which the refractive index was predicted to be negative for one direction of propagation were reported in May of the year 2000.

In 2001, a team of researchers constructed a prism composed of metamaterials (negative index metamaterials) to experimentally test for negative refractive index. The experiment used a waveguide to help transmit the proper frequency and isolate the material.

The experimental demonstration of negative refractive index was followed by another demonstration, in 2003, of a reversal of Snell's law, or reversed refraction. However, in

this experiment negative index of refraction material is in free space from 12.6 to 13.2 GHz. Although the radiated frequency range is about the same, a notable distinction is this experiment is conducted in free space rather employing waveguide.

Furthering the authenticity of negative refraction, the power flow of a wave transmitted through a dispersive left-handed material was calculated and compared to a dispersive right-handed material. The transmission of an incident field, composed of many frequencies, from an isotropic nondispersive material into an isotropic dispersive media is employed. The direction of power flow for both nondispersive and dispersive media is determined by the time-averaged Poynting vector. Negative refraction was shown to be possible for multifrequency signals by explicit calculation of the Poynting vector in the LHM.

Fundamental electromagnetic properties of the NIM

In a slab of conventional material, with an ordinary refractive index – a right-handed material (RHM) – the wave front is transmitted away from the source. In a NIM the wavefront travels toward the source. However, the magnitude and direction of the flow of energy essentially remains the same in both the ordinary material and the NIM. Since, the flow of energy remains the same in both materials (media) the impedance of the NIM matches the RHM. Hence, the sign of the intrinsic impedance is still positive in a NIM.

Light incident on a left-handed material, or NIM, will bend to the same side as the incident beam, and for Snell's law to hold, the refraction angle should be negative. In a passive metamaterial medium this determines a negative real and imaginary part of the refractive index.

Negative refractive index in left-handed materials

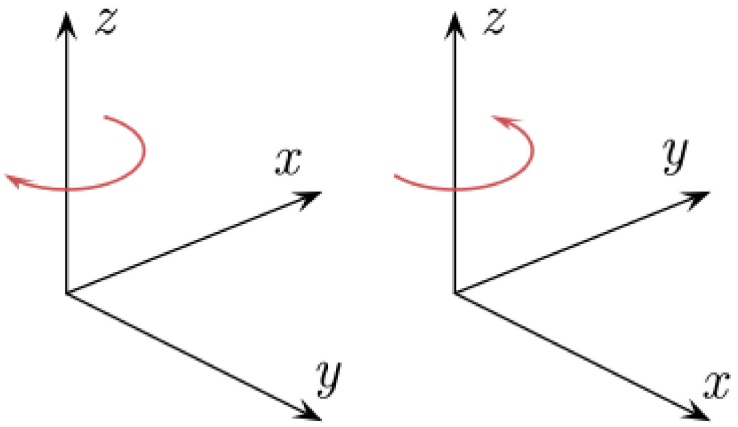

The left-handed orientation is shown on the left, and the right-handed on the right

In 1968 Victor Veselago's paper showed that the opposite directions of EM plane waves and the flow of energy was derived from the individual Maxwell curl equations. In ordinary optical materials, the curl equation for the electric field show a "right hand rule" for the directions of the electric field **E**, the magnetic induction **B**, and wave propagation, which goes in the direction of wave vector **k**. However, the direction of energy flow formed by E × H is right-handed only when *permeability is greater than zero*. This means that when permeability is less than zero, e.g. *negative*, wave propagation is reversed (determined by k), and contrary to the direction of energy flow. Furthermore, the relations of vectors **E**, **H**, and **k** form a "*left-handed" system* – and it was Veselago who coined the term "left-handed" (LH) material, which is in wide use today (2010). He contended that an LH material has a negative refractive index and relied on the steady-state solutions of Maxwell's equations as a center for his argument.

After a 30 year void, when LH materials were finally demonstrated, it could be said that that the designation of negative refractive index is unique to LH systems; even when compared to photonic crystals. Photonic crystals, like many other known systems, can exhibit unusual propagation behavior such as reversal of phase and group velocities. But, negative refraction does not occur in these systems, and not yet realistically in Photonic crystals.

Negative refraction at visible frequencies

As of May 2010 - In previous years, several anomalous studies have announced negative refraction at one single frequency, or other, in the visible spectrum. But the results of two such demonstrations are considered ambiguous by later studies. Another most recent, published, demonstration at one single visible frequency is still not the norm, or common, for the large body of work that has been produced in the field of metamaterials. To date, hundreds of scientific, peer reviewed, articles have been published regading some aspect of metamaterials. This is compared to some minscule number, the studies that have apparent results in the visible spectrum. In an encyclopedia article such as this it is problematic to give undue weight to such studies, until these become common, or part of the norm, for metamaterials.

Moreover, although previous research efforts have announced negative refraction of one single frequency in the visible light spectrum, this most recent (April, 2010) is being reported as "the first one that operates on visible light." Also as before, the stated achievement is for one single frequency in the visible spectrum. In other words there is no broad band capability.

Experimental verification of reversed Cherenkov radiation

Besides reversed values for index of refraction, Veselago predicted the occurrence of reversed Cherenkov radiation (also known simply as CR) in a left-handed medium. In 1934 Pavel Cherenkov discovered a coherent radiation (laser) that occurs when certain

types of media are bombarded by fast moving electron beams. In 1937 a theory built around CR stated that when charged particles, such as electrons, travel through a medium at speeds faster than the speed of light in the medium only then will CR radiate. As the CR occurs, electromagnetic radiation is emitted in a cone shape, fanning out in the forward direction.

CR and the 1937 theory has led to a large array of applications in high energy physics. A notable application are the Cherenkov counters. These are used to determine various properties of a charged particle such as its velocity, charge, direction of motion, and energy. These properties are important in the identification of different particles. For example, the counters were applied in the discovery of the anti-proton and the J particle. Six large Cherenkov counters were used in the discovery of the J particle.

It has been difficult to experimentally prove the reversed Cherenkov radiation.

Paraxial approximation of DNG slabs

Theoretical work, along with numerical simulations, began early in the decade of the new millennium on the capabilities of the DNG slab for subwavelength focusing. The research began with Pendry's proposed "Perfect lens". Several research investigations that followed Pendry's concluded that the "Perfect lens" was possible in theory but not practical. One direction in subwavelength focusing proceeded with the use of negative index metamaterials, but based on the enhancements for imaging with surface plasmons. In another direction researchers explored paraxial approximations of DNG slabs.

US patent on left-handed composite media

The first US patent granted for a fabricated metamaterial is U.S. Patent 6,791,432 B2, titled "Left handed composite media." The listed inventors are David Smith, Sheldon Schultz, Norman Kroll, Richard A. Shelby.

The invention achieves simultaneous negative permittivity and permeability over a common band of frequencies. The material can integrate media which is already composite or continuous, but which will produce negative permittivity and permeability within the same spectrum of frequencies. Different types of continuous or composite may be deemed appropriate when combined for the desired effect. However, the inclusion of a periodic array of conducting elements is preferred. The array scatters electromagnetic radiation at wavelengths longer than the size of the element and lattice spacing. The array is then viewed as an effective medium.

Anomalous dispersion

Propagation of a Gaussian Light Pulse through an Anomalous Dispersion Medium. However the speed of transmitting information is always limited to *c*.

Chapter- 7

Multi-function Structure and Programmable Matter

Multi-function structure

Multi-function material is a composite material. The traditional approach to the development of structures is to address the loadcarrying function and other functional requirements separately. Recently, however, there has been increased interest in the development of load-bearing materials and structures which have integral non-load-bearing functions, guided by recent discoveries about how multifunctional biological systems work.

Introduction

With conventional structural materials, it has been difficult to achieve simultaneous improvement in multiple structural functions, but the increasing use of composite materials has been driven in part by the potential for such improvements. The multi-functions can vary from mechanical to electrical and thermal functions. The most widely used composites have polymer matrix materials, which are typically poor conductors. Enhanced conductivity could be achieved with reinforcing the composite with carbon nanotubes for instance.

Functions

Among the many functions that can be attained are Electrical/thermal conductivity, Sensing and actuation, Energy harvesting/storage, Self-healing capability, Electromagnetic interference (EMI) shielding and recyclability and biodegradability.

Programmable matter

Programmable matter refers to matter which has the ability to change its physical properties (shape, density, moduli, optical properties, etc.) in a programmable fashion, based upon user input or autonomous sensing. Programmable matter is thus linked to the concept of a material which inherently has the ability to perform information processing.

History

Programmable matter is a term originally coined in 1991 by Toffoli and Margolus to refer to an ensemble of fine-grained computing elements arranged in space (Toffoli & Margolus 1991). Their paper describes a computing substrate that is composed of fine-grained compute nodes distributed throughout space which communicate using only nearest neighbor interactions. In this context, programmable matter refers to compute models similar to cellular automata and Lattice Gas Automata (Rothman & Zaleski 1997). The CAM-8 architecture is an example hardware realization of this model. This function is also known as "digital referenced areas" (DRA) in some forms of self-replicating machine science.

In the early 1990s there was a significant amount of work in reconfigurable modular robotics with a philosophy similar to programmable matter.

As semiconductor technology nanotechnology and self-replicating machine technology have advanced, the use of the term programmable matter has changed to reflect the fact that it is possible to build an ensemble of elements which can be "programmed" to change their physical properties in reality, not just in simulation. Thus, programmable matter has come to mean "any bulk substance which can be programmed to change its physical properties."

In the summer of 1998, in a discussion on artificial atoms and programmable matter, Wil McCarthy and G. Snyder coined the term "quantum wellstone" (or simply "wellstone") to describe this hypothetical but plausible form of programmable matter. McCarthy has used the term in his fiction.

In 2002, Seth Goldstein and Todd Mowry started the claytronics project at Carnegie Mellon University to investigate the underlying hardware and software mechanisms necessary to realize programmable matter.

In 2004, the DARPA Information Science and Technology group (ISAT) examined the potential of programmable matter. This resulted in the 2005-2006 study, "Realizing Programmable Matter" which laid out a multi-year program for the research and development of programmable matter.

In 2007, programmable matter was the subject of a DARPA research solicitation and subsequent program.

Approaches to programmable matter

In one school of thought the programming could be external to the material and might be achieved by the "application of light, voltage, electric or magnetic fields, etc." (McCarthy 2006). For example, in this school of thought, a liquid crystal display is a form of programmable matter. A second school of thought is that the individual units of the ensemble can compute and the result of their computation is a change in the ensemble's physical properties. An example of this more ambitious form of programmable matter is claytronics, where the units in the ensemble "compute" and the result is a change in the shape of the ensemble.

There are many proposed implementations of programmable matter. Scale is one key differentiator between different forms of programmable matter. At one end of the spectrum reconfigurable modular robotics pursues a form of programmable matter where the individual units are in the centimeter size range. At the nanoscale end of the spectrum there are a tremendous number of different bases for programmable matter, ranging from shape changing molecules to quantum dots. Quantum dots are in fact often referred to as artificial atoms. In the micrometer to sub-millimeter range examples include claytronics, MEMS-based units, cells created using synthetic biology, and the utility fog concept.

Examples of programmable matter

There are many conceptions of programmable matter, and thus many discrete avenues of research using the name. Below are some specific examples of programmable matter.

"Simple" programmable matter

These include materials that can change their properties based on some input, but do not have the ability to do complex computation by themselves.

Complex fluids

The physical properties of several complex fluids can be modified by applying a current or voltage, as is the case with liquid crystals.

Metamaterials

Metamaterials are artificial composites that can be controlled to react in ways that do not occur in nature. One example developed by David Smith and then by John Pendry and David Schuri is of a material that can have its index of refraction tuned so that it can have a different index of refraction at different points in the material. If tuned properly this could result in an "invisibility cloak."

Shape Changing Molecules

An active area of research is in molecules that can change their shape, as well as other properties, in response to external stimuli. These molecules can be used individually or en masse to form new kinds of materials. For example, J Fraser Stoddart's group at UCLA has been developing molecules that can change their electrical properties.

Robotics-based approaches

Self-Reconfiguring Modular Robotics

Self-Reconfiguring Modular Robotics is a field of robotics in which a group of basic robot modules work together to dynamically form shapes and create behaviours suitable for many tasks. Like Programmable matter SRCMR aims to offer significant improvement to any kind of objects or system by introducing many new possibilities for example: 1. Most important is the incredible flexibility that comes from the ability to change the physical structure and behavior of a solution by changing the software that controls modules. 2. The ability to self-repair by automatically replacing a broken module will make SRCMR solution incredibly resilient. 3. Reducing the environmental foot print by reusing the same modules in many different solutions.

Claytronics

Claytronics is an emerging field of engineering concerning reconfigurable nanoscale robots ('claytronic atoms', or *catoms*) designed to form much larger scale machines or mechanisms. The catoms will be sub-millimeter computers that will eventually have the ability to move around, communicate with other computers, change color, and electrostatically connect to other catoms to form different shapes.

Cellular automata

Cellular automata are a useful concept to abstract some of the concepts of discrete units interacting to give a desired overall behavior.

Quantum wells

Quantum wells can hold one or more electrons. Those electrons behave like artificial atoms which, like real atoms, can form covalent bonds, but these are extremely weak. Because of their larger sizes, other properties are also widely different.

Synthetic biology

Synthetic biology is a field that aims to engineer cells with "novel biological functions." Such cells are usually used to create larger systems (e.g., biofilms) which can be "programmed" utilizing synthetic gene networks such as genetic toggle switches, to change their color, shape, etc.

Chapter- 8

Quantum Dot

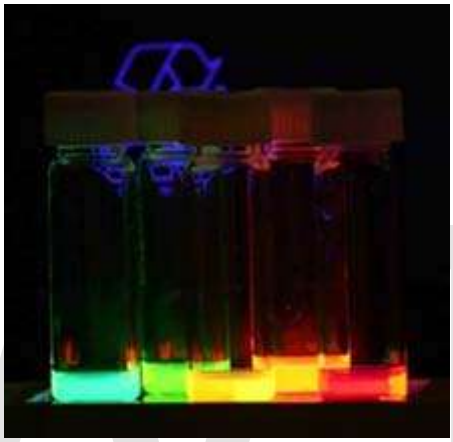

Colloidal quantum dots irradiated with a UV light. Different sized quantum dots emit different color light due to quantum confinement.

A **quantum dot** is a semiconductor whose excitons are confined in all three spatial dimensions. Consequently, such materials have electronic properties intermediate between those of bulk semiconductors and those of discrete molecules. They were discovered at the beginning of the 1980s by Alexei Ekimov in a glass matrix and by Louis E. Brus in colloidal solutions. The term "quantum dot" was coined by Mark Reed.

Researchers have studied quantum dots in transistors, solar cells, LEDs, and diode lasers. They have also investigated quantum dots as agents for medical imaging and hope to use them as qubits.

Stated simply, quantum dots are semiconductors whose electronic characteristics are closely related to the size and shape of the individual crystal. Generally, the smaller the size of the crystal, the larger the band gap, the greater the difference in energy between the highest valence band and the lowest conduction band becomes, therefore more energy is needed to excite the dot, and concurrently, more energy is released when the crystal returns to its resting state. For example, in fluorescent dye applications, this equates to higher frequencies of light emitted after excitation of the dot as the crystal size grows smaller, resulting in a color shift from red to blue in the light emitted. In addition to such tuning, a main advantage with quantum dots is that, because of the high level of control

possible over the size of the crystals produced, it is possible to have very precise control over the conductive properties of the material. Quantum dots of different sizes can be assembled into a gradient multi-layer nanofilm.

Quantum confinement in semiconductors

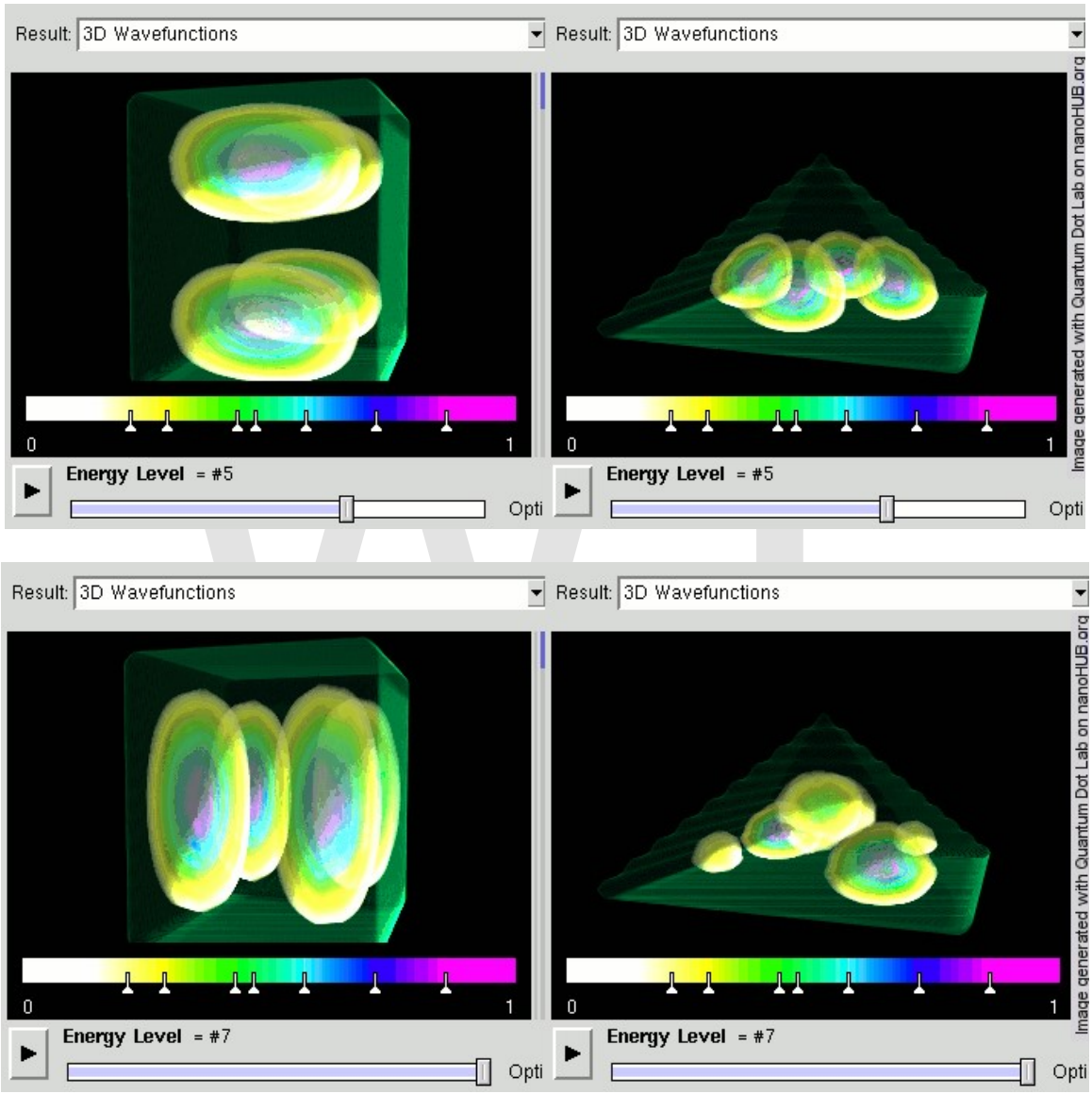

3D confined electron wave functions in a Quantum Dot. Here, rectangular and triangular-shaped quantum dots are shown. Energy states in rectangular dots are more ‘s-type’ and ‘p-type’. However, in a triangular dot the wave functions are mixed due to confinement symmetry.

In an unconfined (bulk) semiconductor, an electron-hole pair is typically bound within a characteristic length, called the exciton Bohr radius. This is estimated by replacing the positively charged atomic core with the hole in the Bohr formula. If the electron and hole

are constrained further, then properties of the semiconductor change. This effect is a form of quantum confinement, and it is a key feature in many emerging electronic structures.

Besides confinement in all three dimensions i.e. Quantum Dot - other quantum confined semiconductors include:

- quantum wires, which confine electrons or holes in two spatial dimensions and allow free propagation in the third.
- quantum wells, which confine electrons or holes in one dimension and allow free propagation in two dimensions.

Production

There are several ways to confine excitons in semiconductors, resulting in different methods to produce quantum dots. In general, quantum wires, wells and dots are grown by advanced epitaxial techniques in nanocrystals produced by chemical methods or by ion implantation, or in nanodevices made by state-of-the-art lithographic techniques.

Colloidal synthesis

Colloidal semiconductor nanocrystals are synthesized from precursor compounds dissolved in solutions, much like traditional chemical processes. The synthesis of colloidal quantum dots is based on a three-component system composed of: precursors, organic surfactants, and solvents. When heating a reaction medium to a sufficiently high temperature, the precursors chemically transform into monomers. Once the monomers reach a high enough supersaturation level, the nanocrystal growth starts with a nucleation process. The temperature during the growth process is one of the critical factors in determining optimal conditions for the nanocrystal growth. It must be high enough to allow for rearrangement and annealing of atoms during the synthesis process while being low enough to promote crystal growth. Another critical factor that has to be stringently controlled during nanocrystal growth is the monomer concentration. The growth process of nanocrystals can occur in two different regimes, “focusing” and “defocusing”. At high monomer concentrations, the critical size (the size where nanocrystals neither grow nor shrink) is relatively small, resulting in growth of nearly all particles. In this regime, smaller particles grow faster than large ones (since larger crystals need more atoms to grow than small crystals) resulting in “focusing” of the size distribution to yield nearly monodisperse particles. The size focusing is optimal when the monomer concentration is kept such that the average nanocrystal size present is always slightly larger than the critical size. When the monomer concentration is depleted during growth, the critical size becomes larger than the average size present, and the distribution “defocuses” as a result of Ostwald ripening.

There are colloidal methods to produce many different semiconductors. Typical dots are made of binary alloys such as cadmium selenide, cadmium sulfide, indium arsenide, and indium phosphide. Although, dots may also be made from ternary alloys such as cadmium selenide sulfide. These quantum dots can contain as few as 100 to 100,000

atoms within the quantum dot volume, with a diameter of 10 to 50 atoms. This corresponds to about 2 to 10 nanometers, and at 10 nm in diameter, nearly 3 million quantum dots could be lined up end to end and fit within the width of a human thumb.

Large batches of quantum dots may be synthesized via colloidal synthesis. Due to this scalability and the convenience of benchtop conditions, colloidal synthetic methods are promising for commercial applications. It is acknowledged to be the least toxic of all the different forms of synthesis.

Fabrication

- Self-assembled quantum dots are typically between 5 and 50 nm in size. Quantum dots defined by lithographically patterned gate electrodes, or by etching on two-dimensional electron gases in semiconductor heterostructures can have lateral dimensions exceeding 100 nm.
- Some quantum dots are small regions of one material buried in another with a larger band gap. These can be so-called core-shell structures, e.g., with CdSe in the core and ZnS in the shell or from special forms of silica called ormosil.
- Quantum dots sometimes occur spontaneously in quantum well structures due to monolayer fluctuations in the well's thickness.
- Self-assembled quantum dots nucleate spontaneously under certain conditions during molecular beam epitaxy (MBE) and metallorganic vapor phase epitaxy (MOVPE), when a material is grown on a substrate to which it is not lattice matched. The resulting strain produces coherently strained islands on top of a two-dimensional "wetting-layer." This growth mode is known as Stranski–Krastanov growth. The islands can be subsequently buried to form the quantum dot. This fabrication method has potential for applications in quantum cryptography (i.e. single photon sources) and quantum computation. The main limitations of this method are the cost of fabrication and the lack of control over positioning of individual dots.
- Individual quantum dots can be created from two-dimensional electron or hole gases present in remotely doped quantum wells or semiconductor heterostructures called lateral quantum dots. The sample surface is coated with a thin layer of resist. A lateral pattern is then defined in the resist by electron beam lithography. This pattern can then be transferred to the electron or hole gas by etching, or by depositing metal electrodes (lift-off process) that allow the application of external voltages between the electron gas and the electrodes. Such quantum dots are mainly of interest for experiments and applications involving electron or hole transport, i.e., an electrical current.
- The energy spectrum of a quantum dot can be engineered by controlling the geometrical size, shape, and the strength of the confinement potential. Also, in contrast to atoms, it is relatively easy to connect quantum dots by tunnel barriers to conducting leads, which allows the application of the techniques of tunneling spectroscopy for their investigation.

The quantum dot absorption features correspond to transitions between discrete,three-dimensional particle in a box states of the electron and the hole, both confined to the same nanometer-size box.These discrete transitions are reminiscent of atomic spectra and have resulted in quantum dots also being called *artificial atoms*.

- Confinement in quantum dots can also arise from electrostatic potentials (generated by external electrodes, doping, strain, or impurities).

Viral assembly

Lee et al. (2002) reported using genetically engineered M13 bacteriophage viruses to create quantum dot biocomposite structures. As a background to this work, it has previously been shown that genetically engineered viruses can recognize specific semiconductor surfaces through the method of selection by combinatorial phage display. Additionally, it is known that liquid crystalline structures of wild-type viruses (Fd, M13, and TMV) are adjustable by controlling the solution concentrations, solution ionic strength, and the external magnetic field applied to the solutions. Consequently, the specific recognition properties of the virus can be used to organize inorganic nanocrystals, forming ordered arrays over the length scale defined by liquid crystal formation. Using this information, Lee et al. (2000) were able to create self-assembled, highly oriented, self-supporting films from a phage and ZnS precursor solution. This system allowed them to vary both the length of bacteriophage and the type of inorganic material through genetic modification and selection.

Electrochemical assembly

Highly ordered arrays of quantum dots may also be self-assembled by electrochemical techniques. A template is created by causing an ionic reaction at an electrolyte-metal interface which results in the spontaneous assembly of nanostructures, including quantum dots, onto the metal which is then used as a mask for mesa-etching these nanostructures on a chosen substrate.

Bulk-manufacture

Conventional, small-scale quantum dot manufacturing relies on a process called “high temperature dual injection” which is impractical for most commercial applications that require large quantities of quantum dots.

A reproducible method for creating larger quantities of consistent, high-quality quantum dots involves producing nanoparticles from chemical precursors in the presence of a molecular cluster compound under conditions whereby the integrity of the molecular cluster is maintained and acts as a prefabricated seed template. Individual molecules of a cluster compound act as a seed or nucleation point upon which nanoparticle growth can be initiated. In this way, a high temperature nucleation step is not necessary to initiate nanoparticle growth because suitable nucleation sites are already provided in the system

by the molecular clusters. A significant advantage of this method is that it is highly scalable.

Cadmium-free quantum dots

Cadmium-free quantum dots are also called “CFQD”. In many regions of the world there is now a restriction or ban on the use of heavy metals in many household goods which means that most cadmium based quantum dots are unusable for consumer-goods applications.

For commercial viability, a range of restricted, heavy metal-free quantum dots has been developed showing bright emissions in the visible and near infra-red region of the spectrum and have similar optical properties to those of CdSe quantum dots.

Cadmium and other restricted heavy metals used in conventional quantum dots is of a major concern in commercial applications. For Quantum Dots to be commercially viable in many applications they must not contain cadmium or other restricted metal elements.

A new type of CFQD can be made from rare earth (RE) doped oxide colloidal phosphor nanoparticles. Unlike semiconductor nanoparticles, excitation was due to UV absorption of host material, which is same for different RE doped materials using same host. Multiplexing applications can be thus realized. The emission depends on the type of RE, which enables very large stokes shift and is narrower than CdSe QDs. The synthesis is aqueous based, which eliminated issues of water solubility for biological applications. The oxide surface might be easier for chemical functionalizion more and chemically stable in various environments. Some reports exist concerning the use of such phosphor nanoparticles on biological targeting and imaging.

Optical properties

An immediate optical feature of colloidal quantum dots is their coloration. While the material which makes up a quantum dot defines its intrinsic energy signature, the nanocrystal's quantum confined size is more significant at energies near the band gap. Thus quantum dots of the same material, but with different sizes, can emit light of different colors. The physical reason is the quantum confinement effect.

The larger the dot, the redder (lower energy) its fluorescence spectrum. Conversely, smaller dots emit bluer (higher energy) light. The coloration is directly related to the energy levels of the quantum dot. Quantitatively speaking, the bandgap energy that determines the energy (and hence color) of the fluorescent light is inversely proportional to the size of the quantum dot. Larger quantum dots have more energy levels which are also more closely spaced. This allows the quantum dot to absorb photons containing less energy, i.e., those closer to the red end of the spectrum. Recent articles in nanotechnology and in other journals have begun to suggest that the shape of the quantum dot may be a factor in the coloration as well, but as yet not enough information is available. Furthermore, it was shown that the lifetime of fluorescence is determined by the size of

the quantum dot. Larger dots have more closely spaced energy levels in which the electron-hole pair can be trapped. Therefore, electron-hole pairs in larger dots live longer causing larger dots to show a longer lifetime.

As with any crystalline semiconductor, a quantum dot's electronic wave functions extend over the crystal lattice. Similar to a molecule, a quantum dot has both a quantized energy spectrum and a quantized density of electronic states near the edge of the band gap.

Qdots can be synthesized with larger(thicker) shells (CdSe qdots with CdS shells). The shell thickness has shown direct correlation to the lifetime and emission intensity.

Applications

Quantum dots are particularly significant for optical applications due to their high extinction co-efficient. In electronic applications they have been proven to operate like a single-electron transistor and show the Coulomb blockade effect. Quantum dots have also been suggested as implementations of qubits for quantum information processing.

The ability to tune the size of quantum dots is advantageous for many applications. For instance, larger quantum dots have a greater spectrum-shift towards red compared to smaller dots, and exhibit less pronounced quantum properties. Conversely, the smaller particles allow one to take advantage of more subtle quantum effects.

WT

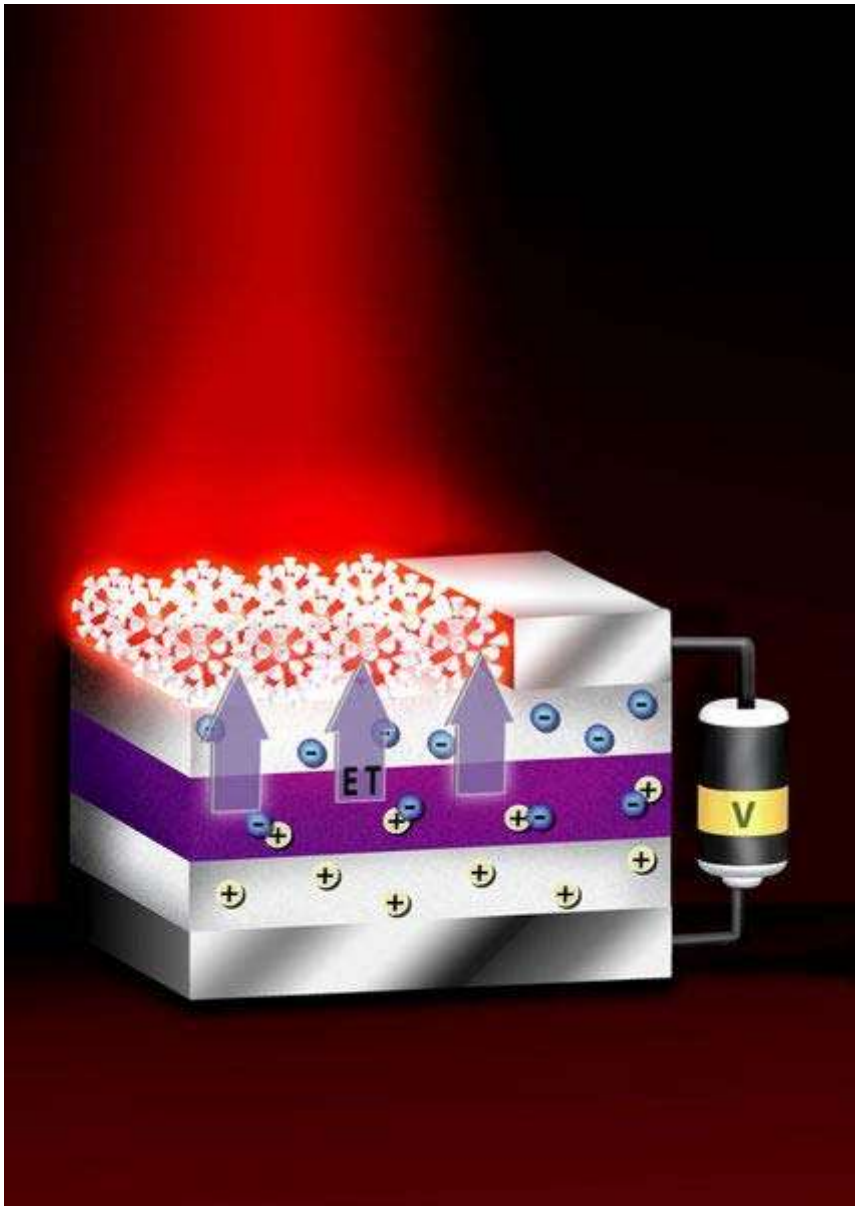

Researchers at Los Alamos National Laboratory have developed a wireless device that efficiently produces visible light, through energy transfer from thin layers of quantum wells to crystals above the layers.

Being zero dimensional, quantum dots have a sharper density of states than higher-dimensional structures. As a result, they have superior transport and optical properties, and are being researched for use in diode lasers, amplifiers, and biological sensors. Quantum dots may be excited within the locally enhanced electromagnetic field produced by the gold nanoparticles, which can then be observed from the surface Plasmon resonance in the photoluminescent excitation spectrum of (CdSe)ZnS nanocrystals. High-quality quantum dots are well suited for optical encoding and multiplexing applications due to their broad excitation profiles and narrow/symmetric emission spectra. The new generations of quantum dots have far-reaching potential for the study of intracellular

processes at the single-molecule level, high-resolution cellular imaging, long-term in vivo observation of cell trafficking, tumor targeting, and diagnostics.

Computing

Quantum dot technology is one of the most promising candidates for use in solid-state quantum computation. By applying small voltages to the leads, the flow of electrons through the quantum dot can be controlled and thereby precise measurements of the spin and other properties therein can be made. With several entangled quantum dots, or qubits, plus a way of performing operations, quantum calculations and the computers that would perform them might be possible.

Biology

In modern biological analysis, various kinds of organic dyes are used. However, with each passing year, more flexibility is being required of these dyes, and the traditional dyes are often unable to meet the expectations. To this end, quantum dots have quickly filled in the role, being found to be superior to traditional organic dyes on several counts, one of the most immediately obvious being brightness (owing to the high extinction coefficient combined with a comparable quantum yield to fluorescent dyes) as well as their stability (allowing much less photobleaching). It has been estimated that quantum dots are 20 times brighter and 100 times more stable than traditional fluorescent reporters. For single-particle tracking, the irregular blinking of quantum dots is a minor drawback.

The usage of quantum dots for highly sensitive cellular imaging has seen major advances over the past decade. The improved photostability of quantum dots, for example, allows the acquisition of many consecutive focal-plane images that can be reconstructed into a high-resolution three-dimensional image. Another application that takes advantage of the extraordinary photostability of quantum dot probes is the real-time tracking of molecules and cells over extended periods of time. Antibodies, streptavidin, peptides, nucleic acid aptamers, or small-molecule ligands can be used to target quantum dots to specific proteins on cells. Researchers were able to observe quantum dots in lymph nodes of mice for more than 4 months.

Semiconductor quantum dots have also been employed for in vitro imaging of pre-labeled cells. The ability to image single-cell migration in real time is expected to be important to several research areas such as embryogenesis, cancer metastasis, stem-cell therapeutics, and lymphocyte immunology.

Scientists have proven that quantum dots are dramatically better than existing methods for delivering a gene-silencing tool, known as siRNA, into cells.

First attempts have been made to use quantum dots for tumor targeting under in vivo conditions. There exist two basic targeting schemes: active targeting and passive targeting. In the case of active targeting, quantum dots are functionalized with tumor-specific binding sites to selectively bind to tumor cells. Passive targeting utilizes the

enhanced permeation and retention of tumor cells for the delivery of quantum dot probes. Fast-growing tumor cells typically have more permeable membranes than healthy cells, allowing the leakage of small nanoparticles into the cell body. Moreover, tumor cells lack an effective lymphatic drainage system, which leads to subsequent nanoparticle-accumulation.

One of the remaining issues with quantum dot probes is their potential in vivo toxicity. For example, CdSe nanocrystals are highly toxic to cultured cells under UV illumination. The energy of UV irradiation is close to that of the covalent chemical bond energy of CdSe nanocrystals. As a result, semiconductor particles can be dissolved, in a process known as photolysis, to release toxic cadmium ions into the culture medium. In the absence of UV irradiation, however, quantum dots with a stable polymer coating have been found to be essentially nontoxic. Then again, only little is known about the excretion process of quantum dots from living organisms. These and other questions must be carefully examined before quantum dot applications in tumor or vascular imaging can be approved for human clinical use.

Another potential cutting-edge application of quantum dots is being researched, with quantum dots acting as the inorganic fluorophore for intra-operative detection of tumors using fluorescence spectroscopy.

Photovoltaic devices

Quantum dots may be able to increase the efficiency and reduce the cost of today's typical silicon photovoltaic cells. According to an experimental proof from 2006 (controversial results), quantum dots of lead selenide can produce as many as seven excitons from one high energy photon of sunlight (7.8 times the bandgap energy). This compares favorably to today's photovoltaic cells which can only manage one exciton per high-energy photon, with high kinetic energy carriers losing their energy as heat. This would not result in a 7-fold increase in final output however, but could boost the maximum theoretical efficiency from 31% to 42%. Quantum dot photovoltaics would theoretically be cheaper to manufacture, as they can be made "using simple chemical reactions." The generation of more than one exciton by a single photon is called multiple exciton generation (MEG) or carrier multiplication.

Light emitting devices

There are several inquiries into using quantum dots as light-emitting diodes to make displays and other light sources, such as "QD-LED" displays, and "QD-WLED" (White LED). In June, 2006, QD Vision announced technical success in making a proof-of-concept quantum dot display and show a bright emission in the visible and near infra-red region of the spectrum. Quantum dots are valued for displays, because they emit light in very specific gaussian distributions. This can result in a display that more accurately renders the colors that the human eye can perceive. Quantum dots also require very little power since they are not color filtered. Additionally, since the discovery of "white-light emitting" QD, general solid-state lighting applications appear closer than ever. A color

liquid crystal display (LCD), for example, is usually powered by a single fluorescent lamp (or occasionally, conventional white LEDs) that is color filtered to produce red, green, and blue pixels. Displays that intrinsically produce monochromatic light can be more efficient, since more of the light produced reaches the eye.

WT